

6-30-1965

Effect of particle size and particle size distribution on the burning rate of barium chromate-boron pyrotechnic delay compositions

Donald J. Freeman
New Jersey Institute of Technology

Follow this and additional works at: <https://digitalcommons.njit.edu/theses>



Part of the [Chemical Engineering Commons](#)

Recommended Citation

Freeman, Donald J., "Effect of particle size and particle size distribution on the burning rate of barium chromate-boron pyrotechnic delay compositions" (1965). *Theses*. 2150.
<https://digitalcommons.njit.edu/theses/2150>

This Thesis is brought to you for free and open access by the Electronic Theses and Dissertations at Digital Commons @ NJIT. It has been accepted for inclusion in Theses by an authorized administrator of Digital Commons @ NJIT. For more information, please contact digitalcommons@njit.edu.

Copyright Warning & Restrictions

The copyright law of the United States (Title 17, United States Code) governs the making of photocopies or other reproductions of copyrighted material.

Under certain conditions specified in the law, libraries and archives are authorized to furnish a photocopy or other reproduction. One of these specified conditions is that the photocopy or reproduction is not to be “used for any purpose other than private study, scholarship, or research.” If a user makes a request for, or later uses, a photocopy or reproduction for purposes in excess of “fair use” that user may be liable for copyright infringement,

This institution reserves the right to refuse to accept a copying order if, in its judgment, fulfillment of the order would involve violation of copyright law.

Please Note: The author retains the copyright while the New Jersey Institute of Technology reserves the right to distribute this thesis or dissertation

Printing note: If you do not wish to print this page, then select “Pages from: first page # to: last page #” on the print dialog screen

The Van Houten library has removed some of the personal information and all signatures from the approval page and biographical sketches of theses and dissertations in order to protect the identity of NJIT graduates and faculty.

EFFECT OF PARTICLE SIZE AND PARTICLE SIZE DISTRIBUTION
ON THE BURNING RATE OF BARIUM CHROMATE-BORON
PYROTECHNIC DELAY COMPOSITIONS

BY

DONALD J.FREEMAN

A THESIS

PRESENTED IN PARTIAL FULFILLMENT OF

THE REQUIREMENTS FOR DEGREE

OF

MASTER OF SCIENCE IN CHEMICAL ENGINEERING

AT

NEWARK COLLEGE OF ENGINEERING

This thesis is to be used only with due regard to the rights of the author. Bibliographical references may be noted, but passages must not be copied without permission of the College and without credit being given in subsequent written or published work.

Newark, New Jersey
1965

APPROVAL OF THESIS

FOR

DEPARTMENT OF CHEMICAL ENGINEERING

NEWARK COLLEGE OF ENGINEERING

BY

FACULTY COMMITTEE

APPROVED: _____

NEWARK, NEW JERSEY

JUNE, 1965

ABSTRACT

The burning rate of barium chromate-boron delay compositions is shown to be related to the 10 percent particle size point on the particle size distribution curve (particle size vs. percent greater than size) for either of the components. The burning rate is also shown to be inversely proportional to the 10 percent point of the barium chromate; and to follow a hyperbolic type relationship with the 10 percent of the boron, decreasing asymptotically as the 10 percent point increases. No correlations were found between the burning rate of the compositions and the average particle diameter, the mean particle diameter, or the 50 percent point for either component.

The average particle diameter (APD) as determined with the Fisher Sub-Sieve Sizer, is presently specified as the measure of the particle size of the components of barium chromate-boron delay compositions. As the validity of the APD is subject to question, other methods of particle size analysis were considered. The Mine Safety Appliances (MSA) Particle Size Analyzer was thus selected for the determination of the particle size distribution of barium chromate and boron.

The APD was found to be closely related to the product of the uniformity index of the sample and either the MSA 50

percent point of the MSA d_m (mean particle diameter.) For barium chromate the APD's were approximately equal to the modified MSA values. A low degree of inequality between the MSA and APD values existed for the boron samples.

ACKNOWLEDGEMENTS

The author is grateful to Professor Michael Frederick for his guidance and counsel throughout the course of this research.

The writer wishes to acknowledge the cooperation and assistance of Picatinny Arsenal in making available the facilities and equipment for experimental work, with special thanks to G. Weingarten of the Pyrotechnics Laboratory.

The writer is indebted to Mrs. Helen Ender for her assistance in the typing of the manuscript.

The writer also expresses his appreciation to his wife, Barbara, whose patience and sacrifices have made completion of this thesis possible.

TABLE OF CONTENTS

	<u>Page</u>
ABSTRACT	iii
ACKNOWLEDGEMENTS	v
TABLE OF CONTENTS	vi
LIST OF ILLUSTRATIONS	viii
LIST OF TABLES	xi
I. INTRODUCTION	1
II. EXPERIMENTAL	8
A. Dispersion of Barium Chromate and Boron	8
1. Method of dispersion	8
2. Selection of dispersing agents	8
B. Use of the Mine Safety Appliances (MSA) Particle Size Analyzer	11
1. Equipment and procedure	11
2. Results	22
C. Preparation of Delay Compositions and Fuzes	23
1. Selection of barium chromate and boron samples	23
2. Blending of compositions	28
3. Loading of delay fuzes	29
D. Burning Rate Testing	33
1. Equipment	33
2. Procedure	35
3. Results	37
III. DISCUSSION	38
A. Dispersion of Barium Chromate and Boron	38
B. Evaluation of Particle Size Analysis Equipment	40
C. Particle Size Distribution of Barium Chromate and Boron	49

	<u>Page</u>
D. Relationship of Burning Rate of Barium Chromate-Boron Delay Compositions to the Particle Size of the Components	61
IV. CONCLUSIONS	81
V. RECOMMENDATIONS	83
VI. BIBLIOGRAPHY	84
VII. APPENDIX	86
A. MSA Particle Size Analysis Tables and Graphs	87
B. Particle Size Frequency Tables and Graphs	107
C. Burning Rate Data and Results	135
D. Glossary	155

LIST OF ILLUSTRATIONS

	<u>Page</u>
1. M112A1 Photoflash Cartridge Assembly- Ordnance Drawing F8848546	2
2. Fuze Assembly - Ordnance Drawing C8848544	3
3. Burning Time and Heat of Reaction of Barium Chromate - Boron Composition vs. Percent Boron	5
4. Feeding Chamber and Centrifuge Tube	12
5. Centrifuge Tubes During Analysis Run	13
6. Centrifuge Tube in Projector for Reading of Sediment Height	14
7. Delay Fuze Housing - from Ordnance Drawing C8848543	30
8. Fuze Housing and Loading Fixture Assembly	31
9. Dennison Four-Ton Multi-Press	31
10. Burning Rate Testing Equipment	34
11. Details of Test Fixture	34
12. 90/10 Squib Assembly - Modified Ordnance Drawing C8879892	36
13. Fisher Sub-Sieve Sizer	41
14. Bausch and Lomb Research Metallograph	46
15. MSA Particle Size Analysis Equipment	48
16. Fisher APD vs MSA 50 Percent Point (Barium Chromate)	54
17. Fisher APD vs MSA 50 Percent Point (Boron)	55
18. Fisher APD vs MSA d_m (Barium Chromate)	56
19. Fisher APD vs MSA d_m (Boron)	57
20. Fisher APD vs Modified MSA 50 Percent Point (Barium Chromate)	63

	<u>Page</u>
21. Fisher APD vs Modified MSA 50 Percent Point (Boron)	64
22. Fisher APD vs Modified MSA d_m (Barium Chromate)	65
23. Fisher APD vs Modified MSA d_m (Boron)	66
24. Effect of Particle Size on Burning Rate of Barium Chromate	73
25. Effect of Particle Size on Burning Rate of Boron	74
26. Burned and Unburned Fuzes	78
27. Particle Size Distribution for Barium Chromate - Lots Baker 38388 and Baker 91104	97
28. Particle Size Distribution for Barium Chromate - Lots Baker 25894 and Baker 26428	98
29. Particle Size Distribution for Barium Chromate - Lots MP 25160 and MP 28303	99
30. Particle Size Distribution for Barium Chromate - Lots MP 32500 and MP 28511	100
31. Particle Size Distribution for Barium Chromate - Lots MP 31801 and MP 30701	101
32. Particle Size Distribution for Barium Chromate - Lot B&C Fine	102
33. Particle Size Distribution for Boron - Lots Trona 571 and Trona 419	103
34. Particle Size Distribution for Boron - Lot HCST 873	104
35. Particle Size Distribution for Boron - Lots HCST 900 and HCST 954	105
36. Particle Size Distribution for Boron - Lots UMC 1992 and UMC 1993	106
37. Size Frequency Curve for Barium Chromate - Lots 125 Baker 30388 and Baker 91104	125

	<u>Page</u>
38. Size Frequency Curve for Barium Chromate - Lots Baker 25894 and Baker 26428	126
39. Size Frequency Curve for Barium Chromate - Lots MP 25160 and MP 28303	127
40. Size Frequency Curve for Barium Chromate - Lots MP 28511 and MP 32500	128
41. Size Frequency Curve for Barium Chromate - Lots MP 30701 and MP 31801	129
42. Size Frequency Curve for Barium Chromate - Lot B&C Fine	130
43. Size Frequency Curve for Boron - Lots Trona 571 and Trona 419	131
44. Size Frequency Curve for Boron - Lot HCST 873	132
45. Size Frequency Curve for Boron - Lots HCST 900 and HCST 954	133
46. Size Frequency Curve for Boron - Lots UMC 1992 and UMC 1993	134

LIST OF TABLES

	<u>Page</u>
1. Wetting and Dispersing Agents	10
2. Reading Schedule for Analysis of Barium Chromate	17
3. Reading Schedule for Analysis of Boron	21
4. Fisher APD for Barium Chromate and Boron Samples	25
5. Chemical Analyses of Barium Chromate Samples	26
6. Chemical Analyses of Boron Samples	27
7. Summary of Delay Compositions	32
8. Methods of Analysis of Particle Size Distribution	43
9. Summary of Particle Size Analysis Results	50
10. Summary of Burning Rate Calculations	62
11. MSA 50 Percent Point vs. Burning Rate for Compositions Containing Baker Barium Chromate	68
12. MSA 50 Percent Point vs. Burning Rate for Compositions Containing Mineral Pigments Barium Chromate	69
13. MSA 10 Percent Point vs. Burning Rate for Compositions Containing Baker Barium Chromate	71
14. MSA 10 Percent Point vs. Burning Rate for Compositions Containing Mineral Pigments Barium Chromate	72
15. MSA Particle Size Analysis of Barium Chromate-Lots Baker 30388 and Baker 91104	87
16. MSA Particle Size Analysis of Barium Chromate-Lots Baker 25894 and Baker 26428	88
17. MSA Particle Size Analysis of Barium Chromate-Lots MP 25160 and MP 28303	89

	<u>Page</u>
18. MSA Particle Size Analysis of Barium Chromate- Lots MP 32500 and MP 28511	90
19. MSA Particle Size Analysis of Barium Chromate- Lots MP 31901 and Mp 30701	91
20. MSA Particle Size Analysis of Barium Chromate- Lot B&C Fine	92
21. MSA Particle Size Analysis of Boron-Lots Trona 419 and Trona 571	93
22. MSA Particle Size Analysis of Boron-Lot HCST 873	94
23. MSA Particle Size Analysis of Boron-Lots HCST 900 and HCST 954	95
24. MSA Particle Size Analysis of Boron-Lots UMC 1992 and UMC 1993	96
25. Size Frequency Data for Barium Chromate- Lot 30388	107
26. Size Frequency Data for Barium Chromate- Lot 91104	108
27. Size Frequency Data for Barium Chromate- Lot 25894	109
28. Size Frequency Data for Barium Chromate- Lot 26428	110
29. Size Frequency Data for Barium Chromate- Lot MP 28303	111
30. Size Frequency Data for Barium Chromate- Lot MP 25160	112
31. Size Frequency Data for Barium Chromate- Lot MP 28511	113
32. Size Frequency Data for Barium Chromate- Lot MP 30701	114
33. Size Frequency Data for Barium Chromate- Lot MP 32500	115

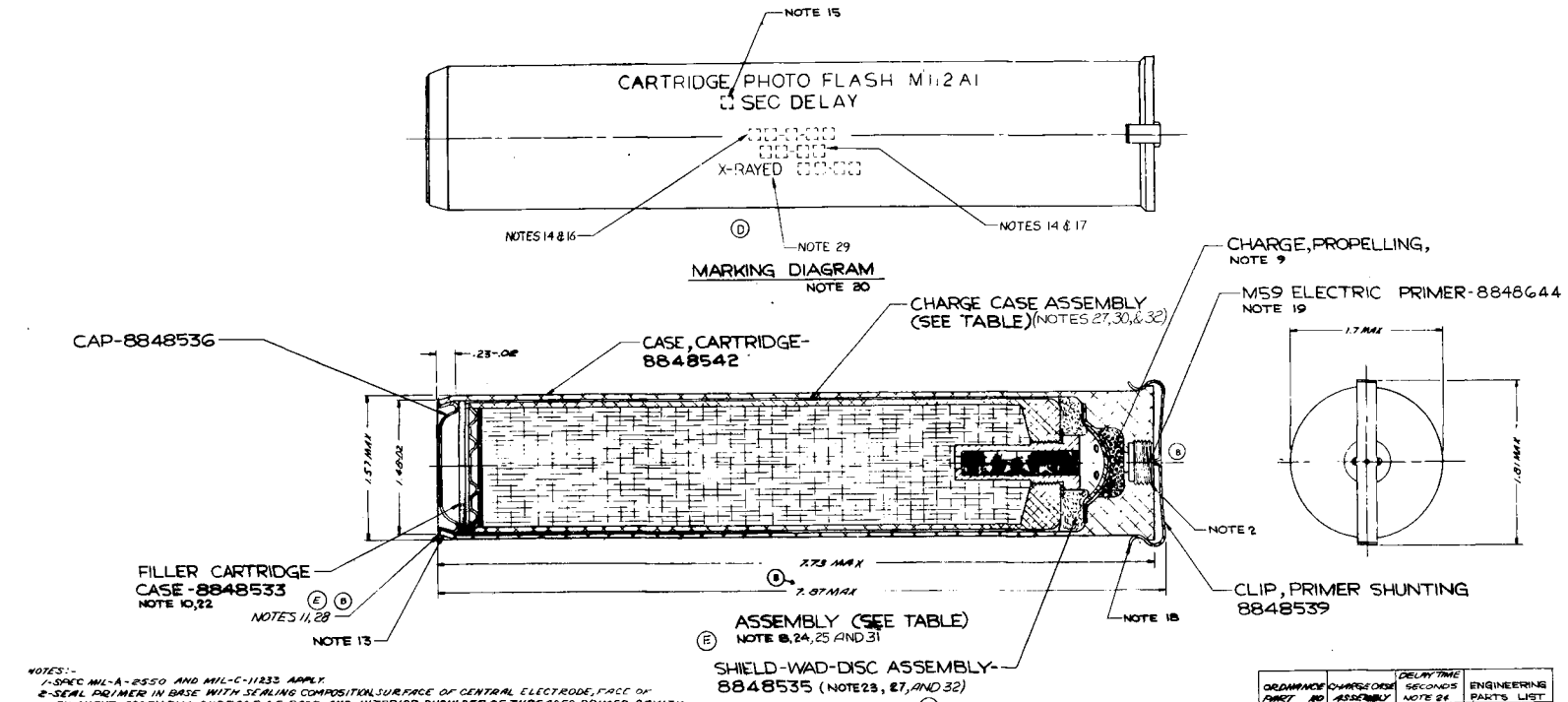
	<u>Page</u>
34. Size Frequency Data for Barium Chromate- Lot MP 31801	116
35. Size Frequency Data for B & C Fine	117
36. Size Frequency Data for Boron-Lot Trona 571	118
37. Size Frequency Data for Boron-Lot Trona 419	119
38. Size Frequency Data for Boron-Lot HCST 873	120
39. Size Frequency Data for Boron-Lot HCST 900	121
40. Size Frequency Data for Boron-Lot HCST 954	122
41. Size Frequency Data for Boron-Lot UMC 1992	123
42. Size Frequency Data for Boron-Lot UMC 1993	124
43. Burning Rate Data-Composition 1	135
44. Burning Rate Data-Composition 2	136
45. Burning Rate Data-Composition 3	137
46. Burning Rate Data-Composition 4	138
47. Burning Rate Data-Composition 5	139
48. Burning Rate Data-Composition 6	140
49. Burning Rate Data-Composition 7	141
50. Burning Rate Data-Composition 8	142
51. Burning Rate Data-Composition 9	143
52. Burning Rate Data-Composition 10	144
53. Burning Rate Data-Composition 11	145

	<u>Page</u>
54. Burning Rate Data-Composition 14	146
55. Burning Rate Data-Composition 15	147
56. Burning Rate Data-Composition 16	148
57. Burning Rate Data-Composition 17	149
58. Burning Rate Data-Composition 19	150
59. Burning Rate Data-Composition 20	151
60. Burning Rate Data-Composition 21	152
61. Burning Rate Data-Composition 23	153
62. Burning Rate Data-Composition 24	154

I. INTRODUCTION

Pyrotechnic delay compositions are physical mixtures of one or more metal powders (fuel) and one or more powdered oxidizing agents. These mixtures ignite and react exothermally at a predetermined rate upon the application of heat or flame; and are characterized by high reaction temperatures, solid combustion products, and the evolution of very small quantities of gas. The oxygen necessary for combustion of the fuel is supplied by the decomposition of the oxidizing agent, thus the combustion of these compositions is not affected by the presence or lack of air.

Time delay fuzes containing pyrotechnic delay compositions loaded under pressure are used in a wide variety of military and non-military; explosive and non-explosive items, due to their simplicity of design, low cost, compactness and resistance to physical abuse. Typical of these compositions is the barium chromate-boron system used in the delay fuze of the M112A1 Photoflash Cartridge (Figure 1), which is fired from aircraft for the purpose of ground illumination during aerial photography missions. The delay fuze, (Figure 2) upon initiation by the black powder expelling charge, delays the functioning of the photoflash charge for 1, 2, or 4 seconds, depending on the intended delay interval. The black powder charge simultaneously expels the charge case



- NOTES:-
- 1-SPEC MIL-A-2550 AND MIL-C-11232 APPLY
 - 2-SEAL PRIMER IN BASE WITH SEALING COMPOSITION SURFACE OF CENTRAL ELECTRODE, FACE OF FILAMENT ASSEMBLY, SURFACE OF BASE AND INTERIOR SHOULDER OF THREADED PRIMER CAVITY MUST BE FREE FROM SEALING COMPOSITION AND ELECTRICALLY CLEAN. AFTER ASSEMBLING PRIMER TO CARTRIDGE CASE, THE CIRCUIT BETWEEN THE PRIMER AND CARTRIDGE CASE SHALL BE TESTED TO DETERMINE ELECTRICAL CONTINUITY AND RESISTANCE. RESISTANCE SHALL BE 0.25 OHM MAX TO 110 OHM MAX. (NOTE 3)
 - 3-SEALING COMPOSITION:

(E) <table border="0" style="width: 100%;"> <tr> <td style="width: 50%;">LAMINAC, NO. 4134</td> <td style="width: 50%;">EXCELINAC BUNWICH</td> </tr> <tr> <td>LUMERSON, DDM (ETHYL 57) (NOTE 7)</td> <td>96.0% ± 1.0%</td> </tr> <tr> <td>1/8" DIA. CLASS 2 SPEC MIL-F-106</td> <td>3.0% ± .25%</td> </tr> </table>	LAMINAC, NO. 4134	EXCELINAC BUNWICH	LUMERSON, DDM (ETHYL 57) (NOTE 7)	96.0% ± 1.0%	1/8" DIA. CLASS 2 SPEC MIL-F-106	3.0% ± .25%	4-PRODUCT OF AMERICAN CYANAMID CO., NEW YORK CITY, NY. (NOTE 6)
LAMINAC, NO. 4134	EXCELINAC BUNWICH						
LUMERSON, DDM (ETHYL 57) (NOTE 7)	96.0% ± 1.0%						
1/8" DIA. CLASS 2 SPEC MIL-F-106	3.0% ± .25%						
5-PRODUCT OF MONSIEUR AGENT CORP., BUFFALO, N.Y. (NOTE 6)							
6-ALL SOURCES MUST COMPLY WITH THE PHYSICAL AND FUNCTIONAL REQUIREMENTS OF THE MANUFACTURER'S TECH INDICATED. ORDNANCE CORP'S ENGINEERING APPROVAL REQUIRED.							
7-ADD CATALYST TO LAMINAC JUST PRIOR TO USE. LIFE OF MIXTURE IS APPROXIMATELY 2 HRS AT 70°F							
8-ASSEMBLY SHALL FREELY ENTER CHAMBER GAGE, 1.5708 IN DIAMETER. SHUNTING CLIP SHALL NOT BE REMOVED FOR GAGING.							
 - 9-CHARGE PROPELLING:-.350-1.5 GRAINS, POWDER, BLACK, CLASS 3, SPEC MIL-P-228. (NOTE 1)
 - 10-USE ONE OR MORE FILLERS, IF NECESSARY TO PREVENT MOVEMENT OF CHARGE CASE ASSEMBLY IN CARTRIDGE CASE.
 - 11-SEAL WITH SEALING COMPOUND TO FORM WATERTIGHT JOINT (NOTE 12, 28)
 - 12-SEALING COMPOUND:

LACQUER, TYPE II, SPEC MIL-L-10887	EXCELINAC BY WEIGHT
0.4, CAS FOR GENDEL SPEC UJ-C-86	60% ± 5%
	40% ± 5%
 - 13-36° CHAMP
 - 14-MARKS INDICATED WITH HIGH LETTERS AND FIGURES USING INK, STENCIL, BLACK NO. 3703B, SPEC TT-1-558.
 - 15-INSERT APPLICABLE DELAY TIME, WITH 1/8" HIGH FIGURE USING INK, STENCIL, BLACK NO. 3703B SPEC TT-1-558.
 - 16-INSERT LOADINGS LOT NUMBERS
 - 17-INSERT DATE, MONTH AND YEAR LOADED.
 - 18-TO BE REMOVED PRIOR TO PLACING PHOTOFLASH CARTRIDGE IN GUN.
 - 19-ASSEMBLY FLUSH TO .023 MAX BELOW FLUSH.
 - 20-MAKE WITH IMPRINT TYPE, USING INK, STENCIL, BLACK NO. 3703B, SPEC TT-F-558.
 - 21-MAX MOISTURE AT TIME OF LOADING TO BE 6.0%.
 - 22-MAX MOISTURE AT TIME OF LOADING TO BE 6.0%.
 - 23-DRY FOR 48 HOURS MIN AT 100°F MIN AT 60% RELATIVE HUMIDITY MAX AND ASSEMBLE WHILE STILL WARM. (NOTES 27, 32, 33)
 - 24-DELAY TIMES APPLY AT 80%.
 - 25-MANUFACTURING REQUIREMENTS-LOADING, ASSEMBLING AND PLACING OF PHOTOFLASH CARTRIDGES MUST BE ACCOMPLISHED IN CONTROLLED PRODUCTION AREAS OF 80% MAX RELATIVE HUMIDITY AND 90°F MAXIMUM TEMPERATURE.

- 26-SIMILAR TO PCANX 78-0-1142, 78-0-1143, AND 78-0-1144
- 27-ASSURE THAT VOLATILES HAVE BEEN THOROUGHLY REMOVED FROM THIS ASSEMBLY BEFORE INSERTING ASSEMBLY IN CARTRIDGE CASE
- 28-SEALING COMPOUND IS TO BE APPLIED ON THE SIDE OF THE SEAT CAP AND ALLOWED TO DRY 98 HRS MIN TO 96 HRS MAX AT ROOM TEMP. THEN SEAT CAP IN POSITION. SEALING COMPOUND IS NOT TO BE APPLIED BY DIPPING THE CAP INTO A CONTAINER OF THE COMPOUND. COMPOUND IS NOT TO BE APPLIED TO INSIDE SURFACE OF CARTRIDGE CASE (NOTE 32)
- 29-MAX EACH CARTRIDGE "X-RAYED" FOLLOWED BY MONTH AND YEAR OF INSPECTION IN NUMERALS APPROX 1/8" HIGH AFTER RADIOGRAPHICAL INSPECTION HAS BEEN PERFORMED
- 30-DRY FOR 16 HOURS MIN AT 100°F MIN AT 60% RELATIVE HUMIDITY MAX, AND ASSEMBLE WHILE STILL WARM
- 31-ALL WORK INVOLVING THE USE OF SOLVENTS (VOLATILES) MUST BE PERFORMED IN AN AREA REMOTE FROM ASSEMBLY OPERATIONS. THE FINAL ASSEMBLY AREA MUST BE FREE OF VOLATILES (SOLVENTS, ETC.)
- 32-PROVIDE ADEQUATE VENTILATION WHILE DRYING TO ASSURE VOLATILE REMOVAL
- 33-USE SHALLOW TRAYS WITH WIRE MESH BOTTOMS

ORDNANCE DRAWING NO.	CHARGE CASE ASSEMBLY	DELAY TIME SECONDS	ENGINEERING PARTS LIST
8848546	8848536	1.00 ± .10	8848546-1
8848546	8848537	1.00 ± .10	8848546-2
8848546	8848538	1.00 ± .10	8848546-3

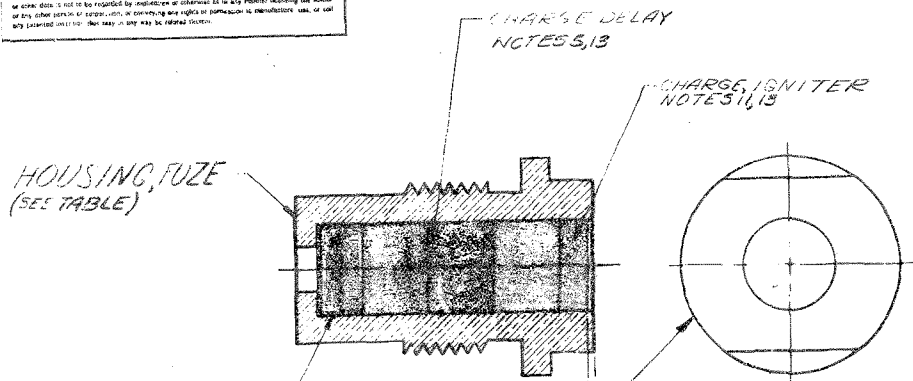
FOR LIST OF PARTS, SEE PRODUCTION PARTS LIST (SEE TABLE). (ORDNANCE PART NO. (SEE TABLE))

PARTIAL DESCRIPTION	TOLERANCES ON DIMENSIONS	FINISH	HEAT TREATMENT	PLATING	INSPECTION	REMARKS
1						
2						
3						
4						
5						
6						
7						
8						
9						
10						
11						
12						
13						
14						
15						
16						
17						
18						
19						
20						
21						
22						
23						
24						
25						
26						
27						
28						
29						
30						
31						
32						
33						
34						
35						
36						
37						
38						
39						
40						
41						
42						
43						
44						
45						
46						
47						
48						
49						
50						
51						
52						
53						
54						
55						
56						
57						
58						
59						
60						
61						
62						
63						
64						
65						
66						
67						
68						
69						
70						
71						
72						
73						
74						
75						
76						
77						
78						
79						
80						
81						
82						
83						
84						
85						
86						
87						
88						
89						
90						
91						
92						
93						
94						
95						
96						
97						
98						
99						
100						

FIGURE 1. M112A1 PHOTOFLASH CARTRIDGE ASSEMBLY- ORDNANCE DRAWING F8848546

NOTICE: When Government drawings, specifications, or other data are used for any purpose other than in connection with a definite Federal Government procurement transaction, the United States Government hereby accepts no responsibility for any alterations whatsoever and the fact that the Government may have furnished, furnished, or may have supplied the data does not constitute an acknowledgment or approval of any other person or organization, or constitute an endorsement or recommendation to manufacture, use, or sell any product or service. The user is to be held responsible.

REVISIONS			
NO.	DESCRIPTION	DATE	APPROVAL
	WAS PCMK 78-2-540A		
	78-2-540F / 78-2-540K		
	EOPA 5856	3-5-68	W. J. B. 120
A	EOPA 32215	7-10-68	W. J. B. 200
B	EOPA 34406	12-16-68	W. J. B. 200
C	EOPA-34599	5-7-65	W. J. B. 5K



STATIC FUSE TIMES (SEC) (RATIO TO FULCRUM)	ORDNANCE PART NO	HOUSING FUZE	DELAY TIME (SECONDS)	DELAY CHARGE (NOTE 5)		IGNITER CHARGE (NOTE 6)		ENGINEERING PARTS LIST
				APPROX WT (MG)	MIN WT (MG)	APPROX WT (MG)	MIN WT (MG)	
AVERAGE RANGE			NOTE 10					
.88-.90	.06-.92	8848544-1, 8848543-1	1	1800		250	150	8848544-1
		8848544-2, 8848543-2	2	2500		300	200	8848544-2
		8848544-3, 8848543-3	4	2500	1300	400	200	8848544-3

- NOTES:-
- 1-SPEC MIL-A-2550 APPLIES.
 - 2-PRIOR TO LOADING, MARK APPLICABLE DELAY TIME ON PERIPHERY OF HEAD WITH $\frac{1}{8}$ HIGH LETTERS AND FIGURES USING INK, STENCIL, BLACK NO. 37038, SPEC TT-I-558. (NOTE 3)
 - 3-IN LIEU OF STENCILING, PERIPHERY OF HEAD MAY BE STAMPED, PRIOR TO LOADING, WITH APPLICABLE DELAY TIME WITH LETTERS AND FIGURES $\frac{1}{8}$ HIGH X .01 DEEP, PROVIDED THAT THIS OPERATION DOES NOT CAUSE ANY DEFORMATION OF THE DELAY COLUMN CAVITY AND DOES NOT INTERFERE WITH SEATING OF THE FUZE.
 - 4-SEAT CUP FIRMLY AGAINST SHOULDER.
 - 5-CHARGE DELAY: APPROX (SEE TABLE) DELAY COMPOSITION. PRESS IN EQUAL INCREMENTS OF 500 MILLIGRAMS MAX AT 36,000 PSI. (NOTES 6, 10)
 - 6-DELAY COMPOSITION (NOTES 7, 15, 16, 17)
 - BARIUM CHROMATE, CLASS A, AVERAGE PARTICLE SIZE $1\frac{1}{2}$ MICRONS SPEC MIL-B-550 - - - - - 95.25% (ADVISORY) (NOTE 9)
 - BORON, SPEC PA-PD-451 - - - - - 4.75% (ADVISORY)
 - 7-THE MINIMUM PERCENT OF BORON TO BE 4.2%.
 - 8-WEIGHTS TO BE ADJUSTED TO GIVE REQUIRED DELAY TIME AND COLUMN HEIGHT.
 - 9-PARTICLE SIZE IS MEASURED WITH FISHER SIEVE SIZER AS DESCRIBED IN PICATINNY ARSENAL REPORT SERIAL NO. MR-12
 - 10-ADJUST DELAY TIME OF FUZE ASSEMBLY SO THAT REQUIRED DELAY TIME OF COMPLETE ROUND IS MET. (NOTE 15)
 - 11-CHARGE, IGNITER: APPROX (SEE TABLE) MILLIGRAMS IGNITING COMPOSITION. PRESS AT 36,000 PSI. (NOTE 12)
 - 12-IGNITING COMPOSITION: (1 SEC) (NOTES 15, 16, 17)
 - BARIUM CHROMATE, CLASS A, AVERAGE PARTICLE SIZE $1\frac{1}{2}$ MICRONS SPEC MIL-B-550 - - - - - 90-1.0% (NOTE 9)
 - BORON, SPEC PA-PD-451 - - - - - 10+1.0%
 - 13-MOISTURE CONTENT AT TIME OF LOADING TO BE 0.1% MAX.
 - 14-SIMILAR TO PCMK 78-2-540A, 78-2-540F AND 78-2-540K.
 - 15-DELAY TIMES ARE CHANGED BY ABSORPTION OF VOLATILES (INCLUDING MOISTURE) BY BOTH THE LOOSE AND PRESSED IGNITING AND DELAY COMPOSITIONS. THEY ARE ALSO AFFECTED BY TEMPERATURE CHANGES (APPROX .001 SEC/°F / SEC DELAY TIME). ADEQUATE PROCESS CONTROLS FOR THESE VARIABLES MUST BE PROVIDED DURING THE ENTIRE CARTRIDGE MANUFACTURING OPERATION.
- PERMIT COMPOSITIONS TO AGE AT 135±5°F IN OPEN CONTAINERS (APPROX 2 WEEKS) UNTIL REPRODUCIBLE STATIC FUSE TIMES ARE OBTAINED ON CONSECUTIVE DAYS THEN COOL COMPOSITION IN CLOSED CONTAINERS (ADVISORY).
- KEEP ONLY A SMALL QUANTITY OF POWDER EXPOSED TO THE AIR AT THE WEIGHING STATION.
- ADVISORY: PROTECT OPEN END OF FUZE WITH CAPPLUG TO EXCLUDE VOLATILES.

FOR LIST OF PARTS, SEE ENGINEERING PARTS LIST (SEE TABLE) ORDNANCE PART NO. (SEE TABLE)

PHYSICAL PROPERTIES	UNLESS OTHERWISE SPECIFIED	ORIGINAL DATE OF DRAWING	PICATINNY ARSENAL
YP	DIMENSIONS ARE IN INCHES	MAR 5, 68	ORDNANCE CORPS
TS	TOLERANCES ON FRACTIONS ON DECIMALS ANGLES		DEPT OF THE ARMY
ELZ	MATERIAL		DOVER, NEW JERSEY
RA	HEAT TREATMENT		
DN	FINAL PROTECTIVE FINISH		
RM			

DATE: 12-16-68
 DRAWN BY: [Signature]
 CHECKED BY: [Signature]
 SUBMITTED BY: [Signature]
 APPROVED BY: [Signature]
 UNIT WT

SCALE: 1/1

CODE IDENT NO. 19203

ENGINEERING PARTS LIST (SEE TABLE)

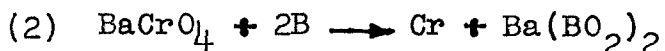
8848544

FIGURE 2. FUZE ASSEMBLY - ORDNANCE DRAWING C8848544

assembly from the cartridge case so that the flash charge will explode safely away from the aircraft after the delay composition has burned. The delay times must have little variation as the photoflash cartridges must be synchronized with the photographic equipment used.

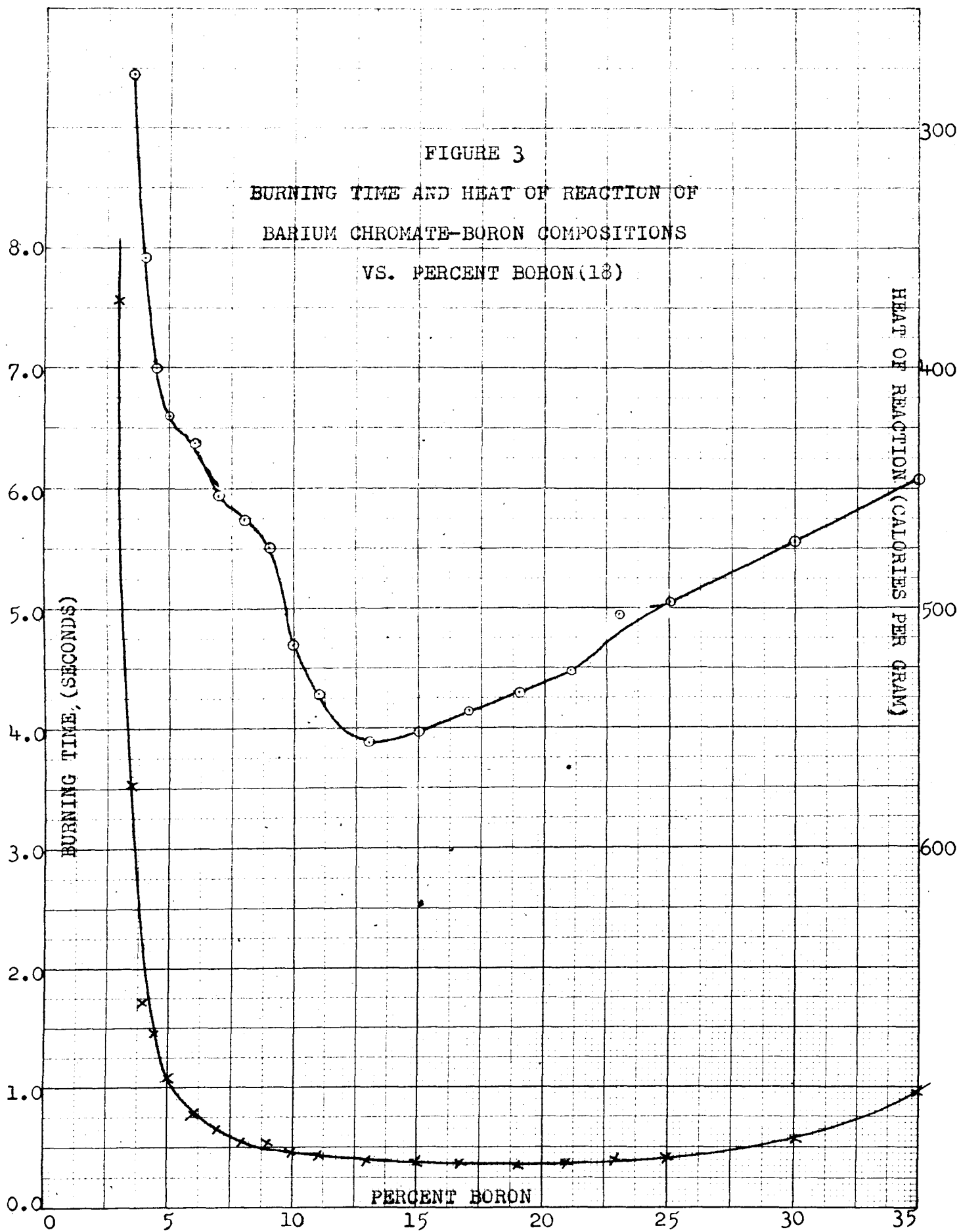
The requirements for this particular application are fulfilled by a 95/5 barium chromate-boron delay composition and a 90/10 barium chromate-boron igniter composition. The 95/5 mixture provides the proper burning rate for the desired delay time, and the 90/10 mixture provides the necessary heat to ignite the delay composition with a high degree of reliability. A graph depicting the burning time and heat of reaction as a function of composition for the barium chromate-boron system is shown in Figure 3 (18).

Barium chromate and boron react in two separate reactions:



Reaction (1) corresponds closely to the reaction of the 95/5 blend, while reaction (2) corresponds to the reaction of the 90/10 blend.

The stoichiometric compositions contain 4.09 percent boron and 7.87 percent boron, respectively, but consideration is given to the fact that boron with as low as 84 percent elemental amorphous boron is specified for use in these



compositions. A maximum of about 92 percent elemental amorphous boron is the best purity now commercially available. Amorphous boron, and not crystalline boron, is intended for use in the barium chromate-boron system because of lower ignition and burning time reproducibility encountered with crystalline boron.

Little is known at present about the mechanism of solid-solid reactions such as those under consideration. However, for reproducible burning times, ease of ignition, and propagation of burning, one of several variables that must be controlled is the particle size of the components of the composition (5, 6).

The particle size of the components is specified as the average particle diameter (hereafter referred to as APD) as determined by the Fisher Sub-Sieve Sizer (1, 3). Comyn, et al (6) show that reproducibility of burning rates of delay compositions prepared in dilute slurries is related not only to the average particle size, but to the particle size distribution of the components as well. For instance, a delay component with an acceptable APD may contain large particles which would prevent that component from blending properly with the other components of the composition and also cause the particles to segregate with handling before pressing into delay fuzes, thus causing erratic burning times of the pressed compositions. A method of specifying

the particle size distribution of the barium chromate and boron may therefore be necessary, in lieu of specifying the APD as the measure of the particle size parameter.

Thus, the particle size distribution-burning rate relationship must be investigated in two steps:

- (1) Using a suitable method for determining the particle size distribution of barium chromate and boron, compare the results of these analyses to the APD of the samples.
- (2) Determine the effect of the particle size distribution or parameters derived from the distribution on the burning rate of the delay compositions blended with various samples of barium chromate and boron.

II. EXPERIMENTAL

A. Dispersion of Barium Chromate and Boron

1. Method of dispersion. A general method of dispersing difficult-to-disperse small particle size materials was developed for both barium chromate and boron. This method, a combination of methods recommended by several investigators (6, 12, 14) is described as follows:

A 0.2 gram sample of barium chromate (or boron) to be dispersed was placed on a 4-inch watch glass and moistened with portions of 25ml of a 0.01 percent stock solution of the dispersing agent undergoing evaluation. The moistened sample was worked into a smooth paste, using a glass rod with a rubber policeman. The paste was washed through a 325 mesh (44 micron) sieve into a Waring Blendor with the remainder of the dispersing agent and sufficient water to dilute the slurry to 250 ml. The blendor was operated for three minutes to complete the dispersion of the sample.

A coarse barium chromate sample, Mineral Pigments 1357, batch 31801, was blended for an additional 4, 7, and 14 minutes, while performing a particle size analysis on the sample after each time period to ascertain that the action of the blendor had not fractured any of the particles.

2. Selection of dispersing agents. Using the method of dispersion just described, various anionic, cationic,

and nonionic surface-active agents (surfactents), (Table 1) and combinations of anionic and nonionic surfactents were evaluated as dispersing agents for barium chromate and boron. As suggested by the Mine Safety Appliances Company (14), the concentration of the surfactents was maintained at about 0.02 percent. The criteria for evaluation of the quality of dispersion were as follows:

- (1) No indication of agglomeration, either visually or under microscopic examination.
- (2) Minimum amount of sediment at the bottom of the test tube initially, after one to three hours, after one day, and after one week.
- (3) Maximum density of dispersion initially, after two to three hours, after one day, and after one week, as determined by the color of the dispersion and the transmission of a light beam through the suspension.

Of the individual surfactents, the nonionic surfactents, Tenlo 70 and Ethofat C/15, and the anionic surfactents, Tamol SN and Lomar PW, appeared to be best for dispersing barium chromate. Ethofat C/15- Lomar PW, Ethofat C/15- Tamol SN, Triton X-100- Tamol SN, and Tenlo 70- Lomar PW mixtures containing 50 percent of each surfactent produced more stable dispersions than any of the individual surfactents, with the most stable dispersion provided by the 0.01 percent Ethofat C/15- 0.01 percent Tamol SN combination.

TABLE 1

WETTING AND DISPERSING AGENTS

Trade Name	Chemical Type	Manufacturer
Nonionic		
Triton X-100	Alkyl aryl polyether (x=10) alcohol	Rohm & Haas
Ethofat C/15	Polyethoxy (x=5) ester of coco fatty acid	Armour
Ethofat O-15	Polyethoxy (x=5) ester of oleic acid	Armour
Span 60	Sorbitan monostearate	Atlas
Span 80	Sorbitan monooleate	Atlas
Tween 60	Polyoxyethylene (20) sorbitan monostearate	Atlas
Tween 80	Polyoxyethylene (20) sorbitan monooleate	Atlas
Tenlo 70	Fatty acid amides	Nopco
Brij 78	Polyoxyethylene (20) stearyl ether	Atlas
_____	Polyoxyethylene glycol (400) monolaurate	Kessler
Anionic		
Lomar PW	Sodium salt of naphthalene sulfonic acid	J. Wolf
Nopcosant. L	_____	Nopco
Tamol SN	Sodium salt of condensed aryl sulfonic acid	Rohm & Haas
Tamol 850	_____	Rohm & Haas
Cationic		
Bromat	Cetyl trimethyl ammonium chloride	Fine Organics
Dibactol	Dimethyl benzyl higher alkyl ammonium chloride	Fine Organics

Preliminary evaluation of individual surfactents for dispersing boron indicated that the best nonionic-anionic combination was Triton X-100 and Tamol 850. Boron was found to be much more difficult to disperse, and to keep dispersed, than barium chromate. This was overcome by adding a small quantity of ammonium hydroxide to the surfactent combination and by increasing the concentration of the Tamol 850 from 0.01 percent to 0.20 percent. Ultimately, an aqueous solution containing 0.01 percent Triton X-100, 0.20 percent Tamol 850, and 0.08 percent ammonium hydroxide provided the most stable dispersions of boron samples.

B. Use of the Mine Safety Appliances (MSA) Particle Size Analyzer

1. Equipment and procedure. The Mine Safety Appliances (MSA) Particle Size Analyzer was selected as the most suitable equipment for analysis of materials smaller than 0.5 micron in size, as was anticipated for the barium chromate and boron under investigation. Illustrations of this equipment are shown in Figures 4 to 6. The general description of the use of this equipment can be found in "MSA Particle Size Analyzer-Operating Procedures and Applications" (14).

The layer sedimentation technique was used in the analytical procedure, so that all settling particles would travel the same verticle distance during sedimentation, providing an undistorted particle size distribution. This method involved placing a thin



FIGURE 4. FEEDING CHAMBER AND CENTRIFUGE TUBE
Tube has been filled with ink to show inside contour.
Note the line at top of the ink level, to which
sedimentation liquid has been filled.



FIGURE 5. CENTRIFUGE TUBES
DURING ANALYSIS RUN

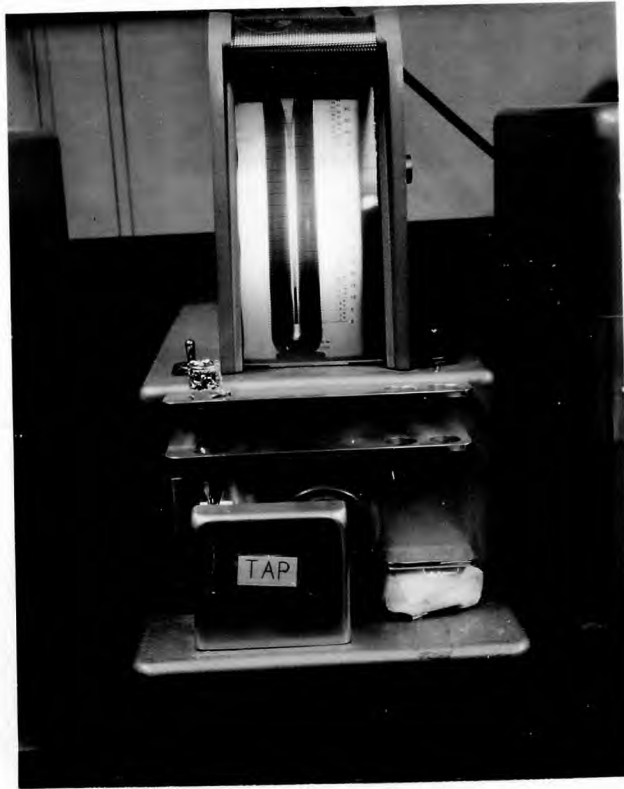


FIGURE 6. CENTRIFUGE TUBE IN PROJECTOR
FOR READING OF SEDIMENT HEIGHT

layer of feeding liquid containing the sample being analyzed on top of the sedimentation liquid in the centrifuge tube. This required the feeding liquid to be approximately 10 percent less dense, 50 percent more viscous, and also miscible with the sedimentation liquid. The feeding and sedimentation liquids must also be excellent dispersants for the samples to be analyzed. The sedimentation liquid was selected during the investigation of the dispersion methods as distilled water containing 0.01 percent - 0.02 percent Ethofat C/15 and 0.01 percent - 0.20 percent Tamol SN. In order to maintain the density and viscosity of the liquid constant, the temperature of the analysis room was maintained at $77 \pm 1^{\circ}\text{F}$ by regulating the air conditioner and steam heat supply. The dispersing properties of ethanol with the proper surfactents were known, as this liquid had been included in the evaluation of dispersing agents for the barium chromate. Thus a 50 percent aqueous solution of ethanol (with surface-active agents) was selected as the feeding liquid.

Selection of the proper feeding liquid has to be accomplished before proceeding with the analyses. Pure liquids that met all the requirements set forth for the feeding liquids were not available, consequently mixtures were investigated. The ethanol-water system provided the greatest promise because of a maximum on the viscosity-composition curve resulting in a viscosity of 2.38 centipoises at 77°F

and 50 percent ethanol by volume, rather than 1.05 centipoise if the system had behaved as an ideal liquid. The density of this mixture is 0.93 grams per cc. These values compare satisfactorily to the criteria that the viscosity be about 50 percent greater than that of the sedimentation liquid, or 1.5 centipoise, minimum, and that the density be about 10 percent lower than that of the sedimentation liquid, or 0.90 grams per cc.

The centrifuge time reading schedule was determined for the barium chromate-water system, starting with Stokes' Law, previously expressed by the equation:

$$t = 18.37 \times 10^8 \mu_0 h / (\Delta \rho) g d^2. \quad (1)$$

Equation (1) reduces to $t = K_g h \cdot 10^2 / g d^2$, where

$$K_g = 18.37 \times 10^6 \mu_0 / (\Delta \rho).$$

For the centrifuge tubes being used, $h = 10$ cm., thus

$$t = K_g \cdot 10 \cdot 10^2 / 980 d^2, \text{ or } t = K_g \cdot 10^3 / 980 d^2. \quad (2)$$

Rounding off, equation (2) becomes: $t = K_g / d^2$, which applies for gravity settling only.

For sedimentation under the influence of centrifugal force, $K_s = K_{\text{cent}} K_g$, where K_{cent} is a constant for the centrifuge being used and s indicates the centrifuge speed in RPM. In turn, $t_s = (1.394/d^2) K_s \dots \dots (3)$. The complete centrifuge time reading schedule for the barium chromate-water system was then calculated, using equation (3).

(Table 2).

TABLE 2

READING SCHEDULE FOR ANALYSIS OF BARIUM CHROMATE

Particle Size (microns)	Centrifuge Speed (RPM)	Reading Time (min:sec)	Sediment Height
20	300	:16	
10		:49	
7		1:08	
5	600	:41	
3		2:05	
2.5		1:28	
2.0		2:36	
1.5	1200	1:29	
1.0		3:55	
0.9		1:45	
0.7	1800	2:56	
0.5		6:26	
0.4		7:17	
0.3		15:14	
0.2	3600	11:04	
0.1		57:09	

It was recommended (14) that the concentration of the barium chromate be high enough to almost fill the capillary tube with settled barium chromate at the conclusion of an analysis run. However, the 0.75 mm centrifuge tubes required so high a concentration of barium chromate in order to obtain a reasonable sediment height in the capillary, that the particles re-agglomerated in the narrowing section of the tube just above the capillary. Substitution of 0.5 mm tubes for the 0.75 mm tubes decreased the necessary concentration of barium chromate by 50 percent, to about 0.7 percent, resulting in the elimination of the tendency of the barium chromate to agglomerate.

After the barium chromate was dispersed as previously described, a medicine-dropper-full was quickly removed from the Waring Blendor and placed in the feeding chamber, which was transferred to a centrifuge tube filled to the bottom of the feeding chamber with sedimentation liquid. The feeding chamber was then removed, leaving a sharp layer of feeding liquid containing the dispersed sample on top of the sedimentation liquid.

Although the tubes were cleaned, gravity settling resulted in barium chromate particles coming to rest on the sloping portion of the sedimentation tube. Upon spinning the tube in the 300 RPM centrifuge for even a few seconds, this material

settled into the capillary. It was concluded that the normal friction between the sloping wall of the tube and the tiny particles was too great to be overcome by gravity. Gravity settling was thus dispensed with and replaced by short, carefully-timed runs with 300 RPM centrifuge. The centrifuge tube was transferred, in turn, to the 600/1200, 1800, and 3600 RPM centrifuges for sedimentation runs, as per the schedule in Table 2. After each run the tube was placed in the projector and the height of the sediment was read.

A constantly re-occurring problem during the analyses was the fouling of the capillary bore with lint and other foreign matters. In order to eliminate this, the following steps were taken:

- (1) All solutions were filtered with membrane filters and kept covered.
- (2) Centrifuge tubes were covered with aluminum foil during analysis of a sample.
- (3) Ethofat C/15 solutions were prepared fresh daily because of the apparent hydrolysis of the surfactent, forming a solid residue.
- (4) Centrifuge tubes with the sedimentation liquid were pre-centrifuged at 3600 RPM for at least one minute to ascertain that there was no dust or lint in the tube.

Distilled water (with surfactents) was used as the sedimentation liquid for boron even though the expected fine

particles (less than 0.1 micron particle size) would require an excessively long time for analysis because:

(1) Considerable numbers of large particles (greater than 20 microns) were anticipated for most of the borons and any "lighter" liquid would have resulted in initial sedimentation at too high a rate.

(2) A degree of familiarity had been gained with the water: ethanol-water system used for barium chromate analyses. Thus, 50 percent aqueous ethanol was again used as the feeding liquid. The centrifuge time reading schedule for the analysis of boron is shown in Table 3.

Most of the technique developed for the barium chromate particle size analyses was applicable to the analysis of the boron samples. However, boron re-agglomerated much more readily than barium chromate, requiring several corrective measures:

(1) Because of the lower density of boron, the sample size was reduced to 0.6 grams per 250 ml of feeding liquid. This resulted in filling the capillary tube to about 40 to 60 percent of the total height. However, in order to counter the readiness of the boron to re-agglomerate, the sample size was cut to 0.35 grams for the most dense boron, and to 0.15 grams for the least dense boron.

(2) The dispersing power of the surfactant was increased by increasing the concentration of the dispersing agent. The concentration of the surfactant used was 0.01 percent Triton X-100,

TABLE 3

READING SCHEDULE FOR ANALYSIS OF BORON

Particle Size (microns)	Centrifuge Speed (RPM)	Reading Time min:sec	Sediment Height
20	300	:43	
10		2:09	
5	600	2:19	
2	1200	3:57	
1.0	1800	6:29	
0.8		5:01	
0.6		10:09	
0.4	3600	7:35	
0.3		10:22	
0.2		27:37	
0.16		30:09	
0.12		59:21	
0.10		59:21	

0.20 percent Tamol 850, and 0.08 percent ammonium hydroxide.

Several of the boron samples contained gritty material that would not pass through the 325 mesh sieve during the dispersion of the samples. This material appeared to consist of discrete particles, and thus was washed into the blender for inclusion in the ensuing particle size analyses.

2. Results. Tables 15 through 24 present the data obtained from the particle size analyses of the barium chromate and boron samples. The particle size distribution, expressed as "percent greater than particle size-d" was calculated and tabulated on the same tables. The particle size distribution curve for each sample of barium chromate and boron (Figures 27 through 36) was drawn on three-cycle log-probability graph paper, with "particle size-d" plotted on the logarithmic scale from 0.1 micron to 100 microns, and "percent greater than particle size-d" plotted on the probability scale from 0.01 percent to 99.99 percent. As no experimental points were obtained beyond the one percent point, the particle size distribution line (or curve) was extrapolated out to the 0.01 percent point.

The particle size curves for the three boron samples containing + 325 mesh (greater than 44 microns) particles were extrapolated toward the intercept at a point greater than 44 microns particle size. All other curves (or lines)

were extrapolated toward the intercept at a point less than 44 microns particle size.

These curves (Figures 27 to 36) provided the data (Tables 25 to 42) for drawing the size-frequency curves (weight percent in particle size class vs. particle size-d)(Figures 37 to 46).

C. Preparation of Delay Composition and Fuzes

1. Selection of barium chromate and boron samples. In order to determine the effect of particle size and particle size distribution on the burning rate of barium chromate-boron delay compositions, all other variables must be held constant. This may be accomplished in two ways:

- (1) By using a number of samples that have been synthesized from one process, by one manufacturer.
- (2) By starting with a sample having a wide particle size distribution, and separating the sample into fractions of various particle sizes.

Assuming that there would be little difference in the nature of impurities or other characteristics on a batch-to-batch basis, samples of barium chromate were obtained from Mineral Pigments Corporation, J.T. Baker Chemical Company, and Barium and Chemicals Company, while samples of boron were obtained from American Potash and Chemical Company, Shieldalloy Corporation, and United Minerals and Chemicals Corporation. These samples were classified according to APD as determined by the Fisher Sub-Sieve Sizer. The average particle sizes

ranged from 0.7 micron to 2.6 microns for the barium chromate, and from 0.5 micron to 2.4 microns for the boron (Table 4).

It was theorized that by separating one sample into particle size fractions, the purity of the fractions should be identical and the only variable would be particle size. Separation of a sample by sieving using micromesh sieves, filtration using millipore porous membrane filters, air elutriation of a fluidized bed, and fractionation by liquid sedimentation was evaluated. The only method which offered promise of a separation was the liquid sedimentation method. Although a rough separation of a barium chromate sample was obtained (MP28303, with an APD of 1.3 micron, was separated into 1.1 micron and 1.9 micron fractions) this method was found to be impractical because sedimentation of the fine particles required a long time to separate and purify the sample, as well as the necessity for handling large amounts of liquid by virtue of the dilute slurries that must be used to prevent premature agglomeration of the dispersed particles.

Because of limited time and facilities, this endeavor was re-appraised and it was decided to use instead the commercial samples, unaltered, for this study. Use of the commercial barium chromate and boron samples meant that factors other than particle size, such as purity and density, had to be considered when determining burning rate correlations, thus chemical analyses of these samples were performed (Tables 5 and 6).

TABLE 4

FISHER APD FOR BARIUM CHROMATE AND BORON SAMPLES

Lot Designation	Fisher APD (microns)
Barium Chromate	
MP 1357-B28303	1.3
MP 1355-B28511	0.9
MP 1358-B32500	2.1
MP 1357-B25160	0.8
MP 1357-B31801	2.6
MP 1355-B30701	0.7
BAKER 26428	1.1
BAKER 30388	0.9
BAKER 25894	1.1
BAKER 91104	0.8
B&C FINE	1.1
BORON	
UMC 1992	2.4
UMC 1993	1.75
TRONA 571	0.7
TRONA 419	0.75
HCST 873	1.0
HCST 900	0.6
HCST 954	0.5

TABLE 5

CHEMICAL ANALYSES OF BARIUM CHROMATE SAMPLES

Lot Designation	Purity (%)	Sulfate (%)	Chloride (%)	Volatile matter at 100°C (%)	Water soluble matter (%)	Loss on ignition at 900°C (%)	Bulk density (gm/cc)
MP 1357- B28303	99.0	0.28	0.00	0.00	0.01	0.14	0.49
BAKER 26428	99.5	0.02	0.00	0.00	0.00	0.00	—
BAKER 30388	99.6	0.04	0.00	0.00	0.00	0.01	0.68
MP 1355- B28511	98.4	0.13	0.06	0.03	0.08	0.64	0.66
MP 1358- B32500	99.0	0.23	0.03	0.00	0.11	0.40	0.75
BAKER 25894	99.9	0.02	0.00	0.00	0.01	0.00	0.57
MP 1357- B25160	98.7	0.32	0.01	0.04	0.01	0.51	0.51
B&C FINE	98.1	0.04	0.02	0.00	0.05	0.41	0.37
MP 1357- B31801	99.1	0.16	0.00	0.00	0.00	0.55	0.88
BAKER 91104	99.2	0.05	0.00	0.03	0.00	0.29	0.50
MP 1355- B30701	98.6	0.20	0.06	0.04	0.02	0.72	0.50

TABLE 6

CHEMICAL ANALYSES OF BORON SAMPLES

Lot Designation	Amorphous boron (%)	Moisture (%)	Total boron (%)	Insoluble matter (%)	Magnesium (%)	Bulk density (gm/cc)
TRONA 571	87.5	0.92	90.9	0.5	3.6	0.21
TRONA 419	84.3	1.99	86.3	0.0	4.9	0.17
HCST 873	84.5	0.80	87.4	4.9	0.5	0.36
HCST 900	81.9	2.48	86.9	0.5	0.6	0.15
HCST 954	86.3	2.42	87.6	0.0	0.1	0.12
UMC 1992	69.7	0.53	91.2	22.6	0.0	0.34
UMC 1993	61.4	0.68	87.5	32.3	0.1	0.28

2. Blending of Compositions. Eleven samples of barium chromate and seven samples of boron were used in the preparation of twenty delay compositions.

Boron is a hygroscopic material, being capable of absorbing 2.55 percent moisture at 30 percent relative humidity and 5.88 percent absorption at 70 percent relative humidity. In order to minimize absorption of boron and yet facilitate manufacture, all blending and loading operations involving barium chromate-boron delay compositions are generally performed under controlled atmosphere conditions of 40 percent maximum relative humidity. The relative humidity was actually maintained between 17 and 30 percent during blending of the compositions used in this study.

The barium chromate and boron were dried in a circulating forced air oven at 135° - 145°F for 16 hours, minimum, and then allowed to cool to room temperature in sealed containers. The barium chromate was passed through a 40 mesh sieve to break up small lumps, preparatory to the blending operation.

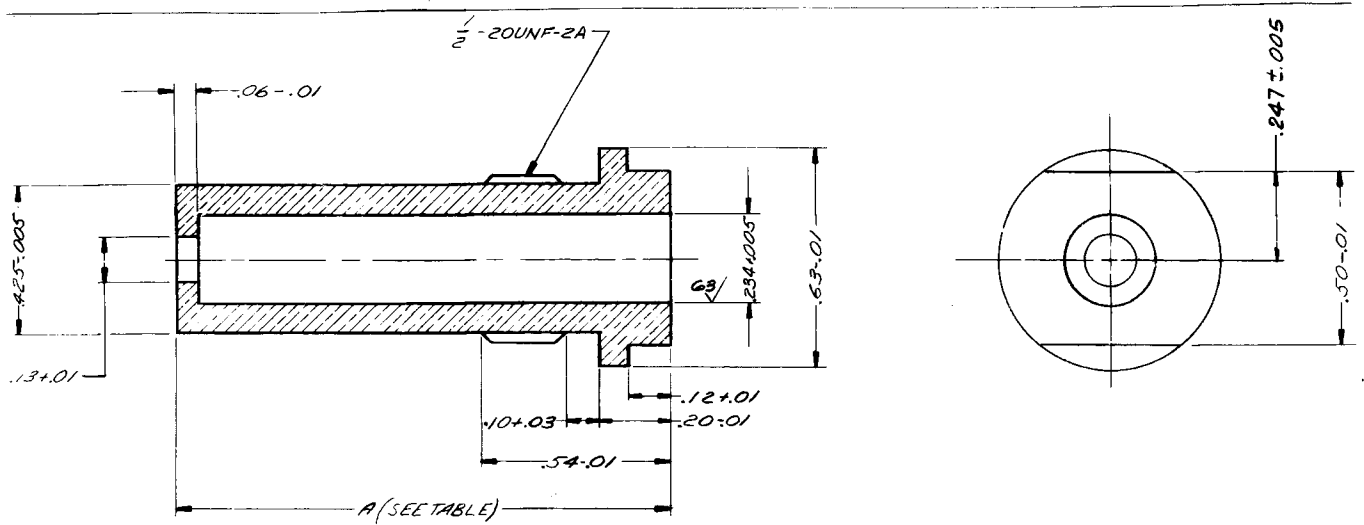
A mixture of 166.7 grams barium chromate, 8.3 grams boron, and approximately 75 ml anhydrous, 99 percent ethanol was blended in a polyethylene cup, using a rubber spatula, until uniform and dry enough for screening. The partially dry composition was then passed through a 40 mesh sieve and air dried until no ethanol vapors could be detected, followed by further drying at 135° - 145° F for 16 hours, minimum, in a circulating forced air oven. The hot, dried composition was

then sealed into a rubber powder container and allowed to stand for a minimum of three weeks before being pressed into delay fuzes.

So that all 20 compositions would have the same blending history, this series of operations was followed without deviation for each composition. These compositions are listed in Table 7.

3. Loading of Delay Fuzes. The delay compositions were loaded into one-second delay housings - Ordnance drawing C8848543 (Figure 7), in accordance with Ordnance drawing C8848544, titled "Fuze Assembly" (Figure 2), with modifications as specified below. All fuze housings were dried at 130^oF for two hours and cooled down to room temperature before being loaded with delay composition.

A fuze housing was placed in the loading fixture (Figure 8) which was then positioned in the Four-Ton Dennison Multi-Press (Figure 9). The loading pressure was set at 36,000 psi. Four equal increments of delay powder ranging from 490 to 575 milligrams and one - 100 milligram increment of 81/19 igniter powder were pressed into the fuze housing with the intention of determining the amount of delay powder that should be loaded per increment, for each delay composition, so as to obtain the longest burning time possible for the complete fuze. Once the proper amount of delay powder was determined (Table 7).



ORDNANCE PART NO.	DIM A	DELAY TIME (SECONDS)
8848543-1	.945-.010	1
8848543-2	1.455±.010	2
8848543-3	1.785-.010	4

- NOTES:-
- 1- SPEC MIL-A-2550 APPLIES.
 - (A) 2- MATERIAL:- FREE CUTTING BRASS ROD, HALF HARD, ASTM B16.
 - 3- SIMILAR TO PCMK 78-2-540M & 78-2-540W.

FIGURE 7. DELAY FUZE HOUSING - FROM ORDNANCE DRAWING C8848543



FIGURE 8. FUZE HOUSING AND LOADING FIXTURE ASSEMBLY



FIGURE 9. DENNISON
FOUR-TON MULTI-PRESS

TABLE 7
SUMMARY OF DELAY COMPOSITIONS

Composition	Barium Chromate Lot	Boron Lot
1	BAKER 30388	TRONA 571
2	MP 1357-B28303	"
3	MP 1355-B30701	"
4	BAKER 91104	"
5	BAKER 26428	"
6	MP 1358-B32500	"
7	B&C FINE	"
8	BAKER 25894	"
9	MP 1355-B28511	"
10	MP 1357-B31801	"
11	MP 1357-B25160	"
14	BAKER 30388	HCST 954
15	"	HCST 873
16	"	UMC 1992
17	"	UMC 1993
19	"	TRONA 419
20	"	HCST 900
21	MP 1355-B30701	HCST 954
23	MP 1358-B31801	UMC 1992
24	MP 1358-B31801	HCST 954

25 delay fuzes were loaded. To aid in proper consolidation a two second minimum dwell time on each increment was used during the pressing operation. As the powder, by virtue of its boron content, was hygroscopic, care had to be taken when weighing and pressing the powder, in order to prevent unnecessary exposure of the powder to atmospheric moisture. This was accomplished by removing such small portions of powder from the main sealed container that the duration of time between removal from the container, weighing the increments, and pressing did not exceed ten minutes. Also, the relative humidity was maintained below 30 percent. In order to calculate the burning rate of the composition in each fuze, the depth of powder was measured with a depth micrometer before and after loading the igniter increment (Tables 43 to 62).

The completed fuzes, after marking and measuring, were sealed into powder cans containing dessicant bags, and held until required for burning rate testing.

D. Burning Rate Testing

1. Equipment. Figure 10 shows the equipment set-up used for the burning rate determinations. The components included a starter circuit, a delay-relay circuit, a twenty-four volt source (two-twelve volt storage batteries connected in series), a chronograph and the test fixture.

The test fixture (Figure 11), was a steel box with an opening at the top for insertion of the delay fuze. In

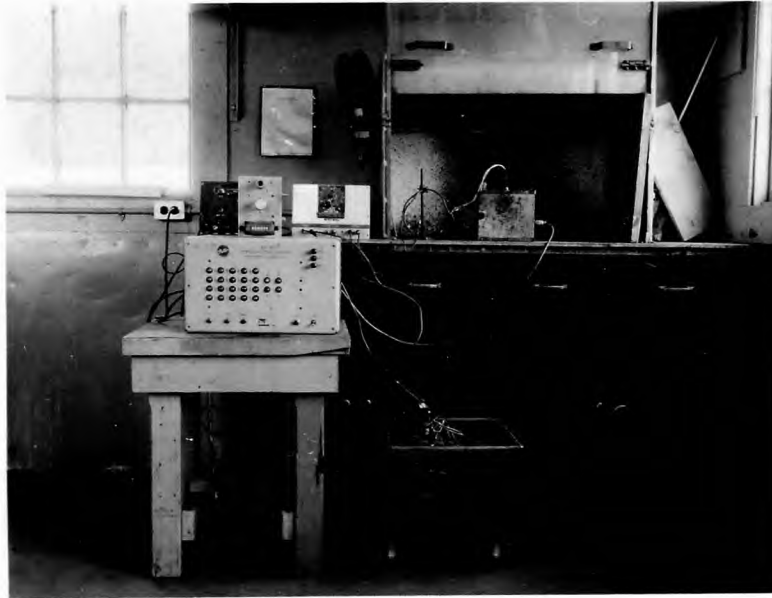


FIGURE 10. BURNING RATE TESTING EQUIPMENT

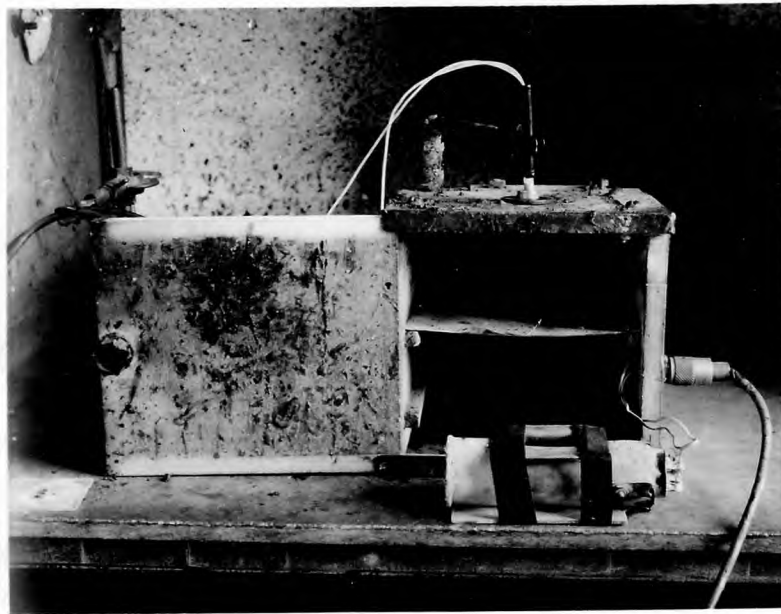


FIGURE 11. DETAILS OF TEST FIXTURE, SHOWING PHOTOCELL, FUZE IN TOP OF BOX, 90/10 SQUIB, AND LEDGE FOR PLACING PHOTOCELL

addition it contained a photocell to pick up the light as the delay burned through, thus sending a signal to stop the chronograph. The purpose of the removable shelf was to allow the photocell to be placed close to delay fuzes that would not emit enough light to energize the photocell from a greater distance. An adapter washer prevented light from leaking around the fuze in the box, causing premature activation of the photocell. A light-proof sliding door was located on the front of the box for servicing the photocell.

The fuze was ignited by a 90/10 electric squib (Figure 12), which was in turn initiated by a pulse from the battery. The starter switch simultaneously started the chronograph and sent a pulse to the squib. The squib, containing 70 milligrams of 90/10 barium chromate-boron igniter powder, ignited the 81/19 barium chromate-boron first-fire charge in the delay fuze, which in turn generated enough heat after burning to ignite the delay composition.

The chronograph used was a model 456 - 1.6 Megacycle Counter Chronograph, manufactured by the Potter Instrument Company. An auxiliary timer was connected to the chronograph to indicate time in multiples of whole seconds of burning time, while the chronograph indicated the decimal part of the burning time.

2. Procedure. With the photocell on the top shelf in the test box and the front door closed, the fuze to be tested was placed in the fuze insert of the box. A 90/10 squib was

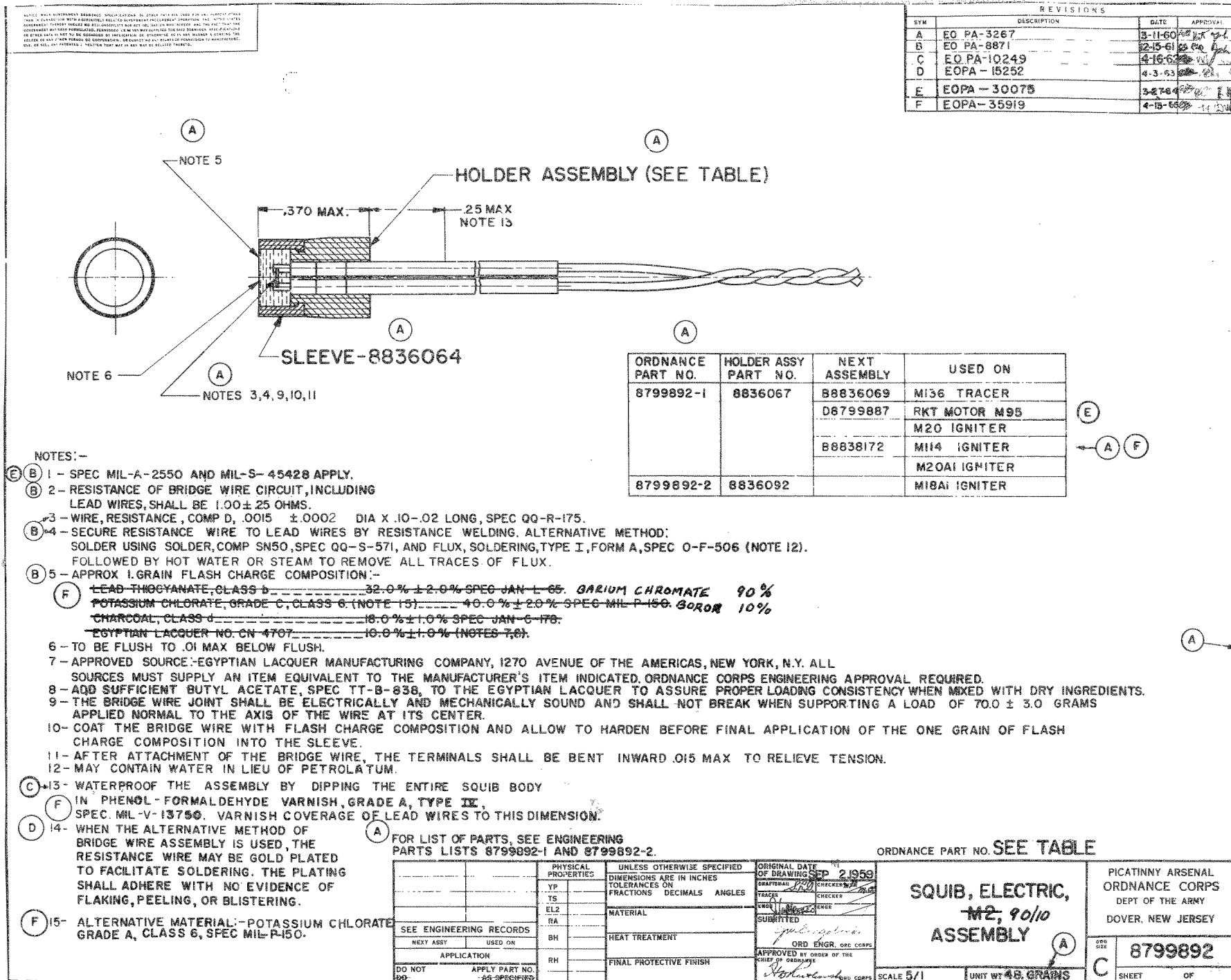


FIGURE 12. 90/10 SQUIB ASSEMBLY - MODIFIED ORDNANCE
DRAWING C8879892

connected into the ignition circuit and positioned above the delay fuze so that it was close to, but did not touch the fuze. The chronograph and auxiliary timer were re-set at zero time and a safety jack was plugged into the delay-relay circuit to complete the circuit. The starter switch was closed, energizing the timing and ignition circuits. After reading the burning time of the fuze from the chronograph and the second timer, the safety jack was removed, breaking the continuity of the circuit. After all the fuzes were burned, ten 90/10 squibs were ignited to determine the squib burning time contribution to the total burning time. In addition, the burning time of ten fuzes loaded with 500 mg of 81/19 igniter composition was tested to determine the burning rate of the igniter composition, thereby permitting the calculation of the igniter burning time contribution to the total burning time.

3. Results. Tables 43 to 62 present the burning rate test data for the 20 compositions tested, along with the depth of the delay and igniter compositions.

III. DISCUSSION

A. Dispersion of Barium Chromate and Boron

The most time consuming phase of this study was the evaluation of dispersing methods and agents for barium chromate and boron; and also the dispersion of the samples being analyzed for particle size distribution. Improper or inadequate dispersion of the samples would have led to erroneous results for the particle size analyses, thus affecting the final correlations of particle size of the components and the burning rate of the compositions. The need for proper dispersion is increased by the reported tendency of particles smaller than five microns to re-agglomerate after being dispersed (4, 6, 7); this tendency becoming greater as the particle size decreases.

Several investigators (7, 12, 14) had recommended the use of a Waring Blendor for dispersing extremely fine powders. Before adopting the use of a Waring Blendor, the question of the fracture of discrete particles as a result of the violent action of the blendor had to be considered. Cadle (4) found that it was difficult to break up particles smaller than 15 microns by any mechanical means. Since most particles of the samples under consideration were smaller than 15 microns, attrition of discrete particles was not considered to occur. To support this, particle size analyses of Mineral Pigments 1357, batch 31801 barium chromate, containing 35 percent of

greater than 15 micron particles, which was blended for 3, 7, 10, and 17 minutes, indicated no change in the concentration of coarse particles as the blending time increased.

Although development of a suitable method of dispersion resulted in a high degree of dispersion, the selection of an optimum surfactent (or combination of surfactents) was necessary, mainly to prevent re-agglomeration of the dispersed sample while settling.

Nonionic surfactents, such as Ethofat C/15, Triton X-100, and Tenlo 70, owe their dispersing power to their ability to "wet" the particles to be dispersed by reducing the surface tension of water from 72 dynes /cm² to 25-35 dynes/ cm². Anionic surfactents such as Tamol SN, Tamol 850, and Lomar PW do not significantly reduce the surface tension and thus "wet" the particles, but disperse them by placing a negative charge on each particle, causing the particles to repel each other. Since the wetting of the particles is an important preliminary step toward preparing a stable dispersion, 50:50 mixtures of nonionic and anionic surfactents were evaluated. As expected, the 0.01 percent Ethofat C/15 - 0.01 percent Tamol SN combination was thus selected as the dispersant for the barium chromate. Boron exhibited a greater tendency to re-agglomerate than did barium chromate so that it was necessary to increase the dispersing power of the surfactent

solution for the preparation of boron dispersions. This was achieved by increasing the concentration of the anionic surfactent from 0.01 percent to 0.20 percent and by adding dilute ammonium hydroxide to the surfactent mixture.

B. Evaluation of Particle Size Analysis Equipment

The specifications for both barium chromate (MIL-B-550A) (1) and boron (PA-PD-451) (3) specify that the APD shall be $1\frac{1}{2}$ micron and 1.0 micron maximum, respectively, as determined with the Fisher Sub-Sieve Sizer. This apparatus measures the flow rate of air through a powder bed under a controlled pressure differential, and automatically relates the flow rate to an average particle size of the sample with the aid of a calculator chart attached to the instrument (Figure 13).

The practice of using the Fisher Sub-Sieve Sizer for particle size analysis of barium chromate and boron is felt to be erroneous for the following reasons:

- (1) The desired APD is at or below the lower limit of usefulness of the Fisher Sub-Sieve Sizer.
- (2) The value obtained is an average particle diameter and does not indicate the particle size distribution which could vary, depending on the manufacturing process.
- (3) Since the APD is based on the total surface area, the reading will be biased toward a low APD, as the smaller particles with a large surface area will have a dispro-

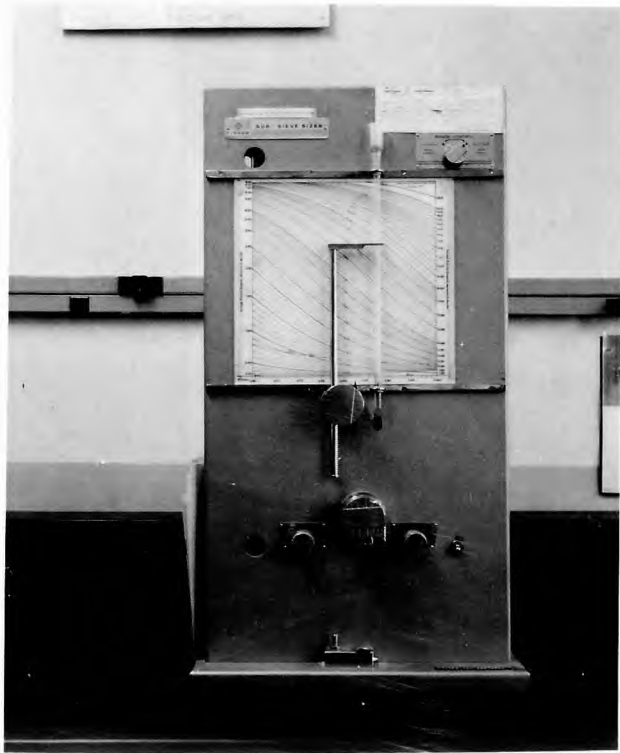


FIGURE 13. FISHER SUB-SIEVE SIZER

portionately large effect on the total surface area.

(4) The Fisher Sub-Sieve Sizer might also be expected to be inadequate for the determination of the APD of a sample with a multi-modal distribution in the one micron size range, as the instrument would be sensitive to the APD of the smallest particle size mode of the sample.

Because of the shortcomings of the Fisher Sub-Sieve Sizer and the values obtained from its use, a more suitable method of particle size analysis was deemed necessary. As the value of an average particle size is questionable, the evaluation of particle size analysis equipment was limited to particle size distribution analyzers.

Table 8 summarizes the methods of analysis of particle size distribution commonly used. Of these, sieving and gas sedimentation are immediately discarded as the anticipated particle size range of barium chromate and boron is below the normal particle size range that can be analyzed by these methods.

Microscopic examination has the advantage of being the most direct method of absolute particle size determination. The method involves the dispersion of a very small portion of the sample and mounting it on a slide or a grid, depending on whether an optical or electron microscope was being used.

As an electron microscope was not available, further

TABLE 8

METHODS OF ANALYSIS OF PARTICLE SIZE DISTRIBUTION

Method	Equipment Required	Normal Size Range (microns)
Sieving	U. S. Standard Sieves	44 - 2000
	Electroformed sieves	5 - 40
Gas Sedimentation	Sharples Micromerograph	5 - 200
Change in electrostatic resistivity	Coulter Counter	0.5 - 100
Microscopy	Optical microscope, using visible light	0.2 - 100
	Electron microscope	0.001 - 5
Liquid sedimentation	a. Gravitational Eagle-Picher Turbidimeter	0.5 - 300
	b. Centrifugal Mine Safety Appliances (MSA) Particle Size Analyzer	0.05 - 50

This apparatus (15), which utilizes the principle of gravitational sedimentation, consists of a condensed light source, a rectangular sedimentation cell, and a photocell and microammeter for measuring the transmitted light. A dilute (approximately 0.02 percent) dispersion of the sample being analyzed is placed in the sedimentation cell and allowed to settle. It is assumed that the particles act as spheres, both when settling and when absorbing light. The rate of settling is in accordance with Stokes' Law, given by the equation:

$$t = 18.37 \times 10^8 \mu_0 h / (\Delta \rho) g d^2, \text{ where}$$

μ_0 = absolute viscosity of the sedimentation liquid—poise

t = time in seconds to settle distance h

$(\Delta \rho)$ = difference in density between sedimentation liquid and settling particles—gm/cm³

d = particle diameter—micron

g = gravitational constant—980 cm/sec²

The particle size distribution is thus a function of the change in concentration of the suspension at a definite level below the surface with time, as measured with a light beam passing through the suspension and energizing the photocell. The lower limit of usefulness of this method is about 0.5 microns, requiring several hours to reach this point.

The Coulter Counter measures the change in resistance of an electrically conductive liquid in an orifice as particles in suspension pass through the orifice and displace

consideration could not be given to this equipment, even though it would be capable of indicating particles as small as 0.001 microns. Another draw-back would be the extreme tediousness of measuring a sufficient number of particles to obtain a distribution curve.

A Bausch and Lomb Research Metallograph was available for particle size analysis (Figure 14). This instrument is theoretically capable of 2000 x magnification and a limit of resolution of 0.20 micron. However, due to the wave length of ordinary white light and the diffraction of light around small particles, the actual limit of resolution is about 0.5 micron or higher, thus the smaller particles would not be included in the analysis. Also, as with electron microscopy, the use of the optical microscope is very time-consuming. Photographing the sample, followed by measuring and counting the particles appears to be a simple operation, however, photographs taken at 2000x magnification were of a very poor quality and could not be used for analytical purposes. Because of the very short depth of focus at this magnification, particles larger than 2 microns would be out of focus when measuring the smallest particles, thus the focus must be continually adjusted when analyzing a sample.

Comyn, et al (5) has recommended the use of the Eagle-Picher Turbidimeter for obtaining the particle size distribution of components of delay powders.

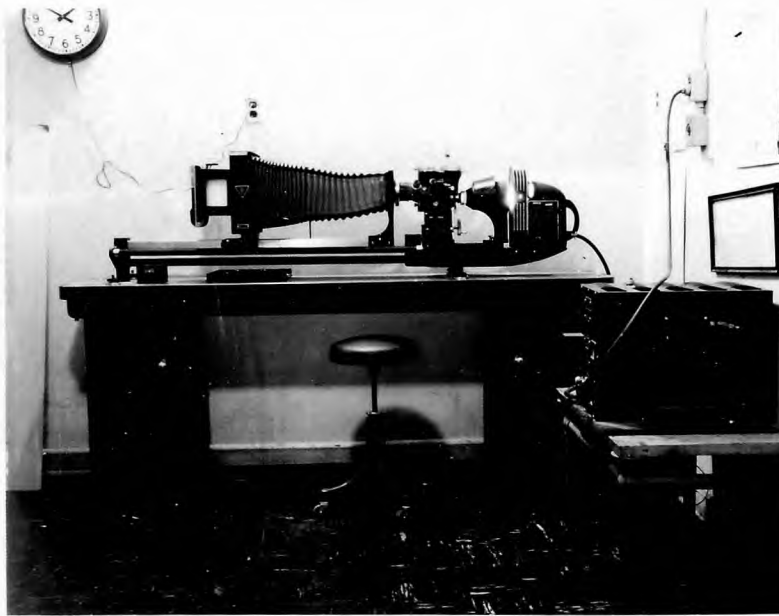


FIGURE 14. BAUSCH AND LOMB RESEARCH METALLOGRAPH

an equal volume of electrolyte while settling in accordance with Stokes' Law, thus producing a voltage pulse proportional to the particle volume. The instrument is intended for analysis of particles as small as 0.5 micron, however, several investigators (9, 13) have reported that the Coulter Counter produced results which indicated that analyzed samples were two to three times coarser than when analyzed by sedimentation or microscopy.

The Mine Safety Appliances (MSA) Particle Size Analyzer, a recent introduction to the particle size analysis field, consists of four constant speed centrifuges (300 RPM, 600/1200 RPM, 1800 RPM, and 3600 RPM) and other accessory equipment (Figure 15). The operational principal is Stokes' Law liquid sedimentation, with the rate of settling augmented by centrifugal force. This method brings the analysis of particles as small as 0.1 micron within the range of practicability, as well as decreasing considerably the time necessary to perform particle size analyses of other, larger materials. The centrifuges have been specifically designed for particle size analysis and have the following special features:

- (1) Constant speed obtained through the use of high quality hysteresis type synchronous motors.
- (2) Stable starting and stopping characteristics, including a maximum rate of acceleration of five radians per second.
- (3) Ability to be stopped and started by an interval timer.

The particle size distribution data can be obtained by placing the sample in the centrifuge tube filled with the sedimentation

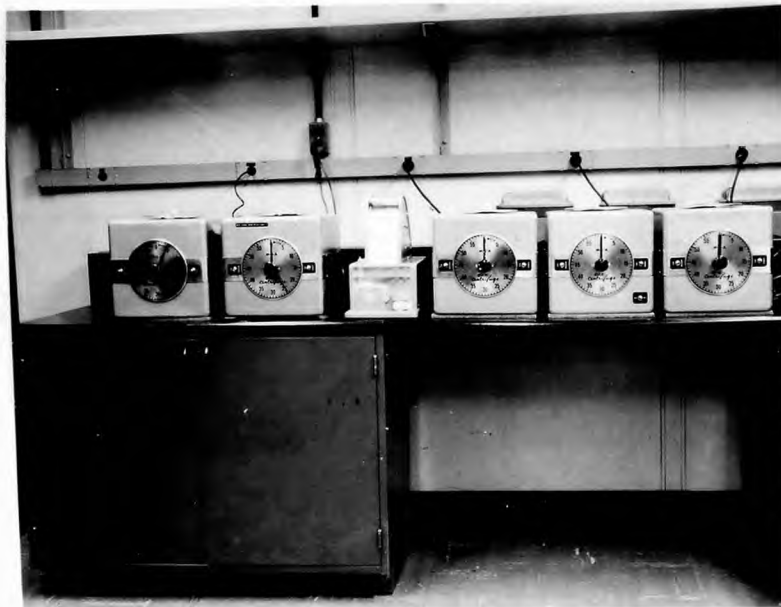


FIGURE 15. MSA PARTICLE SIZE ANALYSIS EQUIPMENT
(Left to right) Two 3600 RPM centrifuges, projector,
300 RPM, 600/1200 RPM, and 1800 RPM centrifuges.

liquid and centrifuging at predetermined speeds and time intervals until all of the sample has settled in the capillary tube while measuring the height of sample in the centrifuge tube capillary bore at the end of each time interval.

In a final comparison of the methods of particle size analysis; microscopy, gravitational liquid sedimentation, and electrostatic resistivity change cannot be considered to be adequate, mainly because of the limitation of these methods to a low particle size of about 0.5 micron. (This does not include electron microscopy, since this method was not considered due to the unavailability of an electron microscope). APD's as determined by the Fisher Sub-Sieve Sizer range as low as 0.5 micron for the samples being evaluated in this study, indicating that the small particles in these samples will be smaller than 0.5 micron.

The only method which appears to be suited for analysis of particle size distribution for particles smaller than 0.5 micron is centrifugal liquid sedimentation, using the MSA Particle Size Analyzer. Consequently, the decision was made to use the MSA Particle Size Analyzer for the particle size analysis of barium chromate and boron.

C. Particle Size Distribution of Barium Chromate and Boron

Inspection of Figures 27 to 36 and 37 to 46 shows that the samples of barium chromate and boron which were not represented by approximately straight lines between the "85 percent and 15 percent greater than particle size= d " points on the log-probability

TABLE 9

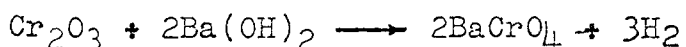
SUMMARY OF PARTICLE SIZE ANALYSIS RESULTS

Lot designation and code number	Fisher APD (microns)	M S A		Uniformity index (U)	U*(M S A)	
		50 percent point (microns)	d _m (microns)		50 percent point (microns)	d _m (microns)
Barium Chromate						
MP 31801 (1)	2.6	10.4	6.38	.293	3.05	1.87
MP 32500 (2)	2.1	11.0	6.98	.286	3.15	2.00
MP 28303 (3)	1.3	3.60	3.65	.477	1.72	1.74
BAKER 26428 (4)	1.1	1.92	1.99	.513	0.99	1.02
B&C FINE (5)	1.1	2.52	2.50	.507	1.28	1.26
MP 25160 (6)	0.8	2.55	2.34	.485	1.24	1.21
BAKER 91104 (7)	0.8	1.67	1.70	.586	0.98	1.00
BAKER 30388 (8)	0.9	1.52	1.54	.607	0.92	0.94
MP 28511 (9)	0.9	1.27	1.75	.383	0.49	0.67
BAKER 25894 (10)	1.1	2.16	2.13	.551	1.19	1.17
MP 30701 (11)	0.7	1.08	1.69	.300	0.32	0.51
Boron						
UMC 1992 (1)	2.4	8.3	7.32	.442	3.67	3.23
UMC 1993 (2)	1.75	5.45	5.35	.433	2.36	2.31
HCST 873 (3)	1.0	1.90	1.73	.450	0.86	0.78
TRONA 419 (4)	0.75	2.47	2.21	.429	1.06	0.95
TRONA 571 (5)	0.7	2.90	2.58	.412	1.19	1.06
HCST 900 (6)	0.6	2.40	2.53	.373	0.90	0.94
HCST 954 (7)	0.5	2.09	2.05	.381	0.80	0.78

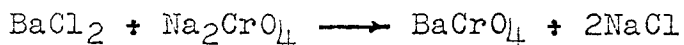
graphs, exhibited definite bi-modal particle size distribution on the size-frequency graphs. The remaining samples were represented by variations of the normal "bell-shaped" curve. The barium chromate samples from J.T. Baker exhibited normal particle size distribution with a high degree of uniformity. On the other hand, the Mineral Pigments barium chromate samples, including four with a bi-modal particle size distribution, were less uniform than the Baker samples.

The uniformity of the components was at first qualitatively estimated from the range of the particle size distribution and the shape of the size-frequency curve for each sample. An algebraic function of the particle size distribution, termed the uniformity index, expresses the particle size uniformity of the samples as a quantitative value. The uniformity indices of the barium chromates range from .286 to .485 for the Mineral Pigments samples and from .513 to .607 for the Baker samples, while the uniformity indices for the boron samples range from .373 to .450. The range of the uniformity index scale is from 1.0 for a sample containing only one particle size species, to zero for a sample with an infinitely wide particle size distribution.

The general difference in particle size distribution between manufacturers of barium chromate led to inquiries as to any differences in the method of manufacture of barium chromate. J.T. Baker manufactures barium chromate as a high purity reagent grade chemical, as indicated by the one-step reaction:



The Mineral Pigments process is represented by the following reaction:



This reaction requires an in-process pH adjustment (no elaboration could be obtained) so that the reaction will proceed toward completion. Consequently, this reaction may take place in two separate steps, depending on the timing of the pH adjustment, and result in a bi-modal particle size distribution. The chemical analyses specified by MIL-B-550A (1) and TL-PD-104 (2) were performed to determine the effects of the different methods of manufacture on the chemical purity (Table 5)

The J.T. Baker barium chromate was found to have a higher purity than the Mineral Pigments barium chromate and contained little or no chloride, sulfate, volatile matter, or moisture; with little or no loss on ignition at 900°C. The Mineral Pigments barium chromate samples had a discernable chloride content as a result of the synthesis reaction, a high sulfate content due to the use of city water for processing, rather than distilled water (the sulfate in the Baker barium chromate comes from the small amount of sulfate impurity in the chromic anhydride), and a high loss on ignition at 900°C, resulting from the volatility of the sodium chloride and any moisture or gases that were not removed in normal drying.

With the exception of a low sulfate content, the barium

chromate sample from Barium and Chemicals Corporation (B & C Fine) had a purity level and impurity content which classified it with the Mineral Pigments samples. This suggested that the Barium and Chemicals process was similar to the Mineral Pigments process, but with greater control of the reaction rate and the use of distilled processing water.

After consideration of the chemical differences of the Baker and Mineral Pigments barium chromate samples, it was felt that classification of the two types might be useful for better correlation of particle size and burning rate results.

In order to compare and evaluate the two methods of particle size analysis, the following graphs were drawn for both barium chromate and boron:

- (1) Fisher APD versus MSA 50 percent point (Figures 16 and 17).
- (2) Fisher APD versus MSA \bar{d}_m (log mean particle diameter) (Figures 18 and 19).

The MSA 50 percent point was indicated as the particle diameter at the point where the log-probability curve intersected the "50 percent greater than d " line, while the MSA \bar{d}_m was the mean particle size obtained by integrating the area under the size-frequency curve. For comparison, the "Fisher APD=MSA \bar{d}_m " and the "Fisher APD=MSA 50 percent point" lines were drawn on the appropriate graphs for both barium chromate and boron. In all cases, the experimental points lay below the theoretical "Fisher APD=MSA" line implying that either the Fisher readings were biased

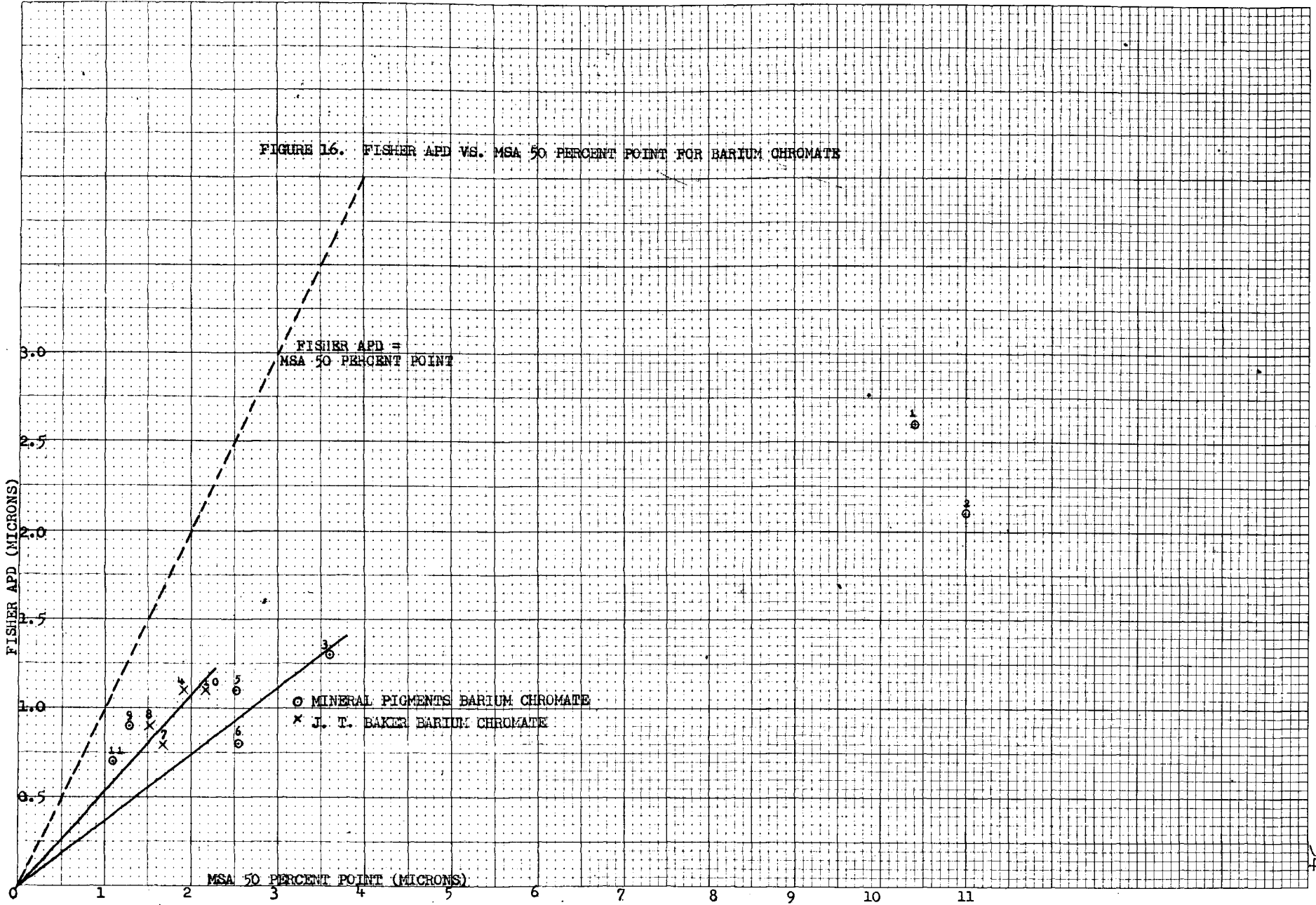


FIGURE 17. FISHER APD VS. MSA 50 PERCENT POINT
FOR BORON

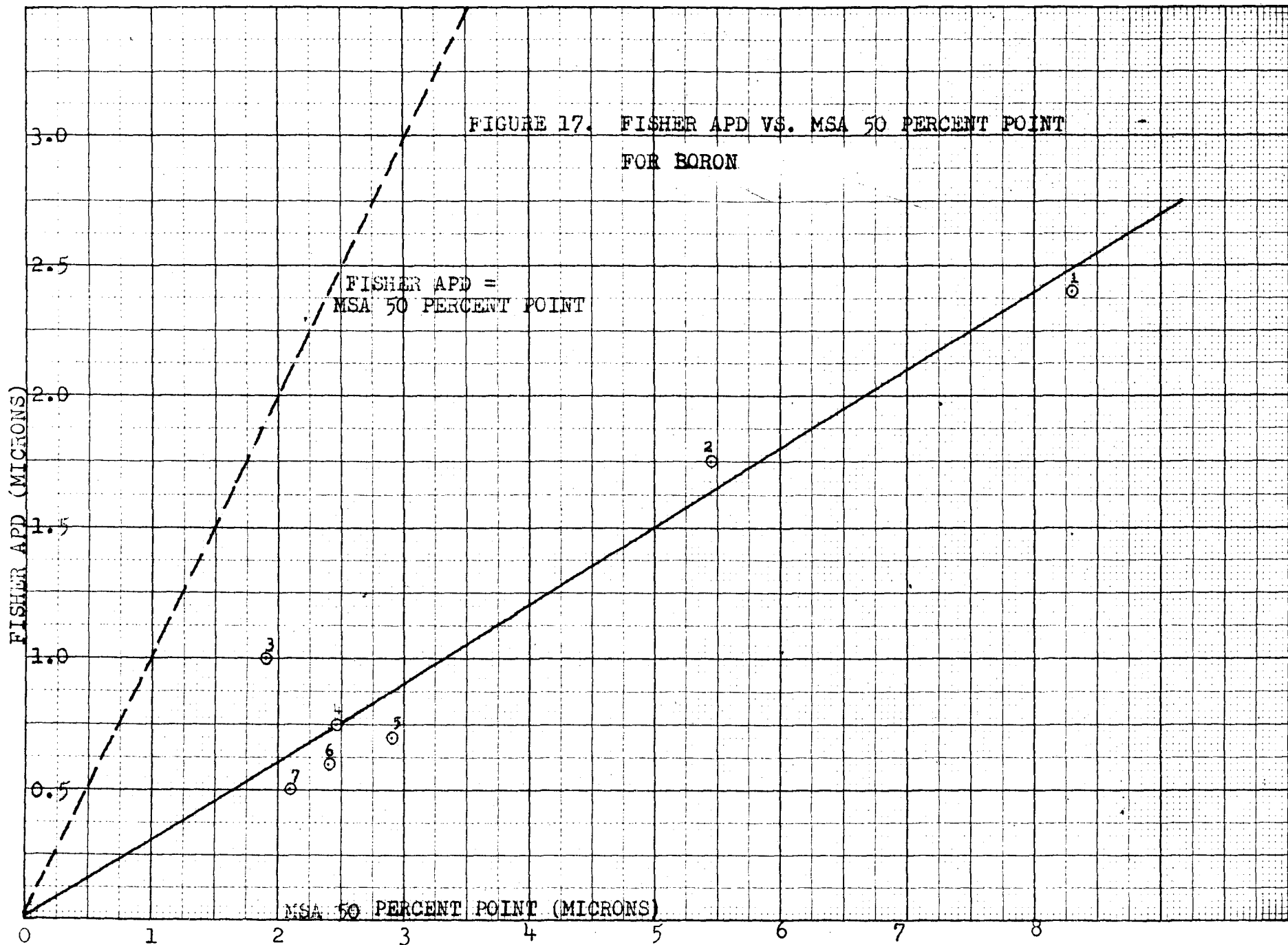
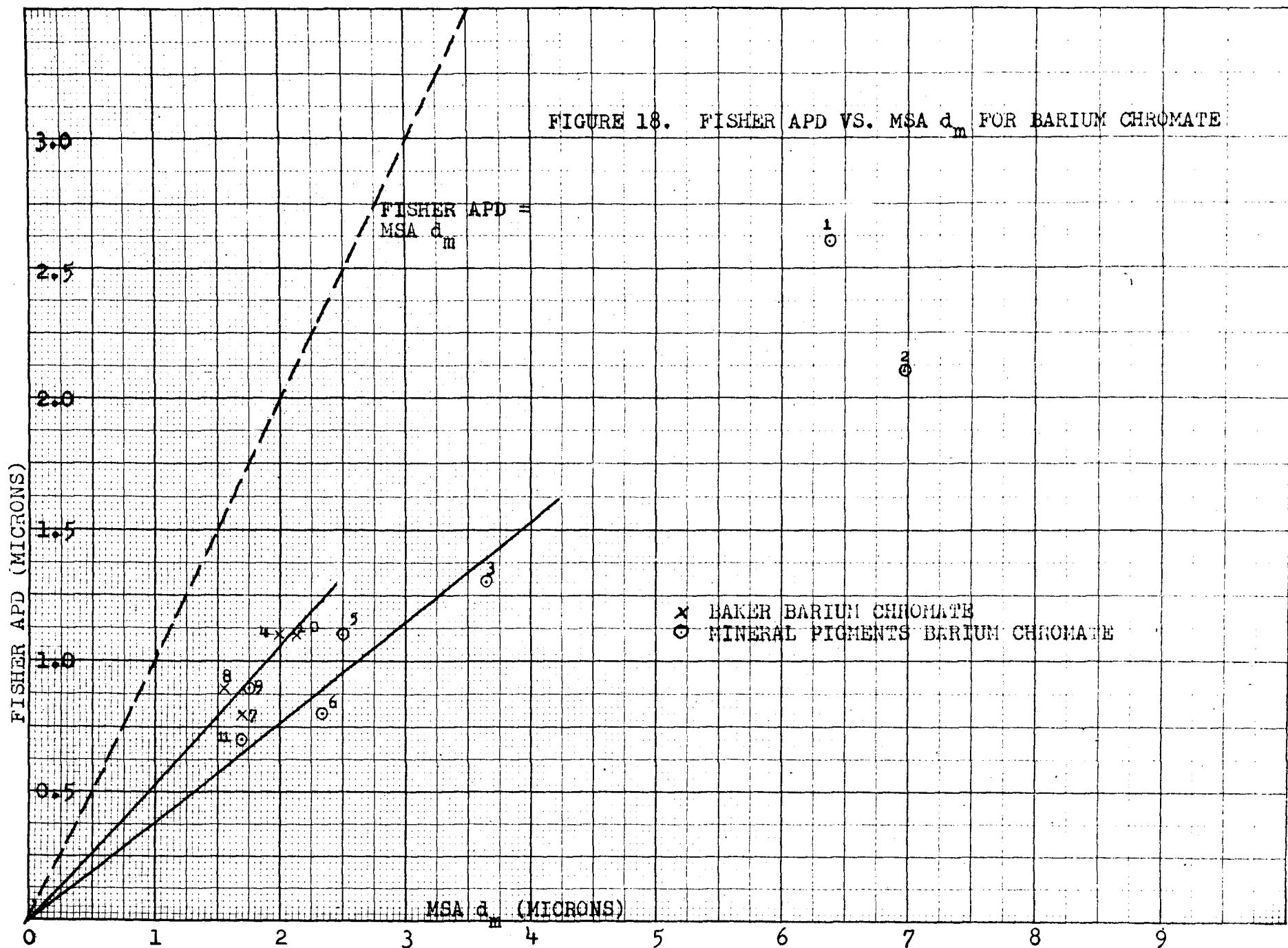
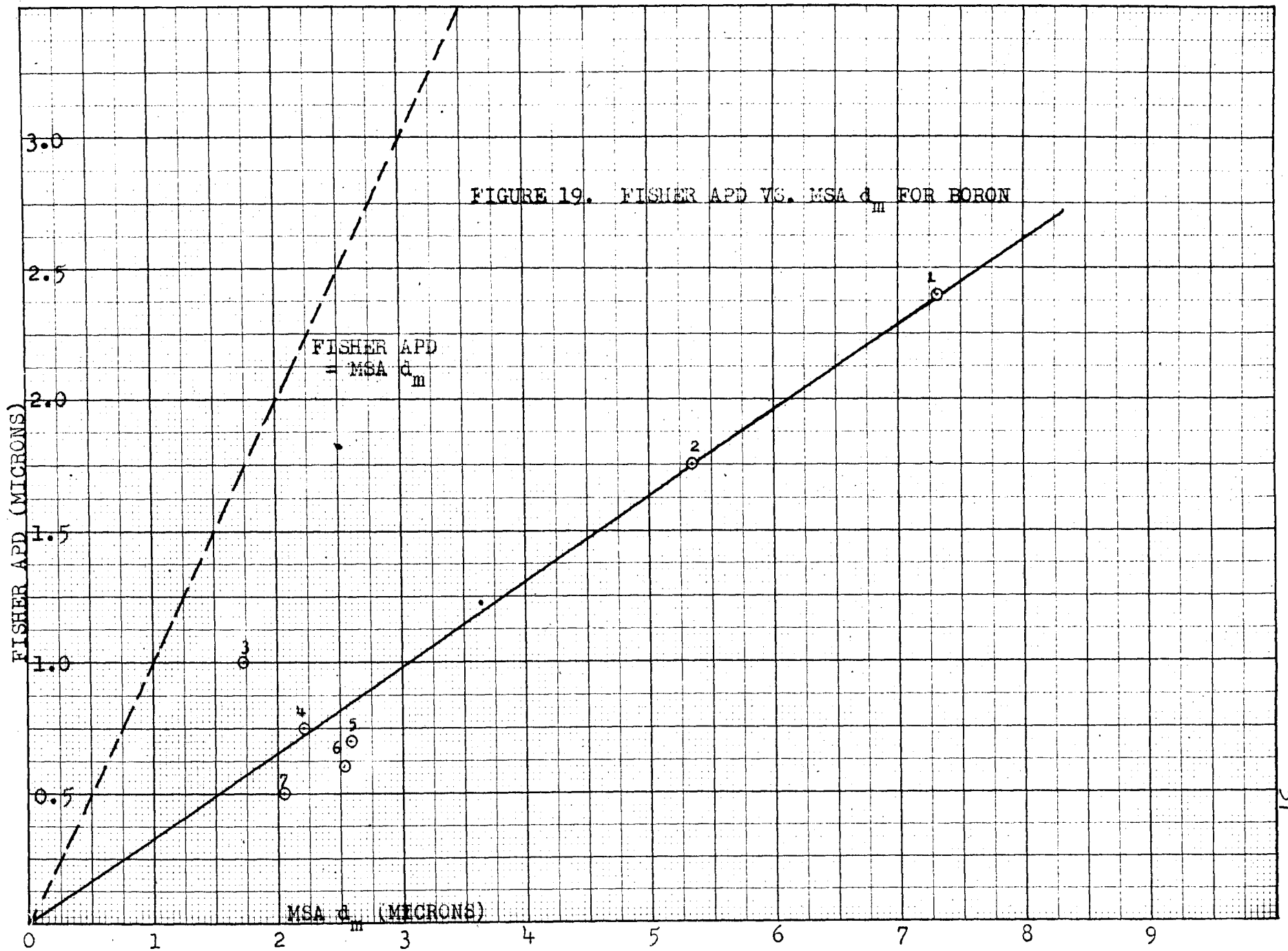


FIGURE 18. FISHER APD VS. MSA d_m FOR BARIUM CHROMATE





toward the low end of the particle size range or that the MSA readings were biased in favor of the larger particles, possibly because of re-agglomeration of the samples. It is believed that the former is actually the case, based on several facts and observations:

- (1) As the APD as determined by the Fisher Sub-Sieve Sizer is related to the total surface area of the sample, the particle size determination will be strongly influenced by the small particles which have a large surface area. This phenomenon would be more pronounced, the smaller the size of the smallest particles in the sample and the larger the particle size range of the sample.
- (2) Since the method of dispersion used was a combination and also an improvement on each of several individual methods of dispersion (4, 12), and since any visible re-agglomeration was eliminated by controlling the concentration of the sample being analyzed, it is improbable that re-agglomeration was responsible for the higher readings obtained with the MSA equipment. The MSA readings also coincided with estimations of the particle size range as determined by microscopic examination. In addition, Irani (12) states that, for a particle size range below 10 microns, if the proper dispersion is achieved, and if the layer technique is utilized, the MSA equipment and the electron microscope repeatedly gave identical particle size distributions.

The barium chromate samples from J.T. Baker and all of the boron samples except HCST873 follow a straight line relationship when plotted on either the Fisher APD=MSA d_m or the Fisher APD=MSA

50 percent point graphs. On both graphs, the Baker barium chromate follows the relationship: $MSA \text{ } \bar{d}_m$ (or $MSA \text{ } 50 \text{ percent point}$) = 1.9 Fisher APD. The two Mineral Pigments bi-modal samples with the primary mode in the large particle range, ie., MP 32500 and MP 31801, exhibit the greatest deviation from either the Fisher $APD=MSA \text{ } \bar{d}_m$ or the Fisher $APD=MSA \text{ } 50 \text{ percent point}$ lines. It will be recalled that one of the shortcomings of the Fisher Sub-Sieve Sizer is that the APD's so obtained are biased in favor of small particles. The smallest particles of these samples are further removed from the value of the mean diameter or the 50 percent point of each sample, as compared to more uniform samples with a normal distribution. The APD for each sample is thus much smaller than the MSA values ($MSA \text{ } 50 \text{ percent point} = 4-5 \text{ APD}$). Conversely, the two Mineral Pigments bi-modal samples with the primary mode in the small particle range, ie, MP 30701 and MP 28511, exhibit the least deviation from the Fisher $APD=MSA \text{ } \bar{d}_m$ and the Fisher $APD=MSA \text{ } 50 \text{ percent point}$ lines. Again, it is reasoned that the size of the smallest particles is relatively close to both the mean diameter and the 50 percent point, the MSA values will not be much larger than the APD's ($MSA \text{ } 50 \text{ percent point} = 1.5 \text{ APD}$). The two remaining Mineral Pigments samples, MP 28303 and MP 25160, as well as the B & C Fine sample, indicated normal size distributions with the exception that the particle size range was greater than the particle size range for the Baker barium chromate samples. The slope of the MSA-APD lines for this group of samples should be intermediate between the two bi-modal groups and slightly less

than the slope of the MSA-APD lines for the Baker samples. Examination of Figures 16 and 18 show that, as expected, the relationships are: MSA 50 percent point (or MSA d_m) = 2.5 APD.

The boron samples were not segregated as to method of manufacture. Table 6 shows the results of the chemical analyses performed on the boron samples. The Trona and HCST samples were similar in purity and composition while each of the UMC samples had a low amorphous boron content. The low amorphous boron content, coupled with the large particle size, high percentage of insoluble matter, "gritty" feeling, and total boron content similar to all other boron samples, led the investigator to believe that the UMC samples contained a high percentage of crystalline boron. All boron samples followed the straight-line relationships MSA d_m = 3.1 APD and MSA 50 percent point = 3.3 APD (Figures 17 and 19), with two qualifications:

- (1) HCST 873 deviated from these lines because of its bi-modal nature, as was explained for the bi-modal barium chromate samples.
- (2) The boron samples with the APD's of less than 0.7 micron show a tendency to deviate from the MSA-APD line to a greater extent because of the sensitivity of the Fisher Sub-Sieve Sizer to progressively smaller particles.

In order to compensate for the apparent effect of the particle size distribution on the Fisher APD's as a result of the non-uniformity of the samples, the product of the MSA d_m or MSA 50 percent point and the uniformity index was plotted against the

Fisher APD for each sample, as indicated in Figures 20 to 23.

The graphs for barium chromate indicate that the Fisher APD is approximately equal to both the modified MSA d_m and the modified MSA 50 percent point. There still appear to be deviations because of the degree of non-uniformity of the samples, but the application of the uniformity index definitely does provide a close correlation between the Fisher APD and both the MSA d_m and the MSA 50 percent point. Similarly, all boron samples with the exception of HCST 873 provided a straight line, indicating the relationship:

$$U \cdot \text{MSA 50 percent point (or } U \cdot \text{MSA } d_m) = 1.4 \text{ APD.}$$

D. Relationship of Burning Rate of Barium Chromate-Boron Delay Compositions to the Particle Size of the Components

Twenty different 95/5 barium chromate-boron delay compositions (Table 7) were pressed into delay fuzes and tested for burning time. The test data is shown in Tables 43 to 62 and the calculated results are summarized in Table 10.

Two major "families" of compositions were represented among the twenty compositions. One "family" included seven compositions in which one lot of boron was blended with eleven different lots of barium chromate. The other major family included seven compositions in which a single lot of barium chromate was blended with seven lots of boron.

Because of the differences in particle size distribution

TABLE 10

SUMMARY OF BURNING RATE CALCULATIONS

Composition	No. of samples	Corrected burning time (sec)	Height of delay composition (in.)	Average (in./sec)	Burning Rate Standard deviation (in./sec)	Coefficient of variation (%)
1	8	0.940	0.764	.810	—	—
2	25	1.064	.775	.728	.0117	1.61
3	25	1.121	.769	.687	.0237	3.45
4	23	1.065	.767	.720	.0192	2.67
5	23	1.065	.751	.704	.0165	2.34
6	25	1.292	.755	.585	.0061	1.04
7	23	0.982	.761	.771	.0182	2.36
8	25	1.048	.773	.738	.0100	1.35
9	19	1.147	.771	.673	.0120	1.78
10	20	1.306	.771	.590	.0067	1.13
11	24	1.313	.757	.577	.0114	1.98
14	8	2.800	.766	.277	—	—
15	9	2.260	.761	.338	—	—
16	11	4.076	.769	.189	.0026	1.35
17	18	5.326	.753	.142	.0016	1.16
19	20	0.911	.767	.842	.0148	1.76
20	19	2.311	.776	.336	.0067	1.96
21	19	2.255	.782	.347	.0062	1.92
23	18	4.820	.772	.160	.0023	1.41
24	20	2.907	.769	.264	.0032	1.23

FIGURE 20. FISHER APD VS. MODIFIED MSA 50 PERCENT POINT FOR BARIUM CHROMATE

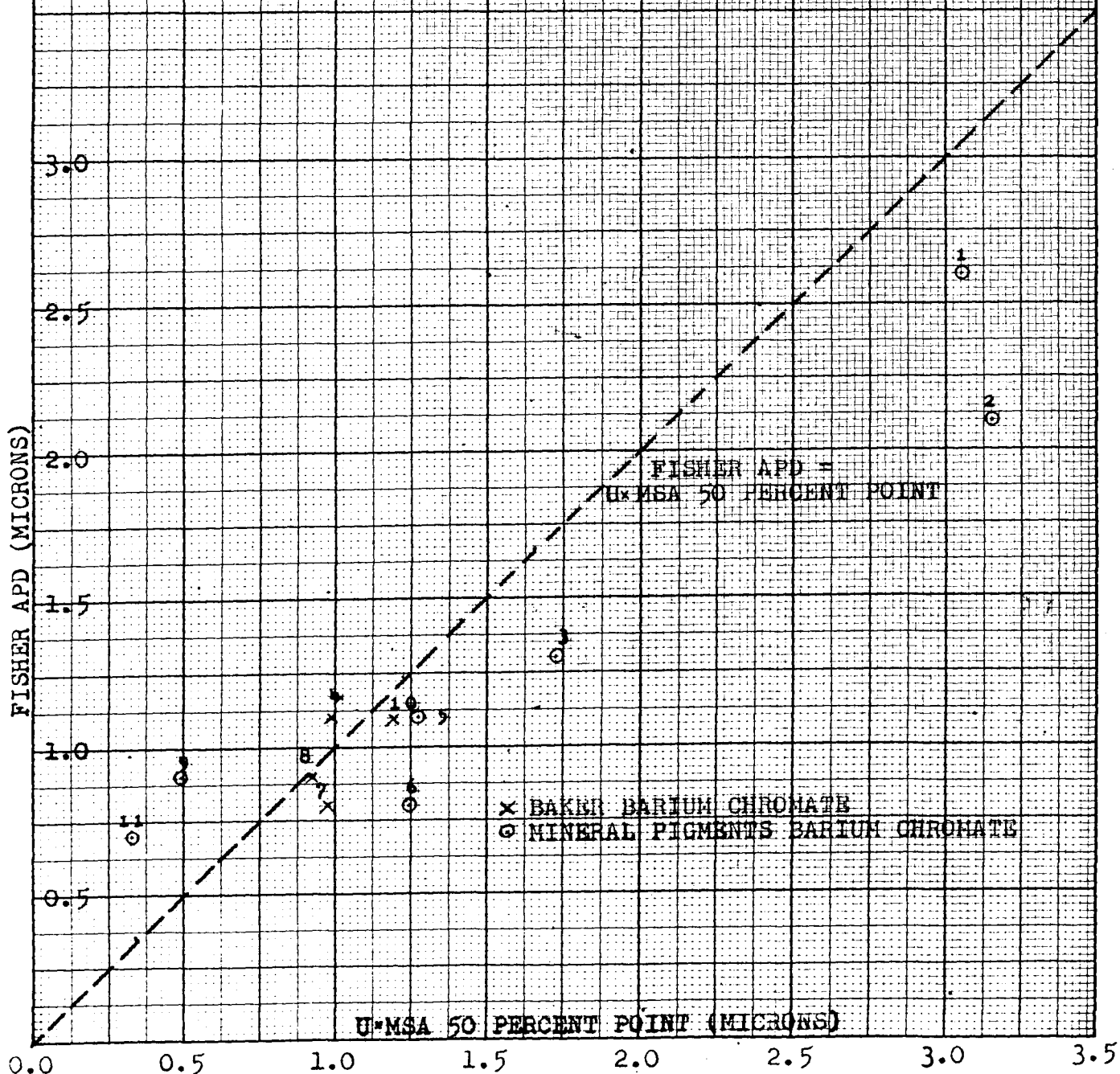
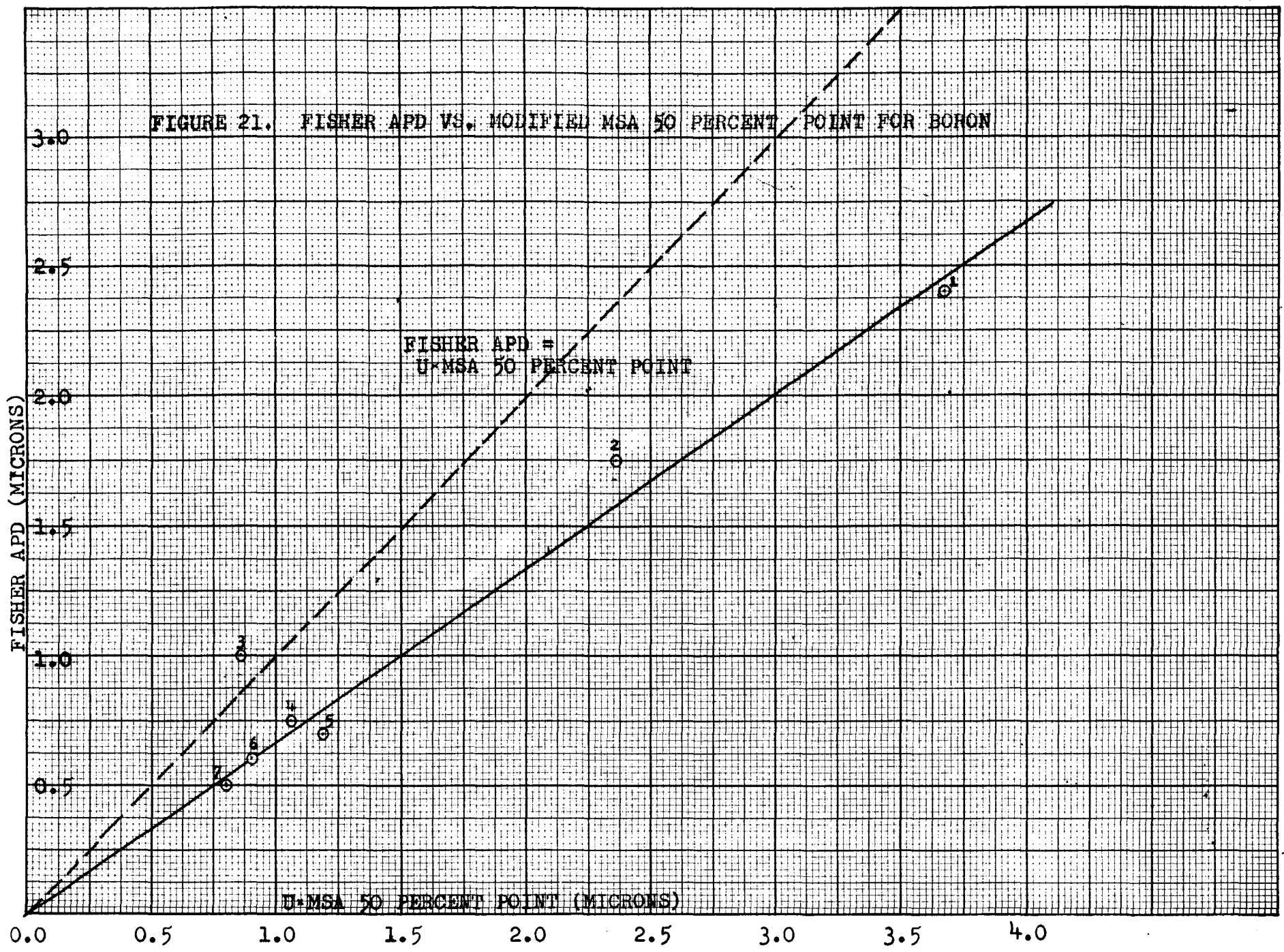


FIGURE 21. FISHER APD VS. MODIFIED MSA 50 PERCENT POINT FOR BORON



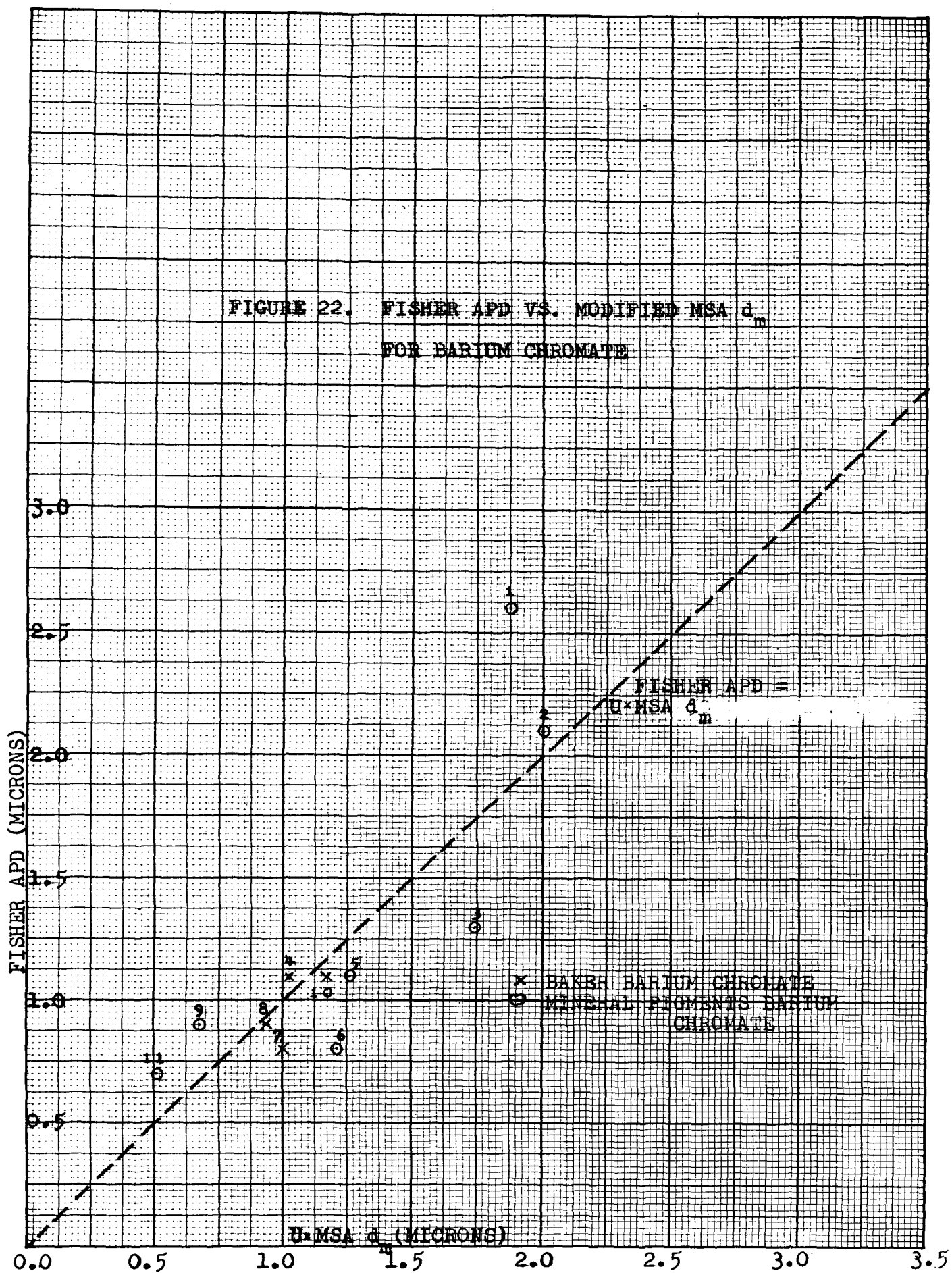
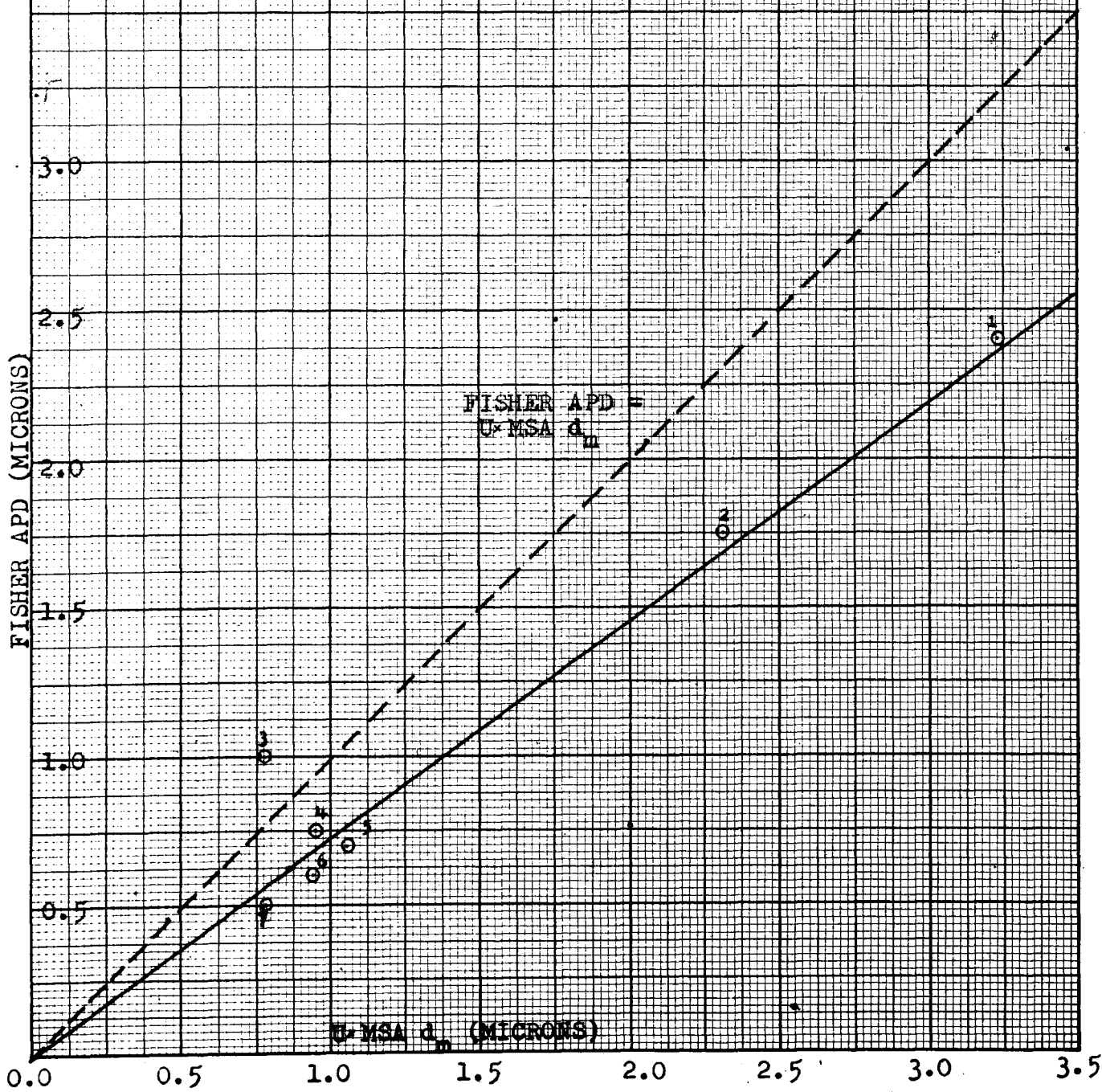


FIGURE 23. FISHER APD VS. MODIFIED MSA d_m
FOR BORON



and chemical purity as a result of the different methods of manufacture, the compositions containing Baker barium chromate were separated from the compositions containing Mineral Pigments barium chromate. This step was taken to minimize the effect of variables other than particle size parameters of the components on the burning rate of the compositions.

The MSA 50 percent point of each component was compared to the burning rate of the compositions for Baker barium chromate (Table 11) and for Mineral Pigments barium chromate (Table 12). These tables have been arranged so as to show the variation of burning rate of the composition as the particle size of either component increases. These tables indicate a general trend toward decreasing burning rate of the compositions as the particle size of either component increases, with several important exceptions. Examination of Table 11 shows that, if burning rate does actually increase as the particle size decreases, Trona 571 and Trona 419 boron samples should be finer than the HCST samples. Table 12 shows that Trona 571 boron should be the finest of the borons in this table, and that B & C Fine barium chromate should be the finest of the Mineral Pigments group of barium chromates, followed by the MP 28303 sample. Similarly, the MSA d_m and the Fisher APD show only limited correlation to the burning rate of the compositions.

Assuming that no other variables, such as purity, density,

TABLE 11

RELATIONSHIP OF THE MSA 50 PER CENT POINT FOR BARIUM CHROMATE AND BORON COMPONENTS
TO THE BURNING RATE OF THE DELAY COMPOSITION (BAKER BARIUM CHROMATE)

Lot designation	Barium Chromate			
	BAKER 30388	BAKER 91104	BAKER 26428	BAKER 25894
MSA 50 percent point	1.52 microns	1.67 microns	1.92 microns	2.16 microns
Boron	HCST 873 1.90 microns	0.338 in./sec		
	HCST 954 2.09 microns	0.277 in./sec		
	HCST 900 2.40 microns	0.336 in./sec		
	TRONA 419 2.47 microns	0.842 in./sec		
	TRONA 571 2.90 microns	0.810 in./sec	0.720 in./sec	0.704 in./sec
	UMC 1992 5.45 microns	0.142 in./sec		0.738 in./sec
	UMC 1993 8.3 microns	0.189 in./sec		

TABLE 12

RELATIONSHIP OF THE MSA 50 PERCENT POINT FOR BARIUM CHROMATE AND BORON COMPONENTS
TO THE BURNING RATE OF THE DELAY COMPOSITION (MINERAL PIGMENTS BARIUM CHROMATE)

Lot designation	MSA 50 percent point	BORON		
		HCST 954	TRONA 571	UMC 1992
		2.09 microns	2.90 microns	8.3 microns
Barium Chromate	MP 30701 1.08 microns	0.347 in./sec	0.687 in./sec	
	MP 28511 1.27 microns		0.673 in./sec	
	B&C FINE 2.52 microns		0.771 in./sec	
	MP 25160 2.55 microns		0.577 in./sec	
	MP 28303 3.60 microns		0.727 in./sec	
	MP 31801 10.0 microns	0.264 in./sec	0.590 in./sec	0.160 in./sec
	MP 32500 11.0 microns		0.585 in./sec	

or degree of crystallinity are involved, the burning rate of the composition should be related to the component particle size only if the composition contains a single particle size for the component, for a theoretical uniformity index of 1.0. This statement is limited to compositions with a particle size small enough to react upon the application of heat for initiation. Consequently, it is felt that a relationship between the burning rate of the compositions and an average particle size of the components can not be expected if the uniformity of the components falls below some empirically determined point.

The particle size distribution curves (Figures 27 to 36) were examined for a correlation to the burning rate of the compositions. As the "x percent was greater than d" point decreased, the correlation of that particle size to the burning rate became more apparent. At the 10 percent point there was a definite correlation between the particle size and burning rate, indicating that the burning rate is limited by the amount of slower burning, coarse particles present. (Tables 13 and 14, Figure 24 and 25.)

The burning rate of the compositions decreases as the particle size (10 percent point) of the barium chromate increases according to a virtually linear relationship (Figure 24). For Mineral Pigments barium chromate samples this rate of decrease is independent of the boron blended with the

TABLE 13

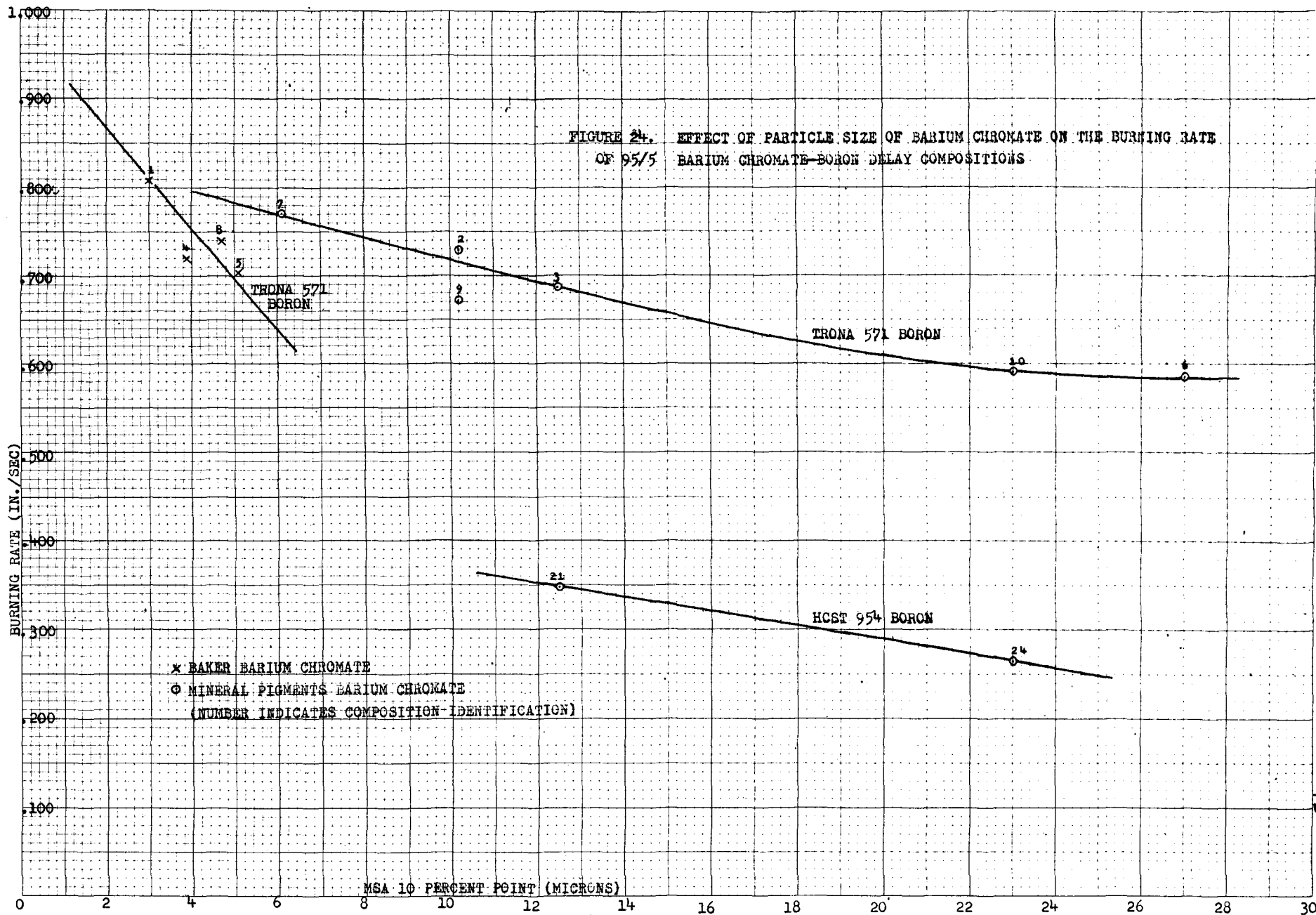
RELATIONSHIP OF THE MSA 10 PERCENT POINT FOR BARIUM CHROMATE AND BORON COMPONENTS
TO THE BURNING RATE OF THE DELAY COMPOSITION (BAKER BARIUM CHROMATE)

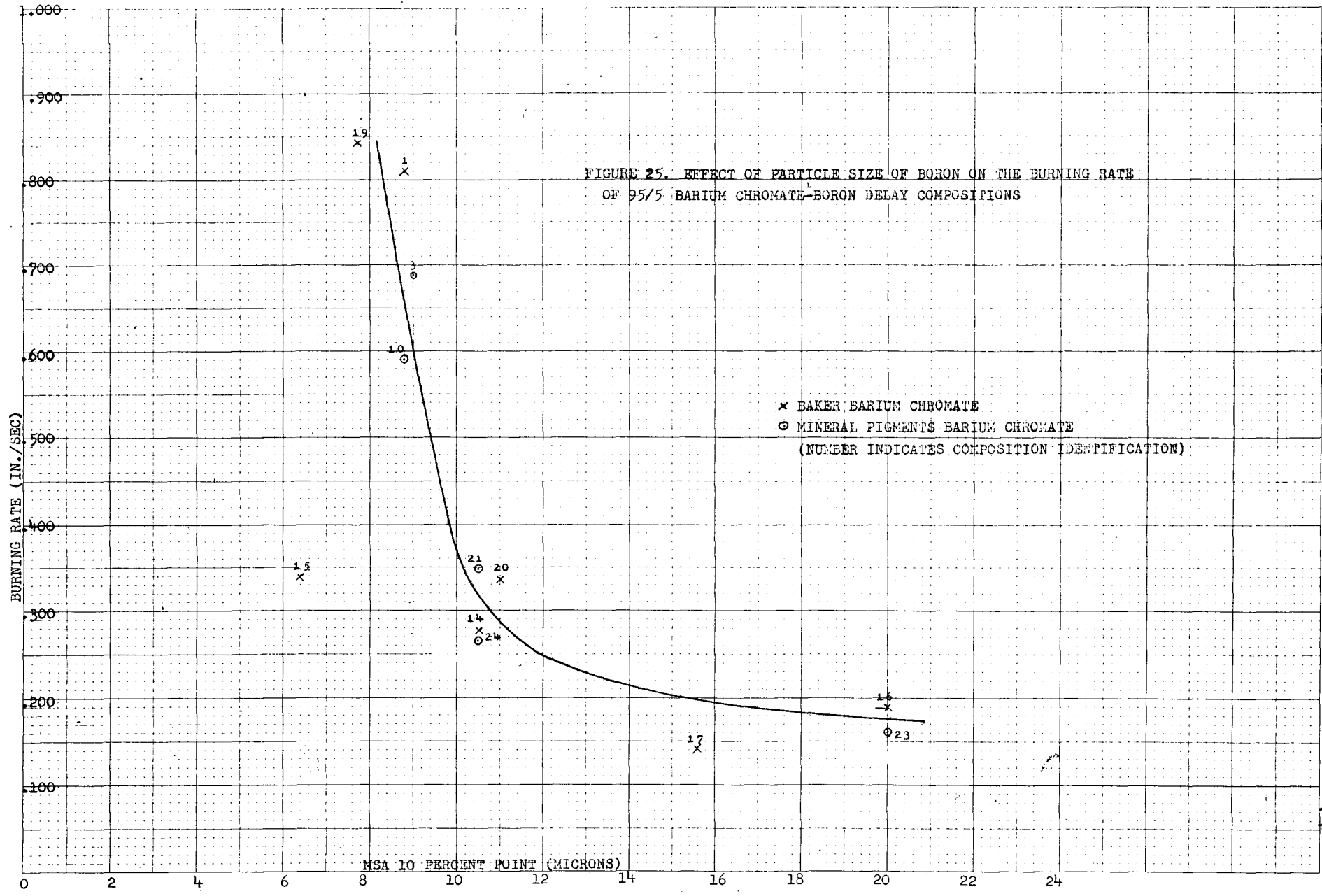
Lot designation	Barium Chromate			
	BAKER 30388	BAKER 91104	BAKER 25894	BAKER 26428
MSA 10 percent point	3.0 microns	3.9 microns	4.7 microns	5.1 microns
TRONA 419 7.7 microns	0.842 in./sec			
Boron TRONA 571 8.8 microns	0.810 in./sec	0.720 in./sec	0.738 in./sec	0.704 in./sec
HCST 900 11.0 microns	0.336 in./sec			
HCST 873 6.3 microns	0.338 in./sec			
HCST 954 10.5 microns	0.277 in./sec			
UMC 1992 20.0 microns	0.189 in./sec			
UMC 1993 15.6 microns	0.142 in./sec			

TABLE 14

RELATIONSHIP OF THE MSA 10 PERCENT POINT FOR BARIUM CHROMATE AND BORON COMPONENTS
TO THE BURNING RATE OF THE DELAY COMPOSITION (MINERAL PIGMENTS BARIUM CHROMATE)

Lot designation	TRONA 571	HCST 954	UMC 1992
MSA 10 percent point	8.8 microns	10.5 microns	20.0 microns
B&C FINE 6.10 microns	0.771 in./sec		
MP 28303 10.2 microns	0.728 in./sec		
MP 28511 10.2 microns	0.673 in./sec		
MP 30701 12.5 microns	0.687 in./sec	0.347 in./sec	
MP 31801 23 microns	0.590 in./sec	0.264 in./sec	0.160 in./sec
MP 32500 27.0 microns	0.585 in./sec		





barium chromate, as evidenced by the slope of the Trona 571 and HCST 954 lines (Mineral Pigments barium chromate) being approximately equal. Figure 24 shows that the burning rate of the composition decreases as the uniformity of the barium chromate decreases, providing further evidence that the burning rate of the compositions is dependent on the coarseness of the components.

The burning rate of the compositions is strongly affected by the boron which is blended with the barium chromate, regardless of the source of the barium chromate (Figure 25). For fine boron samples, the burning rate decreases sharply with an increase in the particle size. However, as the particle size (10 percent point) increases beyond approximately 11 microns, the burning rate decreases only slightly, suggesting a hyperbolic type relationship between burning rate and the particle size of the boron. The significance of these results as applied to actual compositions is as follows:

- (1) As the particle size of the boron increases, the burning rate will level out at a very low burning rate until eventually nonignition of the composition is reached. This is supported by the occurrence of two incompletely burned fuzes out of twenty tested for composition no. 23, containing UMC 1992 boron, the coarsest boron used in this study.
- (2) As the particle size of the boron decreases to a limiting particle size in the low range, the burning rate will become infinite, corresponding to spontaneous combustion. This

is in fact, one of the actual dangers to be considered when dealing with extremely fine boron, both un-mixed or when blended in a delay composition.

The burning rate of the compositions should be related to the particle size only if all other variables were maintained constant. Figure 24 shows that compositions blended with Mineral Pigments barium chromate would be faster burning than Baker Samples of the same particle size. One explanation is that the slight amount of barium sulfate present in the Mineral Pigments samples tends to increase the burning rate of the composition. Other variables, which could either augment or detract from the particle size-burning rate relationships illustrated in Figures 24 and 25 include purity, density, species of impurities, and degree of crystallinity. The various boron samples plotted on Figure 25 do not vary to any great extent from the general curve drawn to represent the data, thus it appears that the particle size expressed as the 10 percent point provides a close correlation to the burning rate, and may be the main factor in the variation of the burning rate. No conclusions can be drawn at this time as to the effect of impurities on the burning rate of the compositions used in this study.

The burning rate standard deviation and coefficient of variation (standard deviation \cdot 100/ave. burning rate) for 17 of the compositions tested are listed in Table 10. No specific

correlations are obvious, but it does appear that as the burning rate decreases, both the coefficient of variation and the standard deviation decrease, indicating that a portion of the burning rate variation is due to an "ignition lag" or other end effects. These effects were minimized by pressing as much delay composition as possible into the fuze housings in order to increase the average burning time of the delay fuzes. Also, elimination of the relay assembly eliminated the possible premature ignition of the heat sensitive relay charge by the heat front preceding the actual burning front. This "anticipatory effect" has been discussed in detail by Gilford, et al (11).

Another factor that should effect the burning rate variation is the amount of gases produced by heating the barium chromate, specified as "loss on ignition at 900°C" on Table 5 . The generation of gas can cause a pressure drop between the burning surface and the outside atmosphere, especially if the solid reaction products result in a heavy slag formation (Figure 26). Werbel (18) found that, for 95/5 barium chromate-boron compositions, the burning rate increased as the ambient pressure increased. Since the pressure drop, and consequently the pressure at the burning surface, is a function of the porosity of the slag, variations in the burning rate will result. No conclusive results were observed to substantiate this theory, except



FIGURE 26. BURNED AND UNBURNED FUZES
Left - burned fuze showing slag formation; center - loaded
delay fuze; right - empty fuze housing.

that composition no.3, containing barium chromate with a high loss of ignition of 0.72 percent had the highest burning rate variation (3.45 percent).

The delay compositions used in this study were blended by spatulation of a thick paste of the composition after being wet with ethanol. The uniformity of the blend was achieved by breaking down agglomerates with the aid of the ethanol, which normally is a dispersing agent for both barium chromate and boron. The components tended to re-agglomerate together more or less uniformly only by virtue of the concentration of the paste and not by any tendency of the liquid vehicle to promote agglomeration.

Complete uniformity of the blends was not achieved, as evidenced by the occasional observation of particles of barium chromate in the compositions. Non-uniformity of a composition could lead to segregation of the components as a result of handling between the blending and pressing operations, in turn causing variations in the burning rate of the delay compositions. The use of barium chromate (or boron) with a high degree of non-uniformity, such as the bi-modal samples from Mineral Pigments, could increase particle segregation. The particles at this point are not discrete particles but agglomerates of delay composition. Since the tendency to agglomerate, as well as the size of agglomerates formed, increases as the discrete particle size decreases, the burning

rate of a delay composition may increase as the apparent particle size increases. This statement is contrary to the results obtained in this experiment, but is credible when it is realized that the large particles are actually agglomerates of much smaller discrete particles. It follows that the use of barium chromate (or boron) with a high degree of non-uniformity, such as the bi-modal samples from Mineral Pigments, would result in varying degrees of agglomeration and, in turn, increased particle segregation. This segregation was not encountered in this study because of the small amounts of delay composition made up and the care taken in handling this composition. However, this process is used widely on a manufacturing scale and the possibility of segregation of particle size is a factor to be considered when discussing particle size.

Another standard method of blending delay powders is the dispersion of the components in a dilute liquid slurry, using a mixer or blendor (6). Although uniform blends should result because of intimate mixing of the particles, it is necessary that the particles be of uniform size, otherwise, differing rates of settling will cause a non-uniformity of the composition, leading to burning rate variations. Further segregation upon handling would be probable.

IV. CONCLUSIONS

1. The burning rate of the barium chromate-boron delay compositions is not related to the Fisher APD, MSA d_m or MSA 50 percent point of either component, but is related to the particle size corresponding to the "10 percent greater than d" point on the particle size distribution curve for the component.
2. The burning rate of the compositions was found to be inversely proportional to the 10 percent point of the barium chromate. However, the burning rate of compositions containing Baker barium chromate decreased at a faster rate with increasing particle size than did the burning rate of compositions containing Mineral Pigments barium chromate. This suggests that other characteristics of the barium chromate, in addition to the particle size, have an effect on the burning rate of the delay compositions.
3. The burning rate of the delay compositions followed a hyperbolic type relationship when plotted against the 10 percent point of the boron, with extreme cases of non-ignition of the composition for coarse boron and spontaneous ignition for compositions containing fine boron. The individual compositions did not deviate from this relationship to any great extent, indicating that particle size is the main characteristic of boron affecting the burning rate of

barium chromate-boron delay compositions.

4. The Mine Safety Appliances (MSA) Particle Size Analyzer is the only apparatus now available, which is suitable for the routine analysis of the particle size distribution of substances containing particles as small as 0.1 micron.
5. The Fisher Sub-Sieve Sizer provides an APD which is biased in favor of the low end of the particle size range. The deviation of the APD from the MSA d_m or the MSA 50 percent point increases as the uniformity of the particle size distribution decreases. The presence of a bi-modal particle size distribution will, based on whether or not the principle mode is toward the small particle size end of the distribution, either decrease or increase the deviation of the APD from the MSA values. This deviation was minimized by multiplying the MSA values by the uniformity index of the samples.
6. The best dispersing agent for the dispersion of barium chromate and boron preparatory to particle size analysis is a 50-50 mixture of a nonionic wetting agent and an anionic dispersing agent.

V. RECOMMENDATIONS

It is recommended that:

1. Further studies be undertaken to investigate the effect of particle size distribution on the burning rate of barium chromate-boron delay compositions and to determine specifications for the desired particle size distribution for barium chromate and boron.
2. The particle size distribution as determined with the MSA Particle Size Analyzer replace the APD as determined with the Fisher Sub-Sieve Sizer for the specification of barium chromate and boron for use in pyrotechnic delay compositions.

VI. BIBLIOGRAPHY

1. Barium Chromate
Military Specification MIL-B-550A
25 September 1958.
2. Barium Chromate
Purchase Description TL-PD-104
U.S. Army Munitions Command, Harry Diamond Laboratories,
Washington, D.C., 8 December 1959, with Amendment 1,
8 June 1961.
3. Boron
Purchase Description PA-PD-451
U.S. Army Munitions Command, Picatinny Arsenal,
Dover, N.J., 12 November 1954.
4. Cadle, R.D.-
Particle Size Determination
New York, Interscience Publishers, Inc., 1955.
5. Comyn, R.H., Couch, M.L., and Mc Intyre, R.E.
Measurement of Particle Size of Components of Gasless
Mixtures
TR-636, U.S. Army Munitions Command, Harry Diamond
Laboratories, Washington, D.C., 28 August 1958.
6. Comyn, R.H., Couch, M.L., and Mc Intyre, R.E.
Specification of Barium Chromate for Use in Gasless
Mixtures
TR-635, U.S. Army Munitions Command, Harry Diamond
Laboratories, Washington, D.C., 17 September 1958.
7. Comyn, R.H., Marcus, I.R., and Mc Intyre, R.E.
"Agglomerate Mixing"
Industrial and Engineering Chemistry, 52, 995-998.
December 1960.
8. Dubrow, Bernard
Determination of the Particle Size and Distribution
of Sub-Sieve Powders
Research and Development Lecture No. 13, U.S. Army
Munitions Command, Picatinny Arsenal,
Dover, N.J., March 1955.
9. Eigsti, D.R., and Dwiggin, R.D.
Particle Size Measurement and Effect of Particle Size
on the Burning Time of Chemical Delay Compositions
Navweps Report 7304, U.S. Naval Ordnance Laboratory,
White Oak, Silver Spring, MD., 16 November 1960.

10. Ellern, Dr. H.
Modern Pyrotechnics
New York, Chemical Publishing Company, Inc., 1964.
11. Gilford, M., Werbel, B., Weingarten, G., and Key, L.
The Anticipatory Effect, A Study of the Burning Mechanism of Delay-Relay Columns
PATR-3047, U.S. Army Munitions Command, Picatinny Arsenal, Dover, N.J., March 1964.
12. Irani, R.R., and Collis, C.F.
Particle Size Measurement, Interpretation and Application
New York, John Wiley and Sons, Inc. 1963
13. Loveland, R.P.
"Methods of Particle Size Analysis"
Symposium on Particle Size Measurement
Philadelphia, American Society for Testing Materials, 1959.
14. MSA Particle Size Analyzer: Operating Procedures and Applications, Pittsburgh, Mine Safety Appliances Company.
15. Musgrave, J.R., and Harner, H.R.
Turbimetric Particle Size Analysis
Joplin, Eagle-Picher Research Laboratories, 1958.
16. Orr, C., and Dallavalle, J.M.
Fine Particle Measurement
New York, The Macmillan Company, 1959.
17. Osipow, L.I.
Surface Chemistry-Theory and Industrial Applications
New York, Reinhold Publishing Corporation, 1962.
18. Werbel, B., and Lopatin, S.
Development of Delay Powders
PATR 2477, U.S. Army Munitions Command, Picatinny Arsenal, Dover, N.J., April 1958.

VII. APPENDIX

TABLE 15

MSA PARTICLE SIZE ANALYSIS OF BARIUM CHROMATE—LOTS BAKER 30388 AND BAKER 91104

Particle Size, d (microns)	Centrifuge Speed (RPM)	Centrifuge Time (min:sec)	BAKER 30388				BAKER 91104			
			Sediment Height		Percent Greater Than		Sediment Height		Percent Greater Than	
			h_1	h_2	d	% ₁	d	% ₂	% ₁	% ₂
20	300	:16	.0	.0	.0	.0	.0	.0	.0	.0
10		:49	.1	.0	.22	.0	.0	.0	.0	.0
7		1:08	.5	.7	1.1	2.4	.0	.0	.0	.0
5	600	:41	1.0	1.5	2.2	5.2	2.0	2.5	4.3	5.8
3		2:05	5.0	2.8	11.2	9.8	6.5	8.9	14.4	20.5
2.5		1:28	7.9	5.0	17.7	17.5	10.5	12.3	23.2	28.5
2.0		2:36	13.5	8.0	30.2	28.0	16.9	17.6	37.3	40.5
1.5	1200	1:29	—	14.0	—	49.0	24.0	25.4	53.0	58.7
1.0		3:55	37.2	23.2	83.3	81.2	37.6	35.5	82.2	82.9
.9		1:45	40.0	24.2	89.6	84.7	39.0	37.0	86.0	85.6
.7	1800	2:56	42.0	26.6	94.0	93.0	42.5	40.5	93.7	93.7
.5		6:26	43.7	28.0	97.7	97.9	45.1	42.7	99.3	98.5
.4		7:17	44.4	28.5	99.4	99.5	45.3	43.0	100.0	99.3
.3		15:14	44.5	28.5	99.6	99.5		43.3		100.0
.2	3600	11:04	44.7	28.6	100.	100.0				

TABLE 16

MSA PARTICLE SIZE ANALYSIS OF BARIUM CHROMATE—LOTS BAKER 25894 AND BAKER 26428

Particle Size, d (microns)	Centrifuge Speed (RPM)	Centrifuge Time (min:sec)	BAKER 25894				BAKER 26428			
			Sediment Height		Percent Greater Than		Sediment Height		Percent Greater Than	
			h ₁	h ₂	d	% ₂	h ₁	h ₂	d	% ₂
20	300	:16	.0	.0	.0	.0	.0	.0	.0	.0
10		:49	.9	.0	11.9	.0	1.4	1.3	2.7	2.4
7		1:08	2.3	1.5	4.9	3.3	3.7	2.3	7.0	4.2
5	600	:41	4.6	4.3	9.9	9.6	6.0	4.8	11.4	8.8
3		2:05	12.3	11.0	26.5	24.5	14.8	12.8	28.2	23.4
2.5		1:28	18.3	16.3	39.4	36.3	28.6	26.7	54.4	48.7
2.0		2:36	26.7	23.9	57.4	53.2	34.8	33.0	66.2	60.3
1.5	1200	1:29	31.5	30.5	67.7	67.8	47.5	47.0	90.3	85.8
1.0		3:55	42.0	40.0	90.3	88.9	48.0	49.0	91.3	89.4
.9		1:45	44.5	41.0	95.7	91.3	50.0	52.0	95.2	94.7
.7	1800	2:56	45.0	44.0	96.8	97.8	51.5	54.5	98.0	99.3
.5		6:26	46.0	44.3	99.0	98.4	52.0	54.5	99.0	99.3
.4		7:17	46.4	44.5	99.8	98.8	52.3	54.6	99.4	99.4
.3		15:14	46.5	44.7	100.0	99.3	52.6	54.9	100.0	100.0
.2	3600	11:04		45.0		100.0				

TABLE 17

MSA PARTICLE SIZE ANALYSIS OF BARIUM CHROMATE—LOTS MP 25160 and MP 28303

Particle Size, d (microns)	Centrifuge Speed (RPM)	Centrifuge Time (min:sec)	MP 25160				MP 28303			
			Sediment Height		Percent Greater Than		Sediment Height		Percent Greater Than	
			h ₁	h ₂	d		h ₁	h ₂	d	
					% ₁	% ₂			% ₁	% ₂
20	300	:16	0.0	0.0	0.0	0.0	0.0	0.0	0.0	0.0
10		:49	0.0	0.0	0.0	0.0	7.0	3.2	14.7	7.1
7		1:08	2.3	3.5	4.4	5.7	12.0	9.0	25.2	20.0
5	600	:41	9.5	13.7	18.1	22.3	17.7	15.2	37.2	33.8
3		2:05	20.6	28.5	39.3	46.3	28.3	25.7	59.5	57.2
2.5		1:28	24.5	32.7	46.7	53.1	33.1	30.3	69.6	67.4
2.0		2:36	29.8	39.2	56.7	63.7	39.7	35.6	83.5	78.2
1.5	1200	1:29	35.0	47.0	66.7	76.3	41.3	38.4	86.8	85.4
1.0		3:55	45.0	53.0	85.7	86.1	46.0	43.0	96.7	95.7
.9		1:45	45.0	54.5	85.7	83.9	46.6	43.4	97.8	96.7
.7	1800	2:56	47.0	56.5	89.5	91.7	46.6	43.9	97.9	97.7
.5		6:26	51.0	59.5	97.2	96.7	47.3	44.5	99.5	99.0
.4		7:17	51.5	60.0	98.0	97.5	47.5	44.9	99.8	100.0
.3		15:14	52.2	60.6	99.3	98.3	47.6	44.9	100.0	100.0
.2	3600	11:04	52.4	61.0	99.8	99.1				
.1		57:09	52.5	61.6	100.0	100.0				

TABLE 18

MSA PARTICLE SIZE ANALYSIS OF BARIUM CHROMATE--LOTS MP 32500 AND MP 28511

Particle Size, d (microns)	Centrifuge Speed (RPM)	Centrifuge Time (min:sec)	MP 32500				MP 28511			
			Sediment Height		Percent Greater Than		Sediment Height		Percent Greater Than	
			h ₁	h ₂	d	% ₂	h ₁	h ₂	d	% ₂
20	300	:16	12.5	18.0	30.9	40.0	.0	.0	.0	.0
10		:49	22.5	25.0	55.6	55.6	4.5	6.3	10.3	12.5
7		1:08	24.6	26.0	60.7	57.8	9.3	9.4	21.4	18.6
5	600	:41	27.8	31.0	68.7	68.8	10.3	10.6	23.7	21.0
3		2:05	29.5	32.7	72.8	72.7	11.7	13.7	26.9	27.1
2.5		1:28	30.3	33.5	74.8	75.5	12.6	15.6	29.0	30.9
2.0		2:36	31.3	34.9	77.3	77.7	14.7	18.4	33.8	36.4
1.5	1200	1:29	32.4	36.0	80.0	80.0	20.7	21.0	47.6	41.6
1.0		3:55	37.0	40.0	91.3	89.0	29.5	28.0	67.8	55.3
0.9		1:45	37.0	40.5	91.3	90.0	32.0	31.0	73.6	61.3
.7	1800	2:56	38.0	42.0	93.8	93.3	37.0	41.0	85.0	81.2
.5		6:26	39.5	43.7	97.6	97.2	41.0	44.5	94.3	88.2
.4		7:17	39.7	44.4	98.0	98.7	47.5	48.4	97.8	95.8
.3		15:14	40.0	44.7	98.8	99.3	43.3	49.5	99.7	98.0
.2	3600	11:04	40.5	45.0	100.	100.	43.5	50.5	100.	99.0
.1		57:09					50.5		100.0	

TABLE 19

MSA PARTICLE SIZE ANALYSIS OF BARIUM CHROMATE—LOTS MP 31801 AND MP 30701

Particle Size, d (microns)	Centrifuge Speed (RPM)	Centrifuge Time (min:sec)	MP 31801				MP 30701			
			Sediment Height		Percent Greater Than		Sediment Height		Percent Greater Than	
			h ₁	h ₂	d	% ₂	h ₁	h ₂	d	% ₂
20	300	:16		11.0		28.6	1.2	0.9	2.8	1.9
10		:49		20.0		51.8	6.8	7.0	15.8	14.8
7		1:08		24.0		62.3	9.8	9.1	22.8	19.2
5	600	:41	17.0	24.4	60.0	63.3	11.7	11.5	27.2	24.3
3		2:05	18.5	27.4	65.2	71.2	14.4	13.8	33.5	29.1
2.5		1:28	18.8	29.4	66.3	76.3	15.3	15.8	35.6	33.3
2.0		2:36	19.4	31.6	68.3	82.0	16.8	16.9	39.1	35.6
1.5	1200	1:29	22.7	32.4	80.0	94.2		18.0		37.9
1.0		3:55	24.0	35.3	84.6	91.7	24.0	25.0	55.8	52.7
0.9		1:45	25.5	35.8	90.0	93.0	27.3	27.7	63.5	58.3
0.7	1800	2:56	26.5	35.9	93.5	93.3	31.0	33.4	72.2	70.0
0.5		6:26	27.5	37.4	97.0	97.0	36.2	40.0	84.2	84.3
0.4		7:17	28.3	37.8	97.7	98.2	39.5	42.0	91.8	88.5
0.3		15:14	28.4	38.2	100.	99.2	41.0	44.5	95.3	93.8
0.2	3600	11:04		38.5		100.0	41.5	45.7	96.5	96.3
0.1		57:09					43.0	47.4	100.0	100.0

TABLE 20

MSA PARTICLE SIZE ANALYSIS OF BARIUM CHROMATE—LOT B&C FINE

Particle Size, d (microns)	Centrifuge Speed (RPM)	Centrifuge Time (min:sec)	B&C FINE			
			Sediment Height		Percent Greater Than d	
			h ₁	h ₂	% ₁	% ₂
20	300	:16	0.2	0.1	0.4	0.2
10		:49	1.8	2.4	3.2	4.2
7		1:08	3.0	4.4	5.3	7.7
5	600	:41	9.0	7.6	16.0	13.3
3		2:05	19.0	21.5	33.9	37.7
2.5		1:28	24.8	29.0	44.2	51.0
2.0		2:36	32.6	37.5	58.2	65.8
1.5	1200	1:29	43.2	46.5	77.0	81.7
1.0		3:55	51.0	54.5	91.0	95.8
.9		1:45	52.0	55.5	92.8	97.5
.7	1800	2:56	53.6	53.7	95.6	97.8
.5		6:26	55.1	56.5	98.2	99.2
.4		7:17	55.5	56.6	98.9	99.3
.3		15:14	55.6	56.7	99.1	99.6
.2	3600	11:04	56.1	56.9	100.0	100.0

TABLE 21

MSA PARTICLE SIZE ANALYSIS OF BORON-LOTS TRONA 419 AND TRONA 571

Particle Size, d (Microns)	Centrifuge Speed (RPN)	Centrifuge Time (min:sec)	TRONA 419			TRONA 571							
			Sediment Height		Percent Greater Than		Sediment Height		Percent Greater Than				
			h ₁	h ₂	d	% ₁	% ₂	h ₁	h ₂	d	% ₁	% ₂	
20	300	:43											
15		1:17	0.0		0.0		0.0	0.0	0.0	0.0	0.0		
10		2:09	0.9		4.2		2.5	1.5	10.2	6.9			
5	600	2:19	6.6		31.0		8.7	6.3	35.5	28.9			
2	1200	3:57	12.3		57.7		14.6	13.6	59.6	62.3			
1.0	1800	6:29	16.7		78.3		20.0	18.5	81.6	84.8			
0.8		5:01	17.6		87.6		20.5	19.0	83.6	87.2			
0.6		10:09	18.3		85.8		21.9	19.5	88.5	89.4			
0.4	3600	7:35	20.1		94.3		23.5	21.0	95.9	96.3			
0.3		10:22	20.9		98.0		24.0	-	97.8	-			
0.2		27:37	21.1		99.0		24.4	21.3	99.5	97.8			
0.16		30:09	21.2		99.6		24.4	21.6	99.5	99.2			
0.12		59:21	21.2		99.6		24.5	21.8	100.0	100.0			
0.10		59:21	21.3		100.0								

TABLE 22

MSA PARTICLE SIZE ANALYSIS OF BORON-LOT HCST 873

Particle Size, d (microns)	Centrifuge Speed (RPM)	Centrifuge Time (min:sec)	LOT HCST 873			
			Sediment Height		Percent Greater Than d	
			h ₁	h ₂	% ₁	% ₂
20	300	:43	0.0	0.0	0.0	0.0
10		2:09	0.0	0.1	0.0	0.7
5	600	2:19	2.9	3.0	19.1	19.9
2	1200	3:57	7.5	7.3	49.3	48.3
1.0	1800	6:29	10.4	10.2	68.5	67.7
.8		5:01	11.0	10.9	72.3	72.3
.6		10:09	11.5	11.3	75.7	74.8
.4	3600	7:35	14.2	14.0	93.4	92.8
.3		10:22	14.5	14.2	95.3	94.1
.2		27:37	15.0	15.0	98.8	99.3
.16		30:09	15.2	15.1	100.0	100.0

TABLE 23

MSA PARTICLE SIZE ANALYSIS OF BORON-HCST 900 AND HCST 954

Particle Size, d (microns)	Centrifuge Speed (RPM)	Centrifuge Time (min:sec)	HCST 900				HCST 954					
			Sediment Height		Percent Greater Than		Sediment Height		Percent Greater Than			
			h ₁	h ₂	d	% ₁	% ₂	h ₁	h ₂	d	% ₁	% ₂
20	300	:43	1.0 ¹		5.6 ¹			0.5 ¹		2.3 ¹		
15		1:17		1.7		7.2		1.3			6.2	
10		2:09	2.2	2.7	12.4	11.5		2.0	2.1	9.2	10.0	
5	600	2:19	5.2	5.4	29.4	23.0		6.1	5.6	28.0	26.7	
2	1200	3:57	10.0	12.6	56.4	53.7		12.0	10.5	55.0	50.0	
1.0	1800	6:29	13.9	19.5	78.5	82.8		16.0	15.1	73.3	71.8	
.8		5:01	16.1	20.0	90.8	85.2		17.0	15.6	77.9	74.2	
.6		10:09	16.2	21.3	91.5	90.6		17.9	16.5	82.1	78.6	
.4	3600	7:35	17.5	22.9	98.8	97.3		19.6	17.3	89.8	82.3	
.3		10:22	17.6	23.0	99.3	97.8		20.1	20.0	92.2	95.2	
.2		27:37	17.7	23.5	100.	100.0		20.4	20.2	93.5	96.2	
.16		30:09	20.7					20.7	20.4	96.3	97.2	
.12		59:21						—	—	—	—	
.10		59:21						21.8	21.0	100.0	100.0	

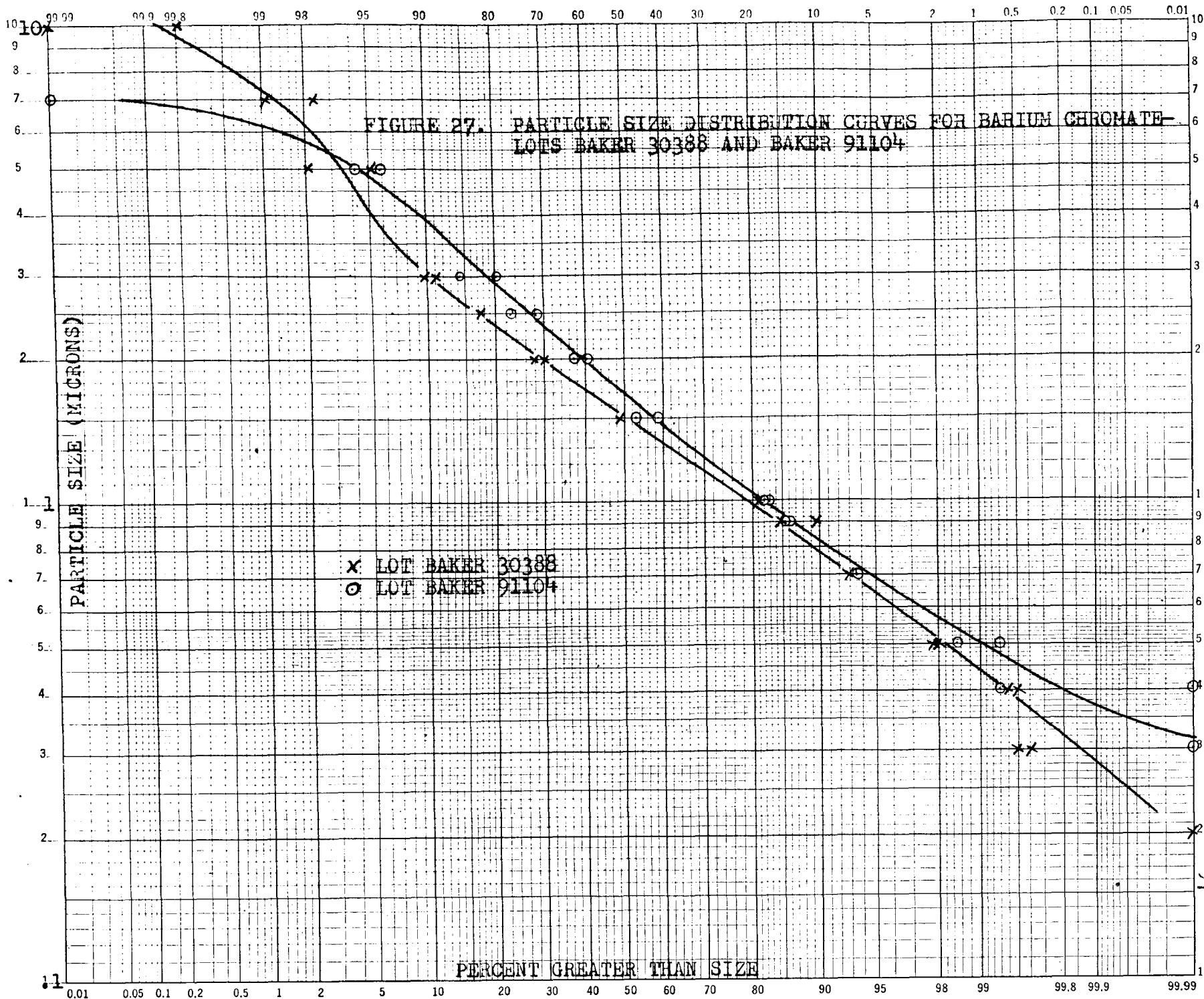
¹ Small portion of sample would not pass through the 325 mesh sieve before being washed directly into the Waring Blender, thus a portion of the greater than 20 microns portion of the sample was actually larger than 44 microns.

TABLE 24

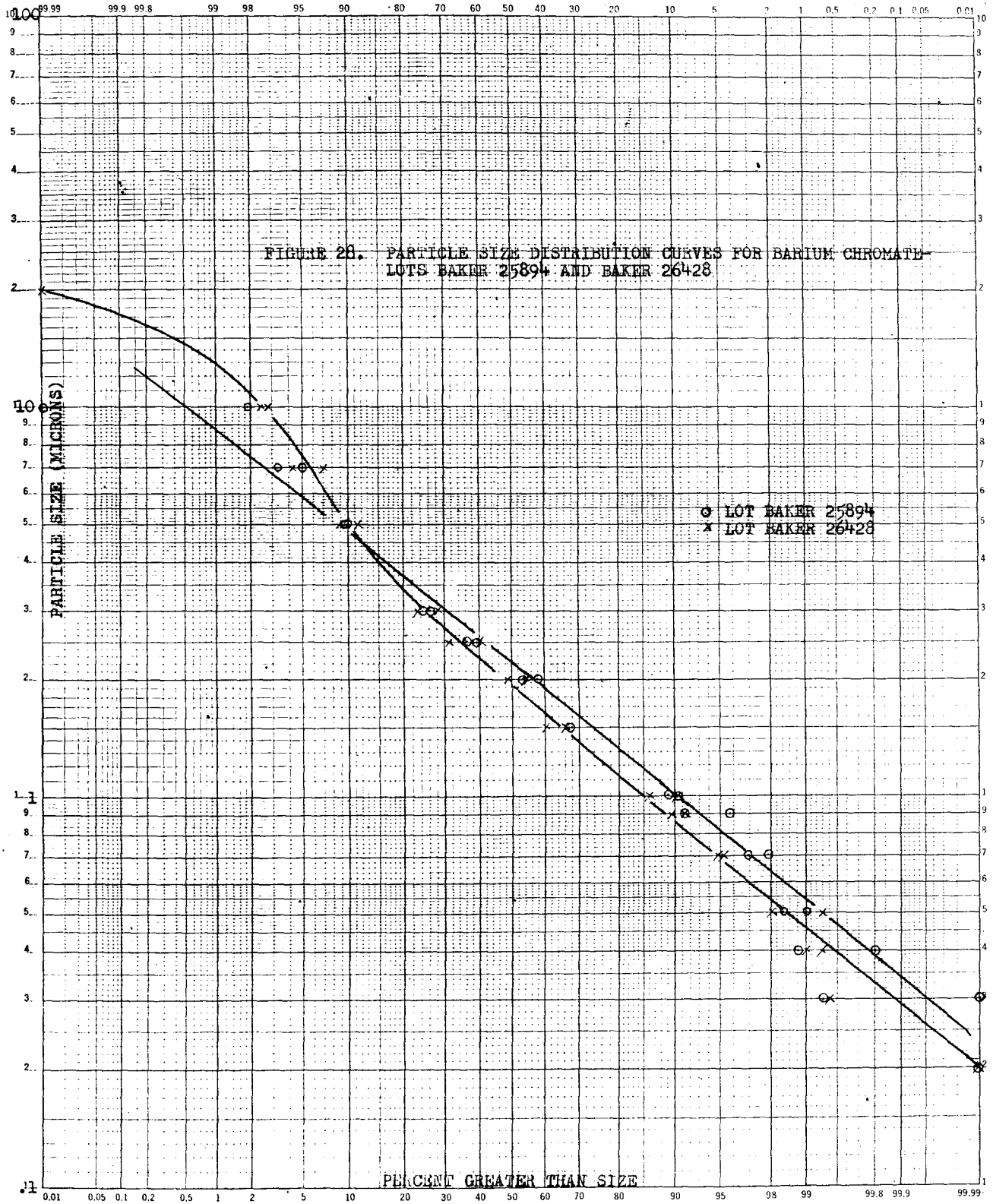
MSA PARTICLE SIZE ANALYSIS OF BORON—LOTS UMC 1992 AND UMC 1993

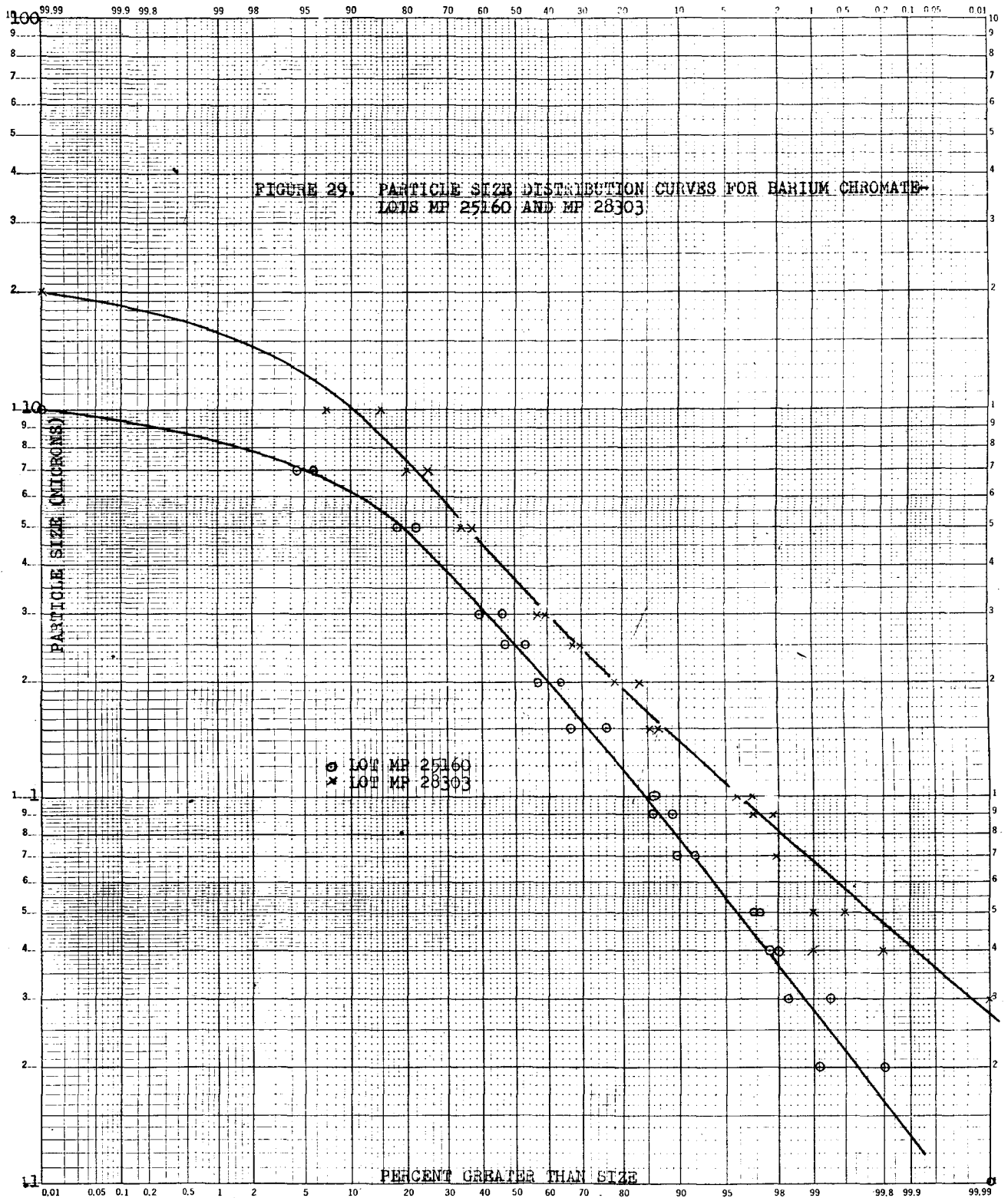
Particle Size, d (microns)	Centrifuge Speed (RPM)	Centrifuge Time (min:sec)	UMC 1992				UMC 1993				
			Sediment Height		Percent Greater Than		Sediment Height		Percent Greater Than		
			h ₁	h ₂	d	% ₁	% ₂	h ₁	h ₂	d	% ₁
25	300	:28	0.	1.5		4.1					
20		:43	3.4		8.0		0.9		4.4 ¹		
15		1:17					2.5			13.4	
10		2:09	20.6	14.5	48.7	39.2	2.5	4.5	12.3	24.1	
5	600	2:19	29.1	26.3	68.7	71.0	13.0	10.5	63.7	56.2	
2	1200	3:57	38.5	34.1	91.0	92.2	18.0	16.3	88.2	87.2	
1.0	1800	6:29	41.8	36.7	98.8	99.2	19.8	18.4	97.2	98.3	
.8		5:01	42.0	36.9	99.3	99.7	20.2	18.6	99.0	99.3	
.6		10:09	42.3	37.0	100.0	100.0	20.3	18.6	99.5	99.3	
.4	3600	7:35					20.4	18.7	100.0	100.0	

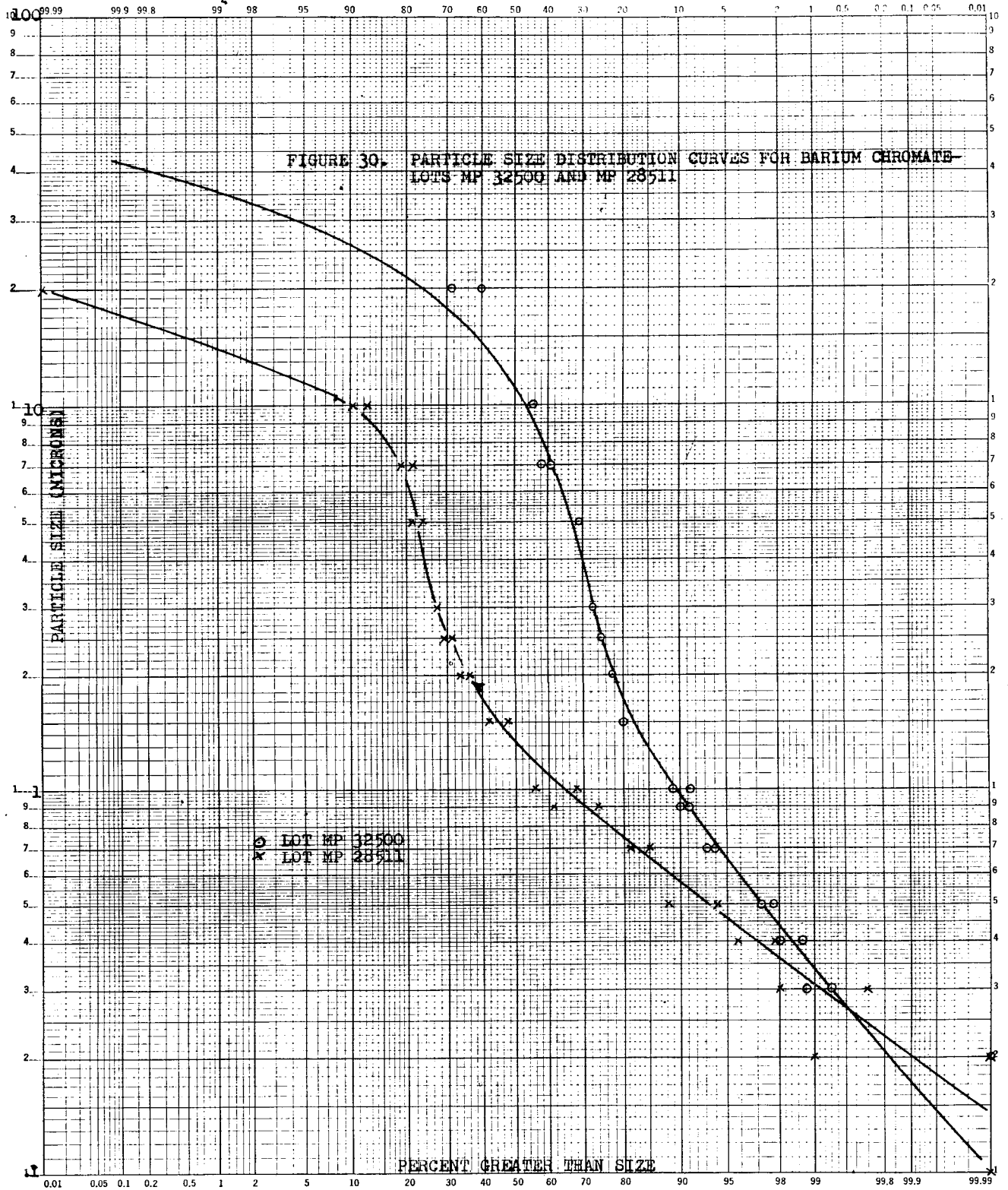
¹A small amount of this sample would not pass through the 325 mesh sieve before being washed directly into the Waring Blendor, thus a portion of the greater than 20 microns sample was actually larger than 44 microns.



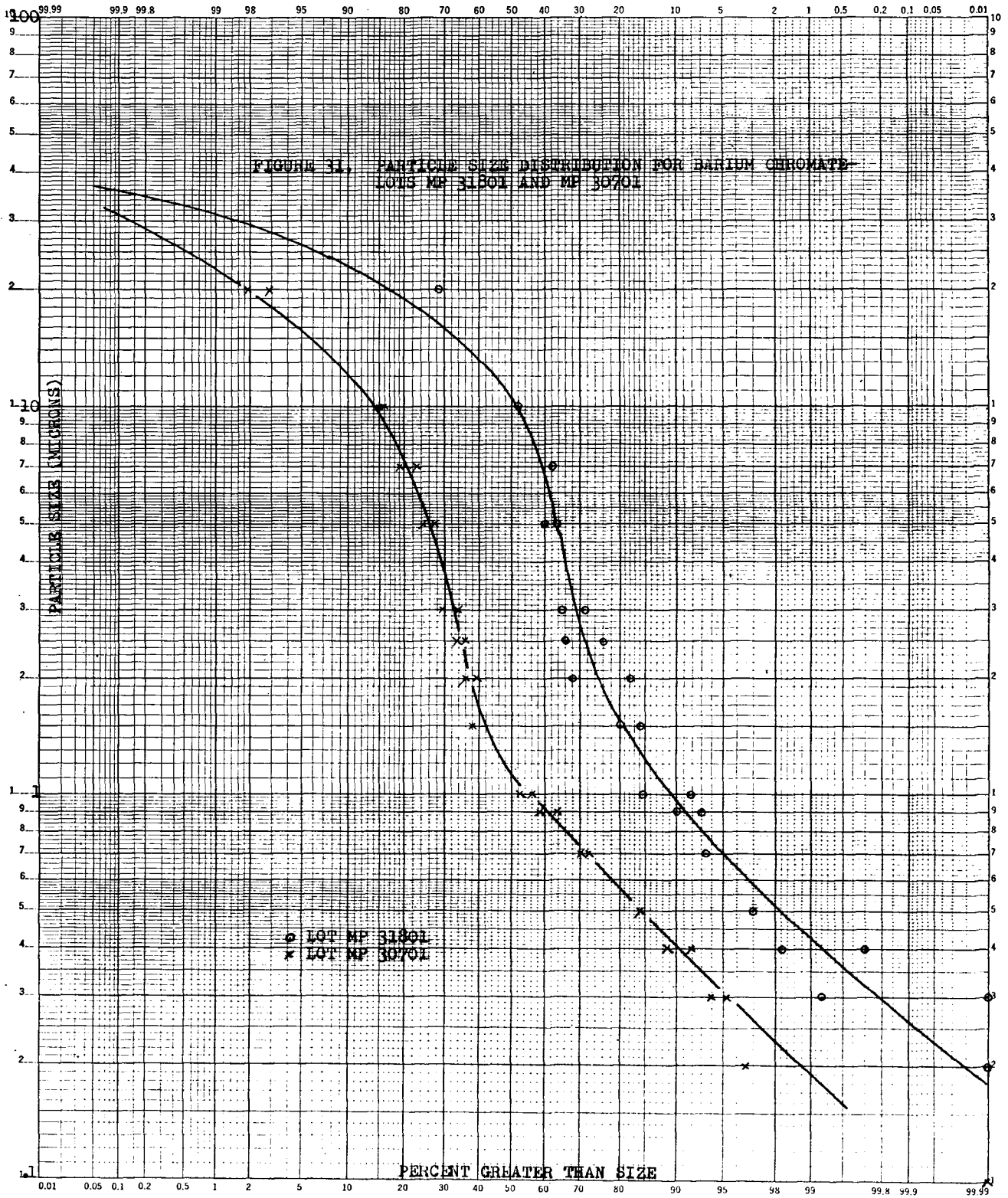
PROBABILITY 46 8040
X 2 LOG CYCLES
KLUFFEL & ESSER CO



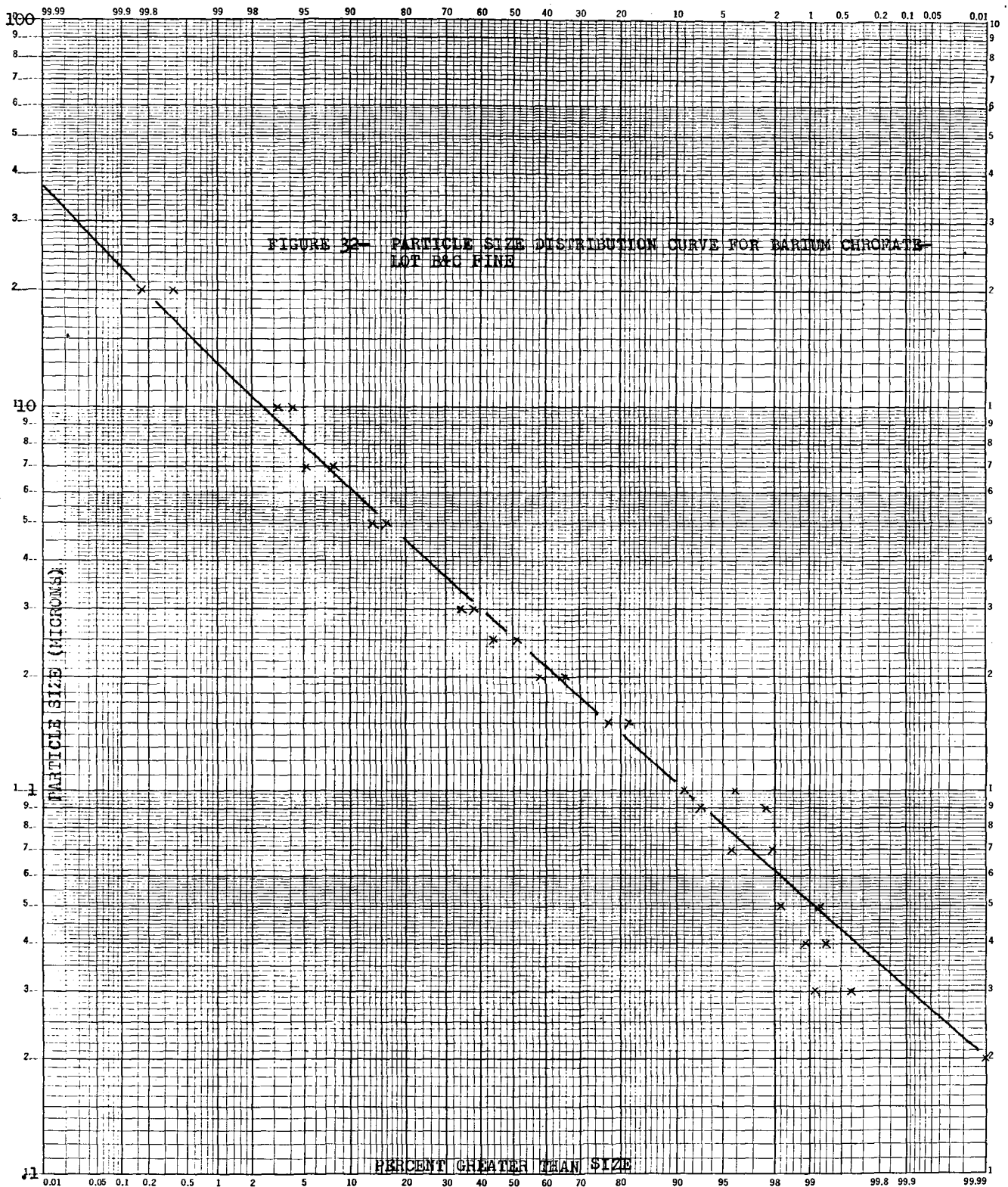


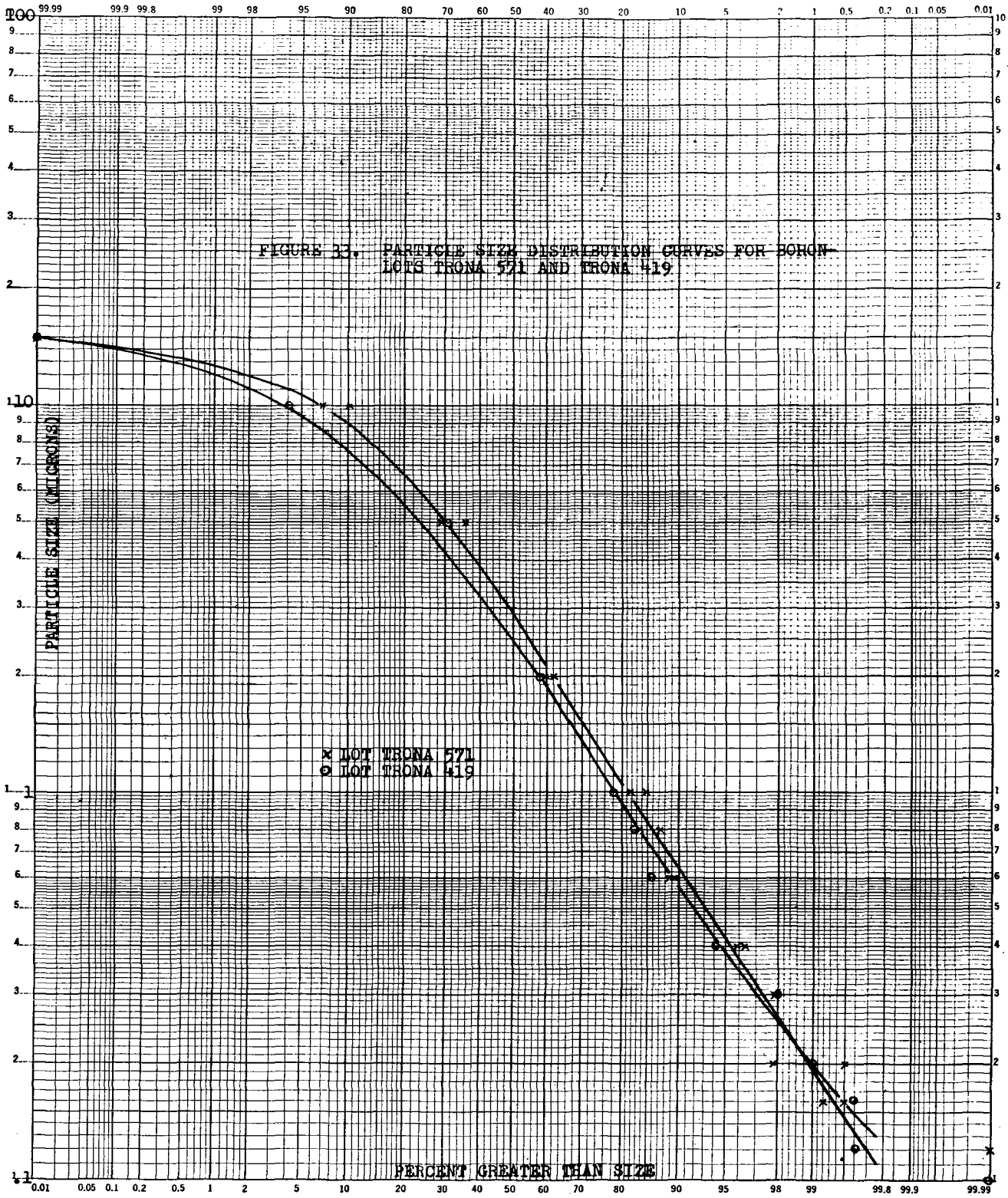


K Σ PROBABILITY 46 8040
 X 2 LOG CYCLES MADE IN U. S. A.
 KEUFFEL & ESSER CO.

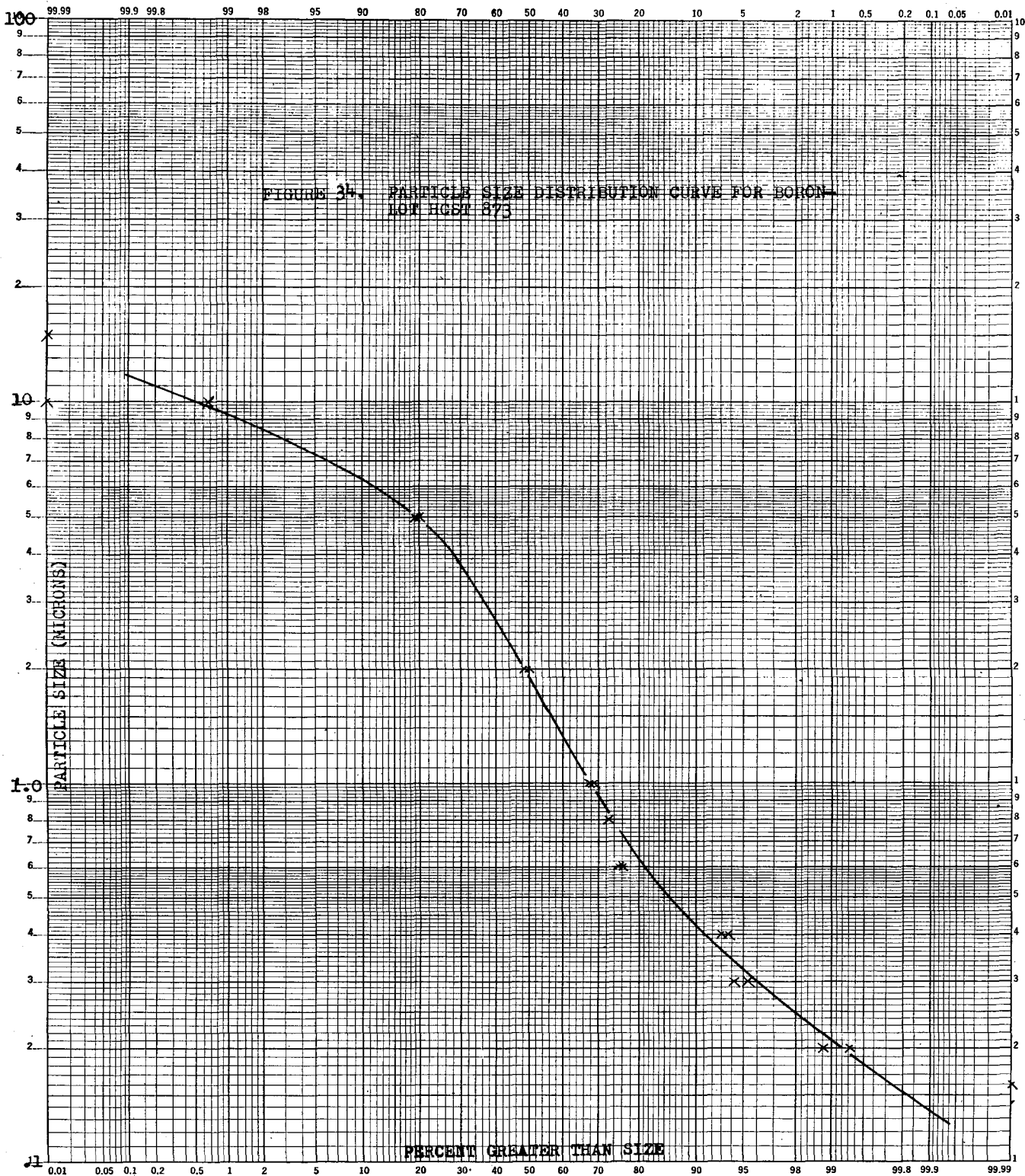


K&E PROBABILITY
X 2 LOG CYCLES
46 8040
MADE IN U.S.A.
KEUFFEL & ESSER CO.





K Σ PROBABILITY 46 8040
X 2 LOG CYCLES MADE IN U. S. A.
KEUFFEL & ESSER CO.



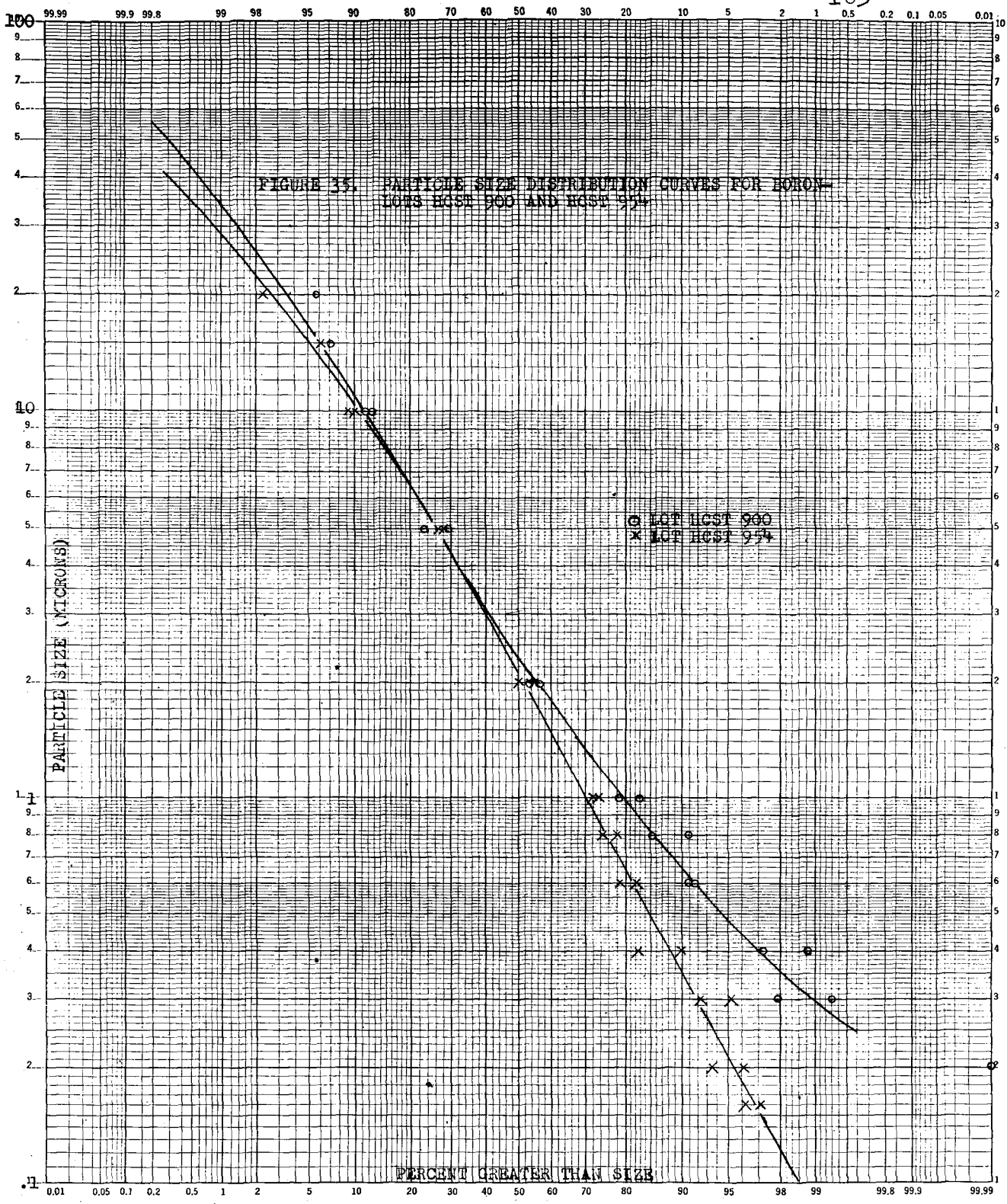


FIGURE 15. PARTICLE SIZE DISTRIBUTION CURVES FOR BORON LOTS HCST 900 AND HCST 954

○ LOT HCST 900
x LOT HCST 954

PERCENT GREATER THAN SIZE

K&E PROBABILITY 46 8040
X 2 LOG CYCLES MADE IN U.S.A.
KEUFFEL & ESSER CO.

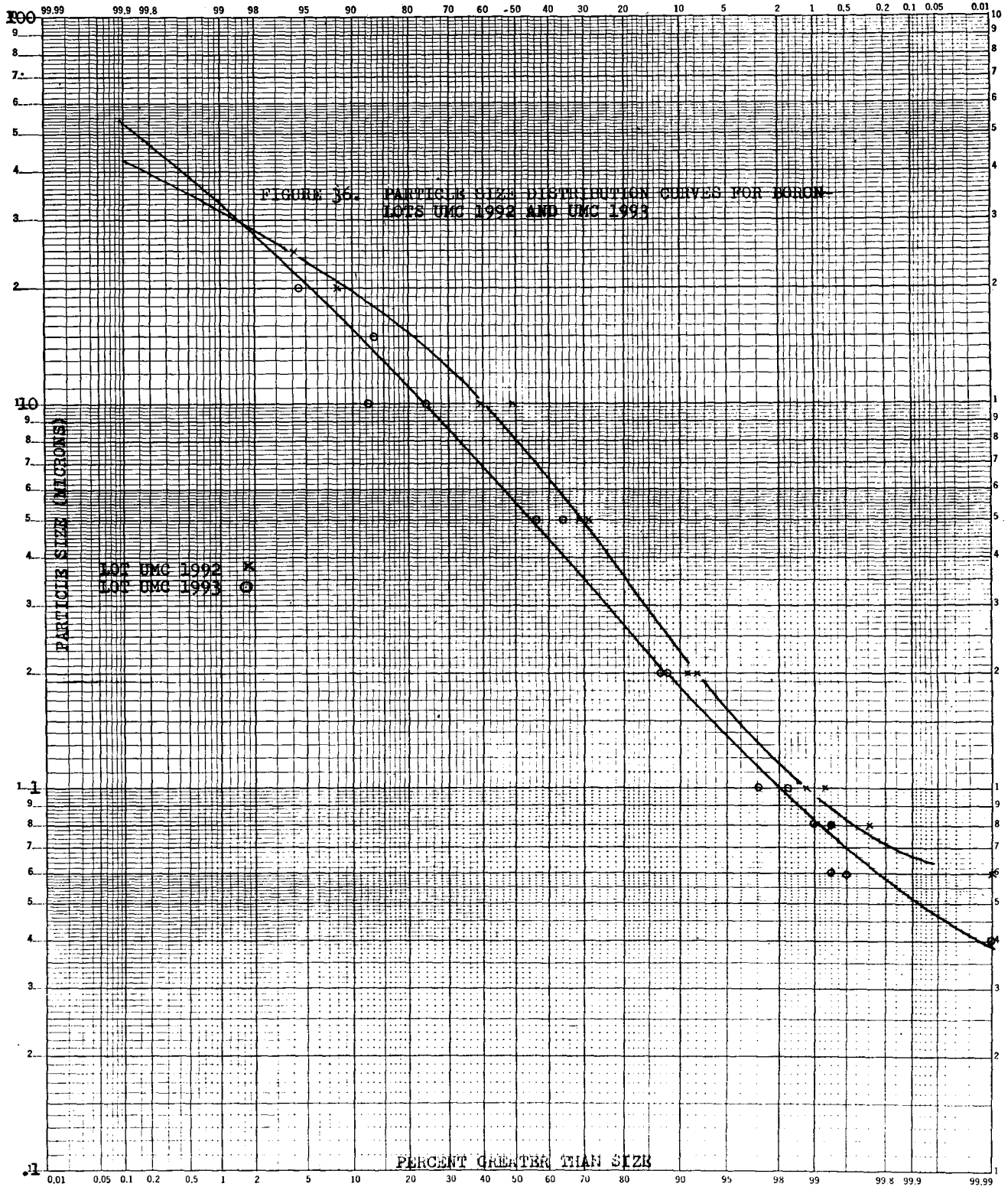


TABLE 25

SIZE FREQUENCY DATA FOR BARIUM CHROMATE-LOT BAKER 30388

Particle Size, \bar{d} (microns)	Mean Particle Size, \bar{d} (microns)	$\log \bar{d}$	Percent Greater Than \bar{d}	Frequency (percent)
10	12.6	1.1	.12	
6.3	7.9	.9	1.85	1.73
4.0	5.0	.7	5.3	3.45
2.5	3.2	.5	16.7	11.4
1.6	2.0	.3	46.0	29.3
1.0	1.26	.1	79.0	33.0
.63	.79	-.1	95.4	16.4
.40	.50	-.3	99.38	3.98
.25	.32	-.5	99.95	.57

TABLE 26

SIZE FREQUENCY DATA FOR BARIUM CHROMATE-LOT BAKER 91104

Particle Size, d (microns)	Mean Particle Size, \bar{d} (microns)	$\log \bar{d}$	Percent Greater Than d	Frequency (percent)
6.3	7.9	.9	.8	
4.0	5.0	.7	9.3	8.5
2.5	3.2	.5	26.5	17.2
1.6	2.0	.3	53.0	26.5
1.0	1.26	.1	81.3	28.3
.63	.79	-.1	96.6	15.3
.40	.50	-.3	99.83	3.23

TABLE 27

SIZE FREQUENCY DATA FOR BARIUM CHROMATE-LOT BAKER 25894

Particle Size, d (microns)	Mean Particle Size, \bar{d} (microns)	$\log \bar{d}$	Percent Greater Than d	Frequency (percent)
25	32	1.5	.00	
16	20	1.3	.04	.04
10	12.6	1.1	.54	.50
6.3	7.9	.9	3.7	3.16
4.0	5.0	.7	15.3	11.6
2.5	3.2	.5	40.0	24.7
1.6	2.0	.3	68.2	28.2
1.0	1.26	.1	89.3	21.1
.63	.79	-.1	97.6	8.3
.40	.50	-.3	99.7	2.1
.25	.32	-.5	99.98	.28

TABLE 28

SIZE FREQUENCY DATA FOR BARIUM CHROMATE-LOT BAKER 26428

Particle Size, d (microns)	Mean Particle Size, \bar{d} (microns)	$\log \bar{d}$	Percent Greater Than d	Frequency (percent)
40	50	1.7		
25	32	1.5	.0	
16	20	1.3	.22	.22
10	12.6	1.1	2.4	2.18
6.3	7.9	.9	6.6	4.2
4.0	5.0	.7	15.0	8.4
2.5	3.2	.5	34.0	19.0
1.6	2.0	.3	61.0	27.0
1.0	1.26	.1	84.7	23.7
.63	.79	-.1	96.1	11.4
.40	.50	-.3	99.4	3.3
.25	.32	-.5	99.95	.55

TABLE 29

SIZE FREQUENCY DATA FOR BARIUM CHROMATE-LOT MP 28303

Particle Size, d (microns)	Mean Particle Size, \bar{d} (microns)	$\log \bar{d}$	Percent Greater Than d	Frequency (percent)
25	32	1.5	.0	
16	20	1.3	.7	.7
1.0	12.6	1.1	10.5	9.8
6.3	7.9	.9	25.5	15.0
4.0	5.0	.7	44.5	19.0
2.5	3.2	.5	68.0	23.5
1.6	2.0	.3	86.3	18.3
1.0	1.26	.1	96.10	9.8
.63	.79	-.1	99.30	3.2
.40	.50	-.3	99.92	.62

TABLE 30

SIZE FREQUENCY DATA FOR BARIUM CHROMATE-LOT MP 25160

Particle Size, d (microns)	Mean Particle Size, \bar{d} (microns)	$\log \bar{d}$	Percent Greater Than d	Frequency (percent)
10	12.6	1.1	.0	
6.3	7.9	.9	10.0	10.0
4.0	5.0	.7	29.0	19.0
2.5	3.2	.5	50.7	21.7
1.6	2.0	.3	70.0	19.3
1.0	1.26	.1	84.4	14.4
.63	.79	-.1	93.3	8.9
.40	.50	-.3	97.4	4.1
.25	.32	-.5	99.28	1.88
.16	.20	-.7	99.81	.53

TABLE 31

SIZE FREQUENCY DATA FOR BARIUM CHROMATE-LOT MP 28511

Particle Size, d (microns)	Mean Particle Size, d (microns)	$\log \bar{d}$	Percent Greater Than d	Frequency (percent)
25	32	1.5		
16	20	1.3	.25	.25
10	12.6	1.1	10.4	10.15
6.3	7.9	.9	20.7	10.3
4.0	5.0	.7	24.2	3.5
2.5	3.2	.5	30.0	5.8
1.6	2.0	.3	41.3	11.3
1.0	1.26	.1	62.0	20.7
.63	.79	-.1	86.1	24.1
.40	.50	-.3	97.0	10.9
.25	.32	-.5	99.67	2.67
.16	.20	-.7	99.98	.31

TABLE 32

SIZE FREQUENCY DATA FOR BARIUM CHROMATE-LOT MP 30701

Particle Size, d (microns)	Mean Particle Size, \bar{d} (microns)	$\log \bar{d}$	Percent Greater Than d	Frequency (percent)
40	50	1.7	.02	
25	32	1.5	.58	.56
16	20	1.3	5.0	4.42
10	12.6	1.1	15.0	10.0
6.3	7.9	.9	22.7	7.7
4.0	5.0	.7	28.7	6.0
2.5	3.2	.5	34.2	5.5
1.6	2.0	.3	40.0	5.8
1.0	1.26	.1	53.5	13.5
.63	.79	-.1	75.5	22.0
.40	.50	-.3	90.04	14.9
.25	.32	-.5	97.4	7.0
.16	.20	-.7	99.54	2.14

TABLE 33

SIZE FREQUENCY DATA FOR BARIUM CHROMATE-LOT MP 32500

Particle Size, d (microns)	Mean Particle Size, d (microns)	$\log \bar{d}$	Percent Greater Than d	Frequency (percent)
40	50	1.7	.15	
25	32	1.5	13.3	13.15
16	20	1.3	35.0	21.7
10	12.6	1.1	53.0	18.0
6.3	7.9	.9	64.0	11.0
4.0	5.0	.7	70.0	6.0
2.5	3.2	.5	74.8	4.8
1.6	2.0	.3	80.4	5.6
1.0	1.26	.1	89.0	8.6
.63	.79	-.1	95.3	6.3
.40	.50	-.3	98.4	3.1
.25	.32	-.5	99.67	1.27
.16	.20	-.7	99.91	.24

TABLE 34

SIZE FREQUENCY DATA FOR BARIUM CHROMATE-LOT MP 31801

Particle Size, \bar{d} (microns)	Mean Particle Size, \bar{d} (microns)	$\log \bar{d}$	Percent Greater Than \bar{d}	Frequency (percent)
25	32	1.5	6.2	6.2
16	20	1.3	32.0	26.0
10	12.6	1.1	51.5	19.5
6.3	7.9	.9	61.0	9.5
4.0	5.0	.7	66.0	5.0
2.5	3.2	.5	71.2	5.2
1.6	2.0	.3	79.4	8.2
1.0	1.26	.1	88.6	9.2
.63	.79	-.1	96.4	7.8
.40	.50	-.3	99.3	2.9
.25	.32	-.5	99.93	.63

TABLE 35

SIZE FREQUENCY DATA FOR BARIUM CHROMATE--LOT B & C FINE

Particle Size, d (microns)	Mean Particle Size, \bar{d} (microns)	$\log \bar{d}$	Percent Greater Than \bar{d}	Frequency (percent)
40	50	1.7		
25	32	1.5	.06	.06
16	20	1.3	.43	.37
10	12.6	1.1	2.3	1.87
6.3	7.9	.9	9.3	7.0
4.0	5.0	.7	24.7	15.4
2.5	3.2	.5	50.5	25.8
1.6	2.0	.3	73.8	23.3
1.0	1.26	.1	90.6	16.8
.63	.79	-.1	97.6	7.0
.40	.50	-.3	99.58	1.98
.25	.32	-.5	99.95	.37

TABLE 36
 SIZE FREQUENCY DATA FOR BORON-LOT TRONA 571

Particle Size, \bar{d} (microns)	Mean Particle Size, \bar{d} (microns)	$\log \bar{d}$	Percent Greater Than \bar{d}	Frequency (percent)
16	20	1.3	.0	
10	12.6	1.1	6.4	6.4
6.3	7.9	.9	22.2	15.8
4.0	5.0	.7	39.0	16.8
2.5	3.2	.5	55.0	16.0
1.6	2.0	.3	69.0	14.0
1.0	1.26	.1	81.2	12.2
.63	.79	-.1	89.8	8.6
.40	.50	-.3	95.2	5.4
.25	.32	-.5	98.1	2.9
.16	.20	-.7	99.32	1.2
.10	.126	-.9	99.8	.5

TABLE 37
 SIZE FREQUENCY DATA FOR BORON-LOT TRONA 419

Particle Size, \bar{d} (microns)	Mean Particle Size, \bar{d} (microns)	$\log \bar{d}$	Percent Greater Than \bar{d}	Frequency (percent)
16	20	1.3	.0	
10	12.6	1.1	3.5	3.5
6.3	7.9	.9	16.0	12.5
4.0	5.0	.7	32.3	16.3
2.5	3.2	.5	49.6	17.3
1.6	2.0	.3	64.6	15.0
1.0	1.26	.1	77.0	12.4
.63	.79	-.1	87.4	10.4
.40	.50	-.3	94.3	6.9
.25	.32	-.5	97.8	3.5
.16	.20	-.7	99.43	1.63
.10	.126	-.9	99.93	.50

TABLE 38

SIZE FREQUENCY DATA FOR BORON-LOT HCST 873

Particle Size, d (microns)	Mean Particle Size, \bar{d} (microns)	$\log \bar{d}$	Percent Greater Than d	Frequency (percent)
16	20	1.3	.00	
10	12.6	1.1	.05	.05
6.3	7.9	.9	10.02	10.15
4.0	5.0	.7	28.0	17.2
2.5	3.2	.5	42.5	14.5
1.6	2.0	.3	54.0	11.5
1.0	1.26	.1	66.6	12.6
.63	.79	-.1	79.3	12.7
.40	.50	-.3	91.0	11.7
.25	.32	-.5	98.0	7.0
.16	.20	-.7	99.80	1.8

TABLE 39

SIZE FREQUENCY DATA FOR BORON-LOT HCST 900

Particle Size, \bar{d} (microns)	Mean Particle Size, \bar{d} (microns)	$\log \bar{d}$	Percent Greater Than \bar{d}	Frequency (percent)
63			.12	
40	50	1.7	.64	.52
25	32	1.5	2.3	1.66
16	20	1.3	5.5	3.2
10	12.6	1.1	11.6	6.1
6.3	7.9	.9	20.8	9.2
4.0	5.0	.7	32.8	12.0
2.5	3.2	.5	48.8	16.0
1.6	2.0	.3	64.0	15.2
1.0	1.26	.1	79.0	15.0
.63	.79	-.1	90.05	11.5
.40	.50	-.3	96.9	6.4
.25	.32	-.5	99.6	2.7
.16	.20	-.7	99.99	.39
.10	.126	-.9		

TABLE 40
 SIZE FREQUENCY DATA FOR BORON-LOT HCST 954

Particle Size, d (microns)	Mean Particle Size, \bar{d} (microns)	$\log \bar{d}$	Percent Greater Than d	Frequency (percent)
40	50	1.7	.35	
25	32	1.5	1.55	1.2
16	20	1.3	4.6	3.0
1.0	12.6	1.1	10.06	6.0
6.3	7.9	.9	20.0	9.4
4.0	5.0	.7	31.5	11.5
2.5	3.2	.5	44.7	13.2
1.6	2.0	.3	57.4	12.7
1.0	1.26	.1	70.0	12.6
.63	.79	-.1	80.4	10.4
.40	.50	-.3	88.2	7.8
.25	.32	-.5	93.4	5.2
.16	.20	-.7	96.6	3.2
.10	.126	-.9	98.5	1.9

TABLE 41

SIZE FREQUENCY DATA FOR BORON-LOT UMC 1992

Particle Size, d (microns)	Mean Particle Size, \bar{d} (microns)	$\log \bar{d}$	Percent Greater Than d	Frequency (percent)
63			.0	
40	50	1.7	.05	.05
25	32	1.5	4.0	3.95
16	20	1.3	18.4	14.4
10	12.6	1.1	41.0	22.6
6.3	7.9	.9	61.0	20.0
4.0	5.0	.7	75.5	14.5
2.5	3.2	.5	88.0	12.5
1.6	2.0	.3	95.0	7.0
1.0	1.26	.1	98.8	3.8
.63	.79	-.1	99.93	1.13

TABLE 42
 SIZE FREQUENCY DATA FOR BORON-LOT UMC 1993

Particle Size, d (microns)	Mean Particle Size, \bar{d} (microns)	$\log \bar{d}$	Percent Greater Than d	Frequency (percent)
63			.03	
40	50	1.7	.44	.41
25	32	1.5	2.6	2.16
16	20	1.3	9.5	6.9
10	12.6	1.1	24.0	14.5
6.3	7.9	.9	43.0	19.0
4.0	5.0	.7	64.0	21.0
2.5	3.2	.5	81.0	17.0
1.6	2.0	.3	92.2	11.2
1.0	1.26	.1	97.8	5.6
.63	.79	-.1	99.68	1.88
.40	.50	-.3	99.99	.31

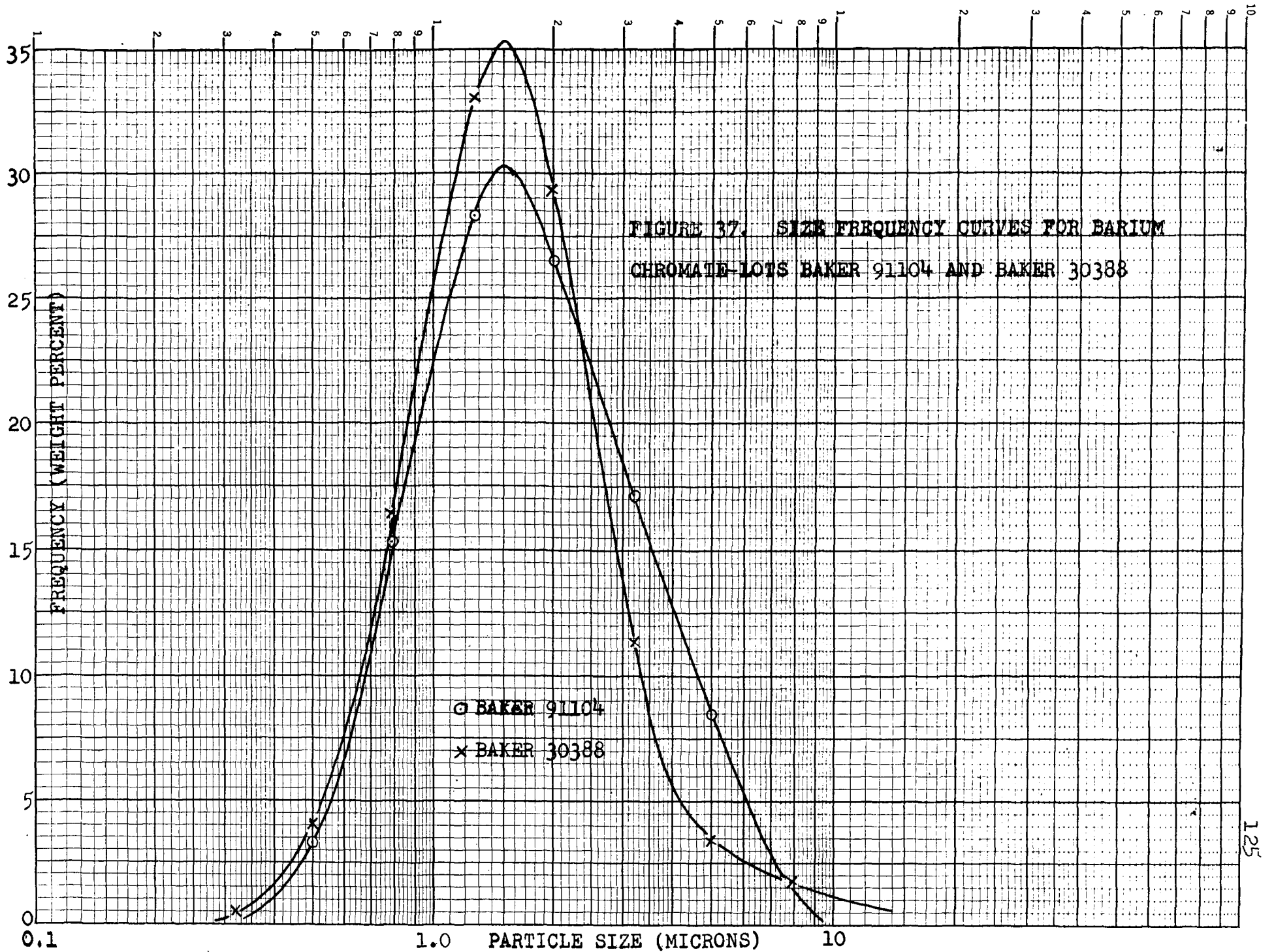


FIGURE 37. SIZE FREQUENCY CURVES FOR BARIUM CHROMATE-LOTS BAKER 91104 AND BAKER 30388

o BAKER 91104
x BAKER 30388

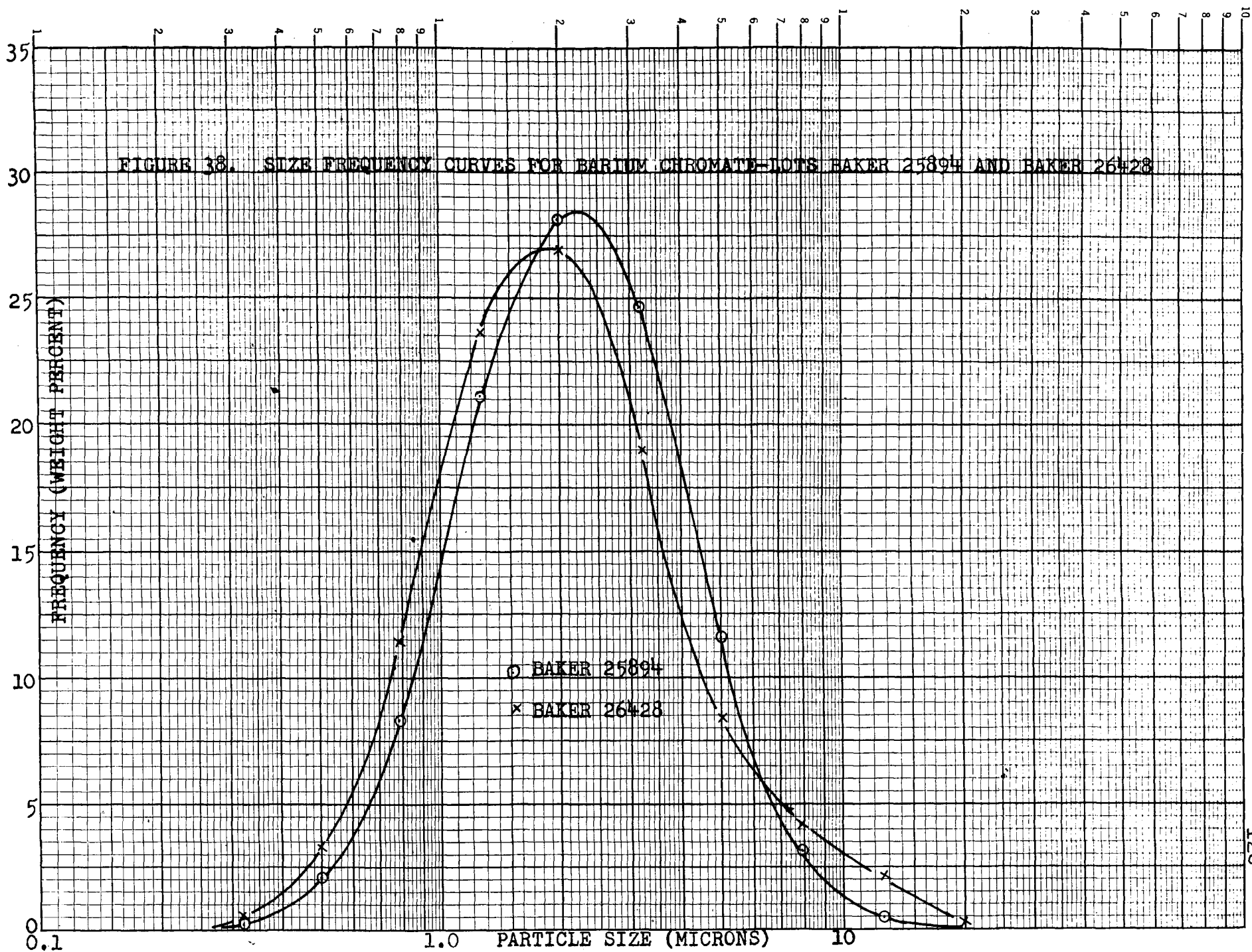
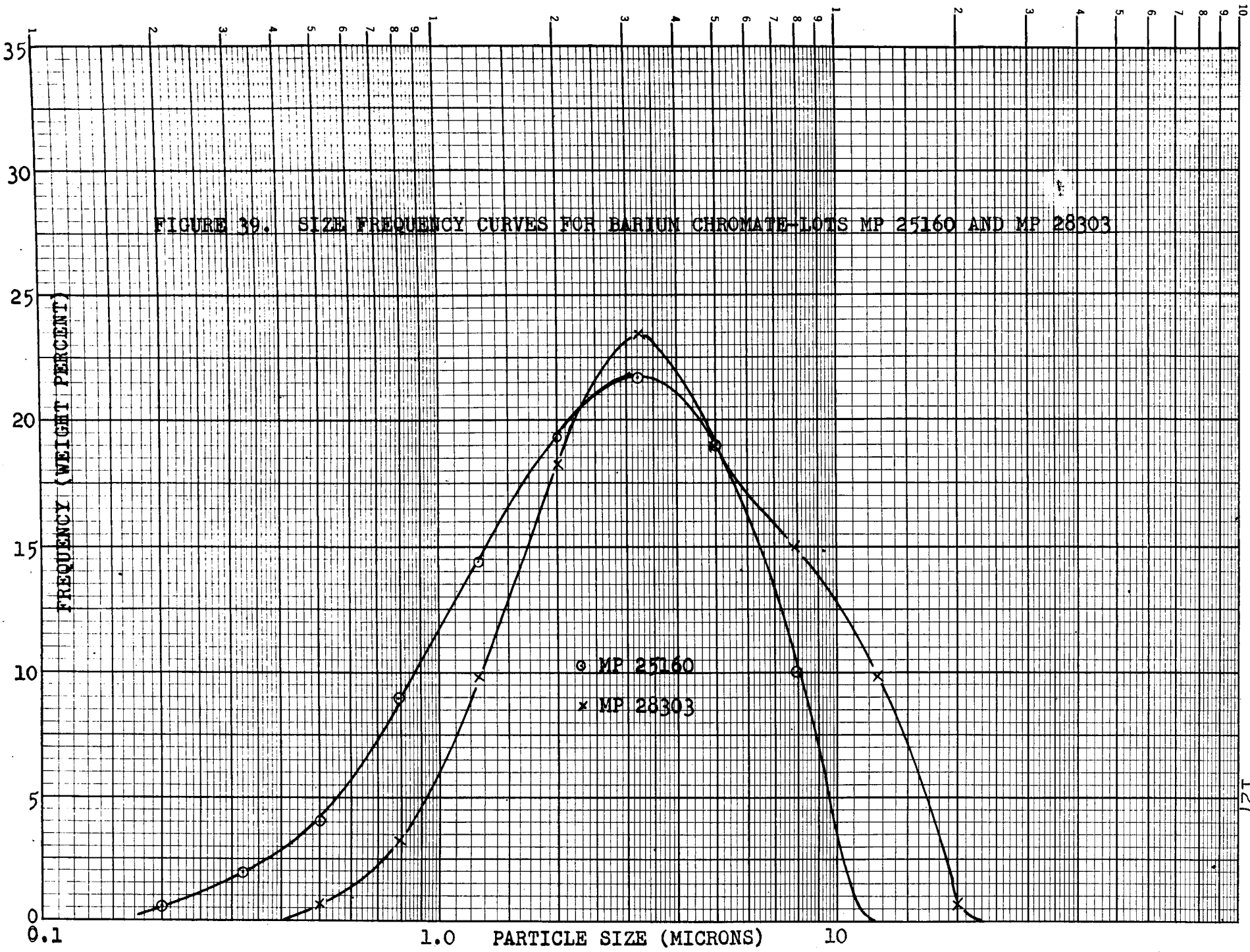


FIGURE 39. SIZE FREQUENCY CURVES FOR BARIUM CHROMATE-LOTS MP 25160 AND MP 28303



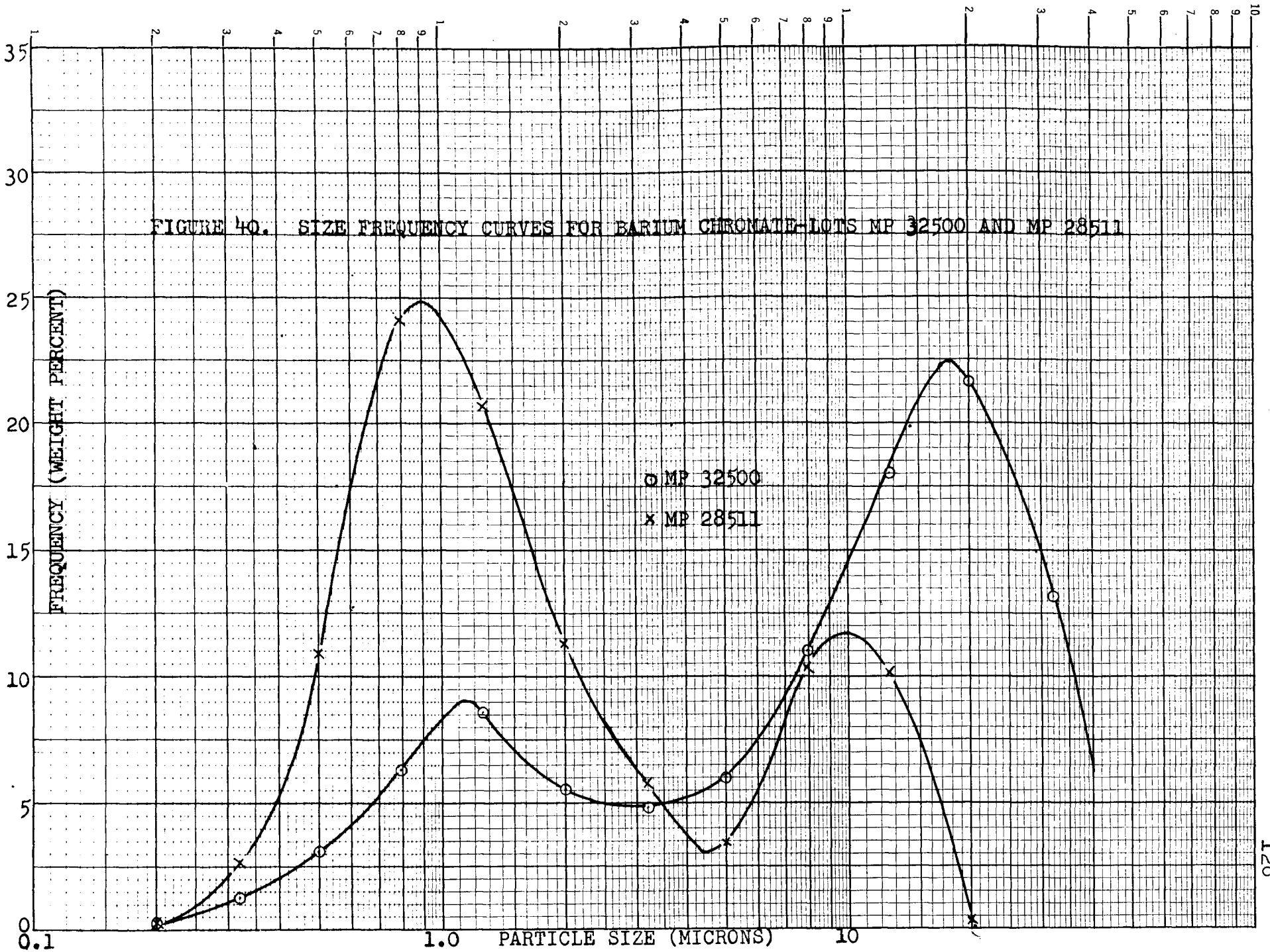


FIGURE 40. SIZE FREQUENCY CURVES FOR BARIUM CHROMATE- LOTS MP 32500 AND MP 28511

○ MP 32500
x MP 28511

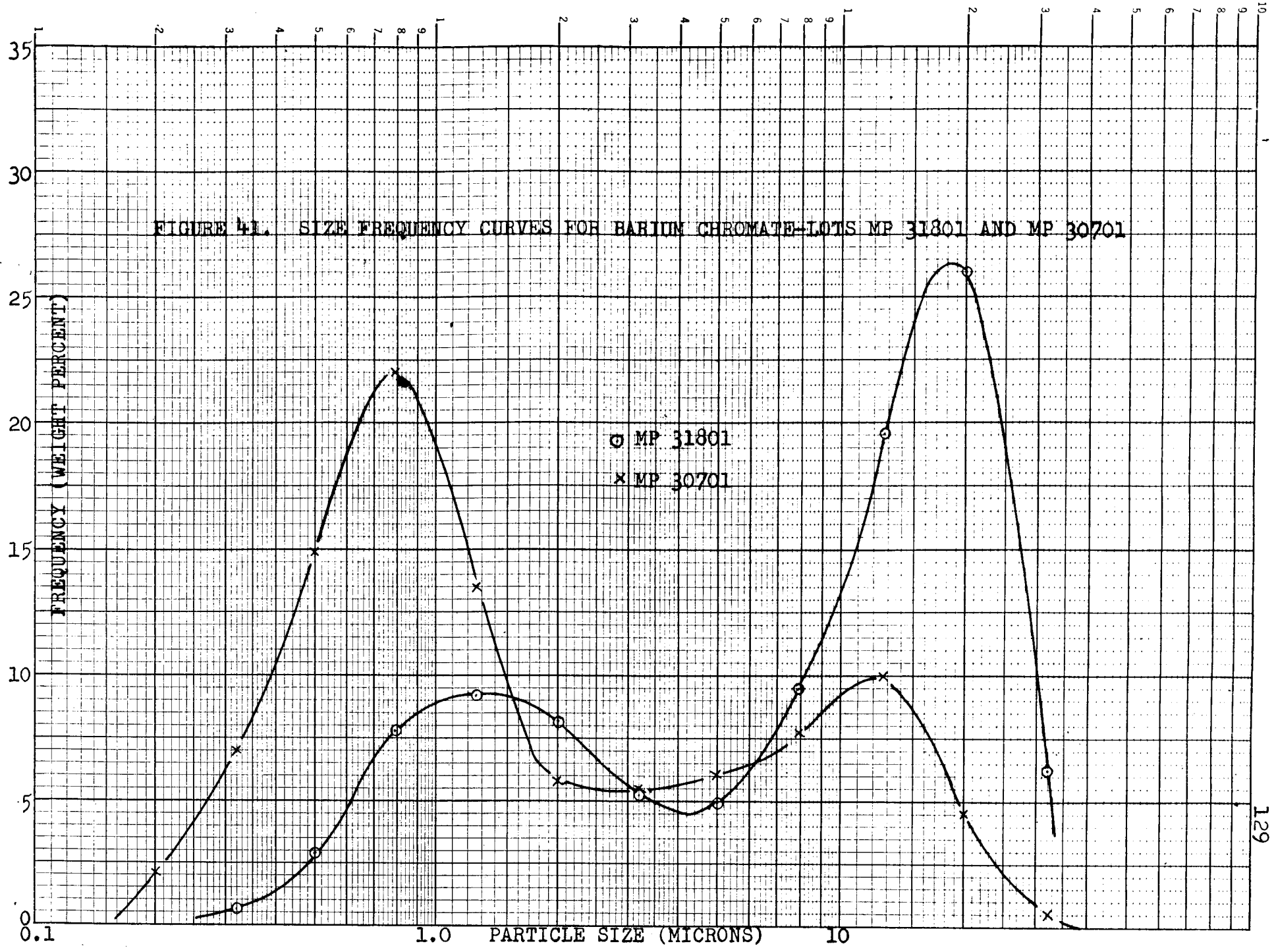
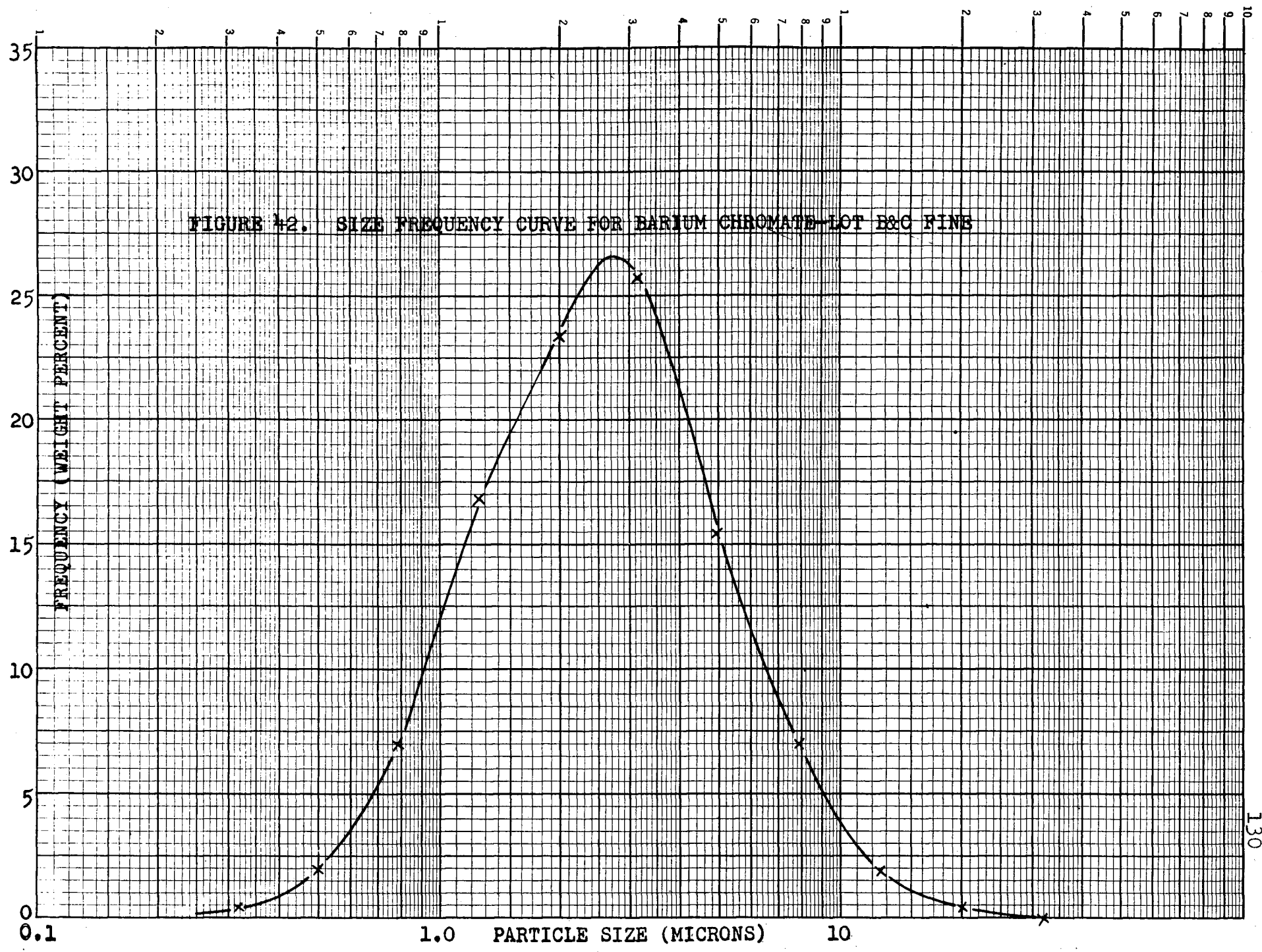


FIGURE 41. SIZE FREQUENCY CURVES FOR BARIUM CHROMATE-LOTS MP 31801 AND MP 30701

○ MP 31801
× MP 30701



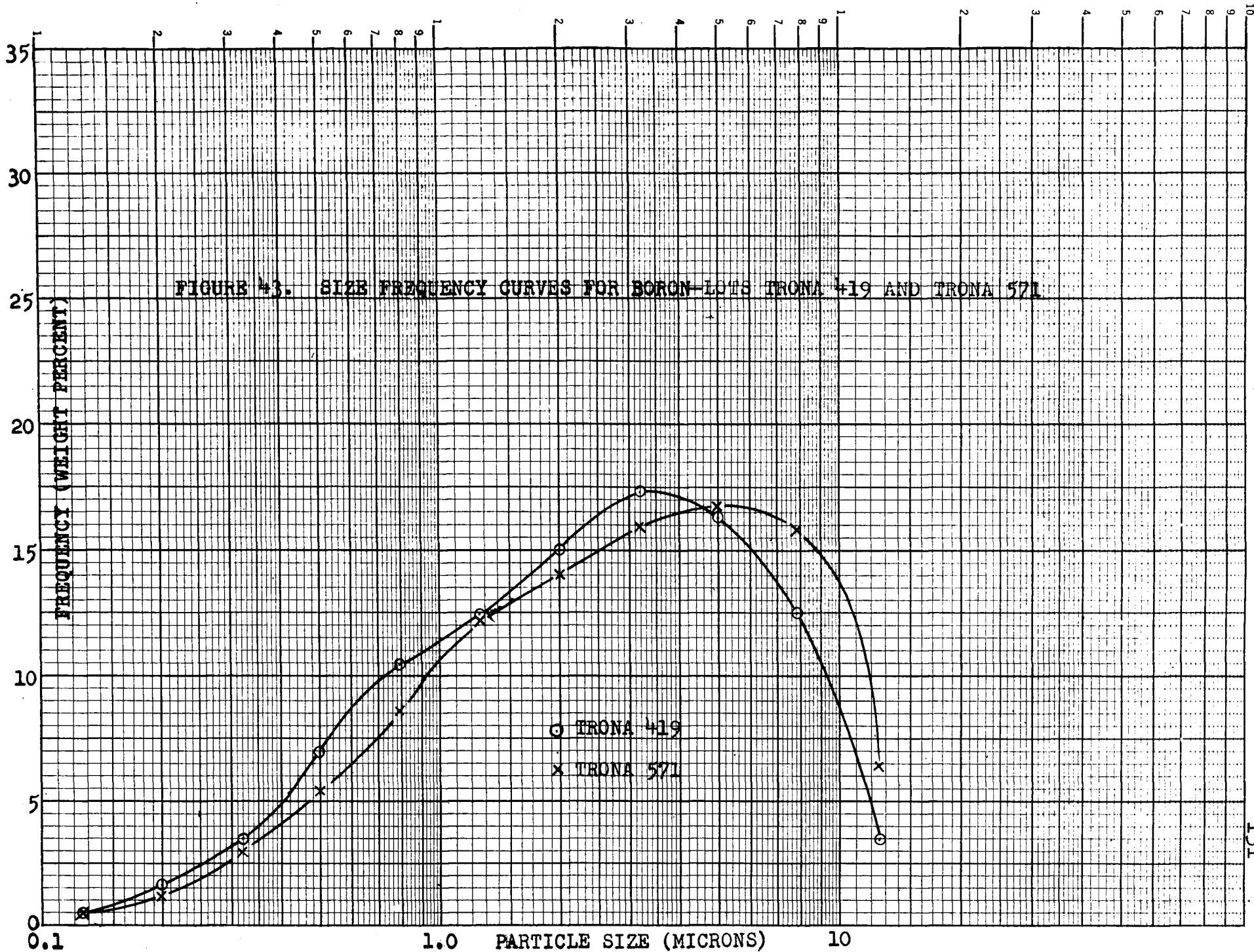
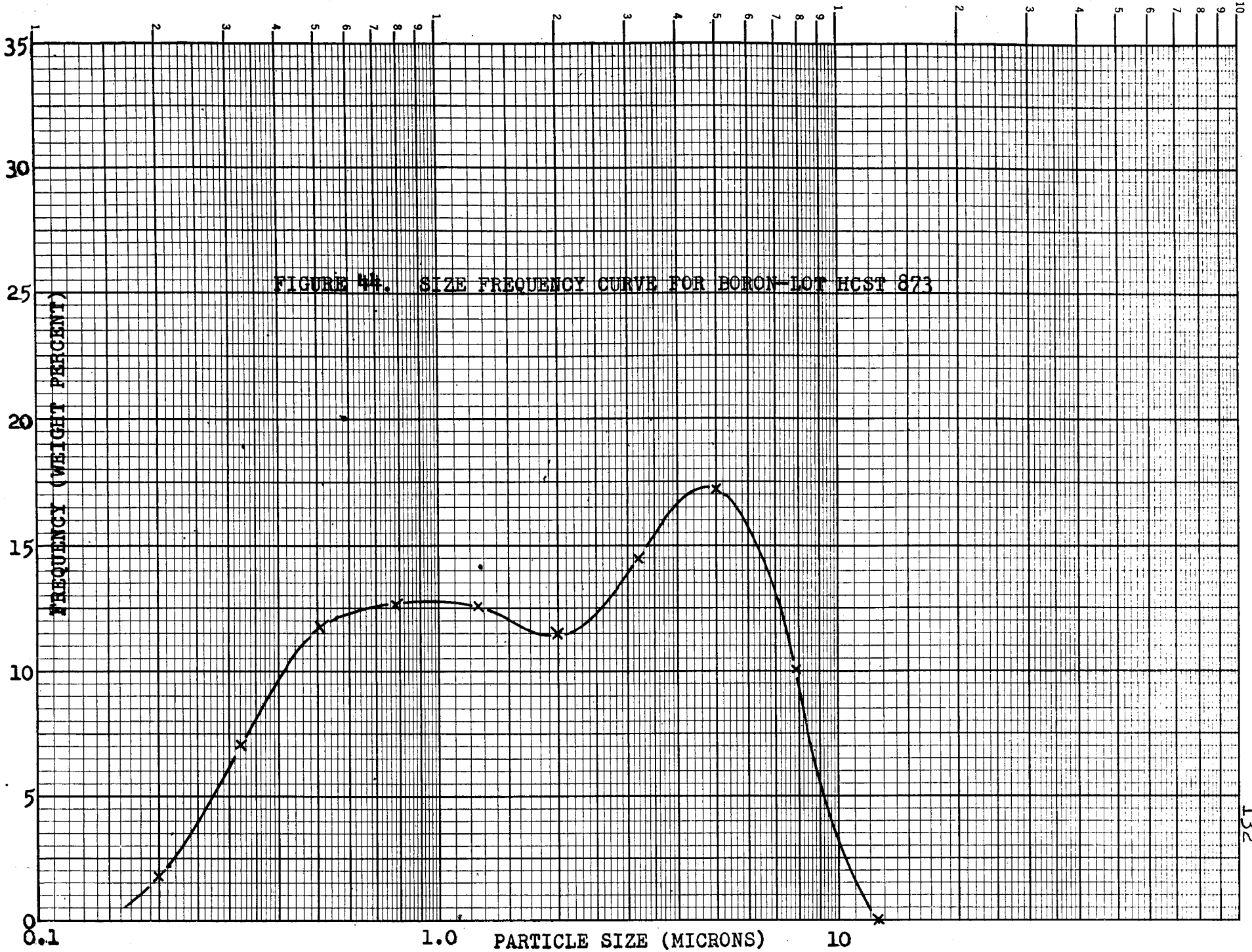
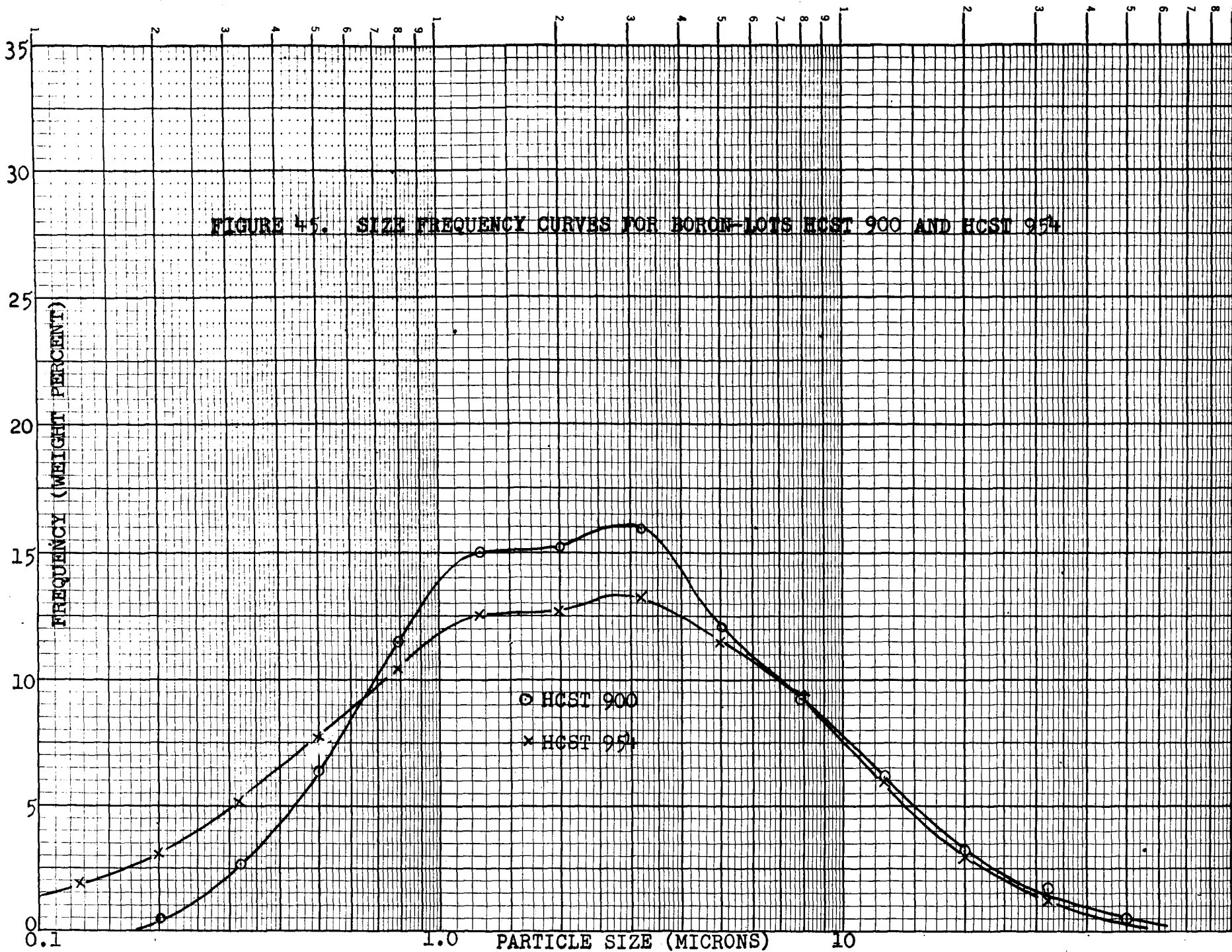


FIGURE 43. SIZE FREQUENCY CURVES FOR BORON-LOTS TRONA +19 AND TRONA 571

O TRONA +19
X TRONA 571





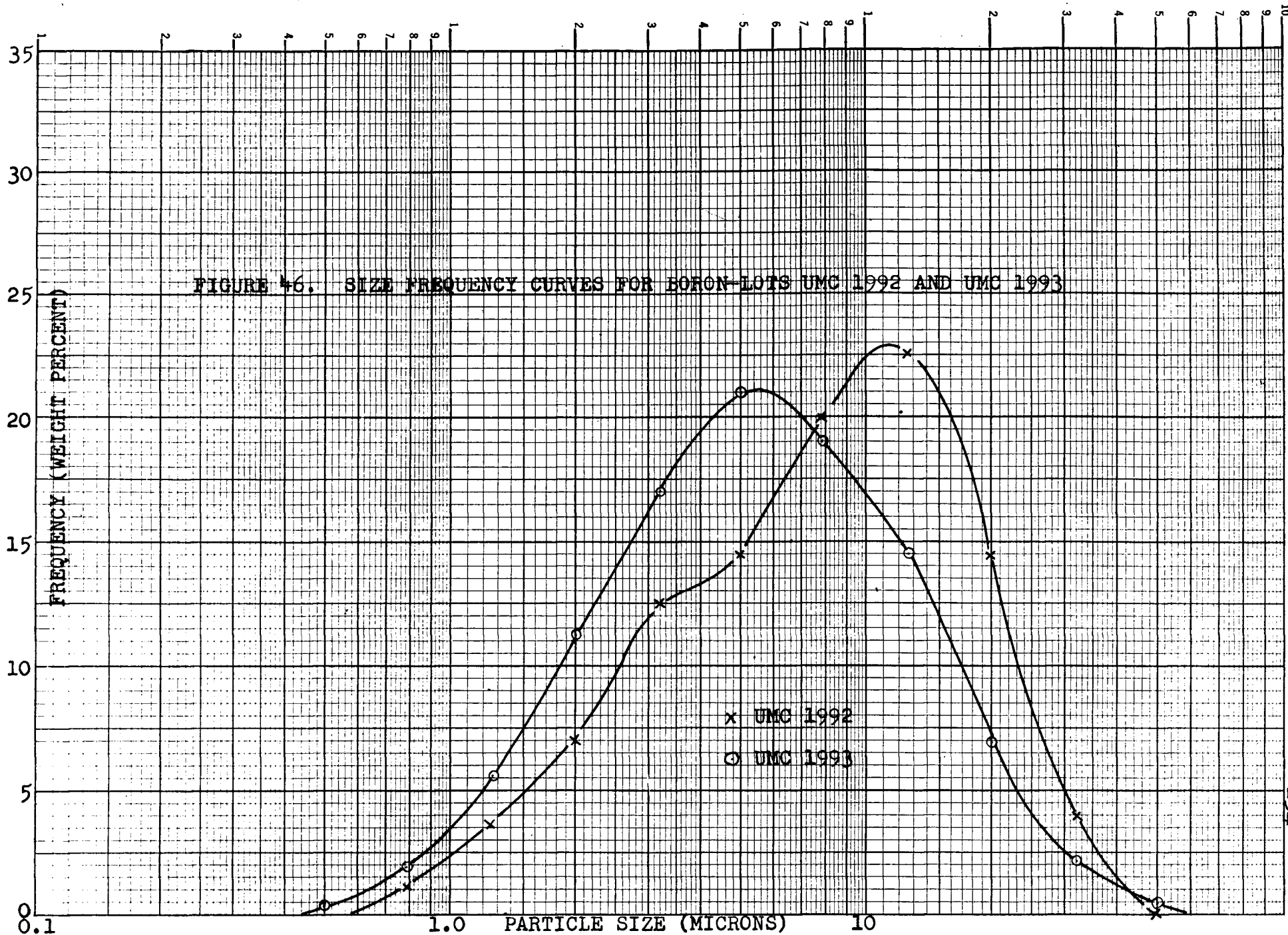


FIGURE 46. SIZE FREQUENCY CURVES FOR BORON LOTS UMC 1992 AND UMC 1993

TABLE 43

BURNING RATE DATA-COMPOSITION 1

Depth of Column Before Igniter Loading (in.)	Column After Igniter Loading (in.)	Fuze Burning Time (sec)	Composition Burning Rate (in./sec)
.049	.015	1.004	.799
.535	.017	.999	.800
.056	.019	.998	.797
.044	.009	1.011	.798
.051	.016	.952	.798
.050	.014	.988	.813
.048	.015	.967	.812
.060	.025	.963	.831

TABLE 44

BURNING RATE DATA—COMPOSITION 2

Depth of Column		Fuze	Composition
Before igniter Loading (in.)	After igniter Loading (in.)	Burning Time (sec)	Burning Rate (in./sec)
.039	.000	1.089	.746
.040	.006	1.125	.719
.045	.004	1.119	.720
.053	.017	1.056	.755
.038	.003	1.118	.725
.041	.003	1.111	.728
.037	.000	1.115	.728
.038	.001	1.121	.723
.037	.001	1.138	.713
.043	.007	1.132	.711
.047	.009	1.086	.740
.046	.012	1.087	.738
.058	.018	1.098	.732
.054	.022	1.072	.741
.052	.018	1.106	.719
.016	-	1.115	.748
.042	.006	1.105	.730
.044	.008	1.132	.710
.038	.004	1.106	.733
.035	.001	1.116	.729
.038	-	1.105	.735
.042	.007	1.128	.715
.034	-	1.124	.782
.041	.005	1.113	.726
.033	.001	1.112	.732

TABLE 45

BURNING RATE DATA -COMPOSITION 3

Depth of Column		Fuze	Composition
Before igniter Loading (in.)	After igniter Loading (in.)	Burning Time (sec)	Burning Rate (in./sec)
-	.045	1.176	.670
-	.050	1.201	.652
-	.047	1.097	.718
-	.042	1.132	.700
-	.049	1.132	.694
-	.049	1.087	.723
-	.047	1.085	.726
-	.046	1.113	.708
-	.046	1.171	.672
-	.046	1.132	.696
-	.042	1.112	.696
-	.051	1.174	.666
-	.046	1.219	.645
-	.052	1.139	.686
-	.045	1.106	.714
-	.049	1.160	.676
-	.046	1.131	.697
-	.051	1.148	.682
-	.048	1.099	.716
-	.041	1.195	.663
-	.049	1.206	.650
-	.043	1.156	.684
-	.043	1.123	.704
-	.044	1.187	.665
-	.049	1.173	.668

TABLE 46

BURNING RATE DATA-COMPOSITION 4

Depth of Column		Fuze	Composition
Before Igniter Loading (in.)	After Igniter Loading (in.)	Burning Time (sec)	Burning Rate (in./sec)
.051	.016	1..40	.699
.045	.013	1.259	.634
.048	.013	1.098	.729
.043	.016	1.147	.700
.044	.011	1.111	.724
.053	.019	1.089	.730
.055	.018	1.125	.705
.045	.013	1.086	.739
.032	.021	1.068	.757
.050	.011	1.048	.765
.049	.014	1.085	.738
.050	.015	1.091	.732
.050	.014	1.128	.707
.054	.019	1.135	.699
.052	.018	1.108	.718
.042	.014	1.156	.694
.049	.014	1.116	.716
.052	.014	1.110	.717
.052	.013	1.111	.719
.054	.020	1.101	.721
.054	.019	1.088	.731
.055	.013	1.156	.687
.048	.013	1.101	.727
.050	.016	1.109	.712

TABLE 47

BURNING RATE DATA-COMPOSITION 5

Depth of Column		Fuze	Composition
Before Igniter	After Igniter	Burning	Burning Rate
Loading (in.)	Loading (in.)	Time (sec)	(in./sec)
.065	.026	1.134	.691
.068	.029	1.135	.688
.064	.023	1.132	.694
.064	.028	1.098	.714
.067	.029	1.119	.698
.059	.026	1.089	.724
.063	.022	1.097	.718
.055	.025	1.085	.730
.066	.030	1.103	.709
.060	.024	1.122	.702
.070	.032	1.154	.674
.075	.037	1.112	.695
.079	.039	1.092	.705
.063	.026	1.090	.720
.067	.033	1.154	.675
.066	.029	1.079	.725
.049	.011	1.126	.711
.069	.029	1.096	.712
.075	.040	1.080	.715
.059	.024	1.104	.715
.067	.035	1.126	.692
.073	.032	1.096	.709
.057	.022	1.130	.699

TABLE 48

BURNING RATE DATA-COMPOSITION 6

Depth of Column		Fuze	Composition
Before Igniter	After Igniter	Burning	Burning Rate
Loading (in.)	Loading (in.)	Time (sec)	(in./sec)
.056	.019	1.354	.580
.061	.022	1.339	.599
.057	.018	1.344	.585
.062	.024	1.318	.592
.056	.019	1.346	.585
.059	.019	1.348	.582
.064	.025	1.343	.580
.067	.028	1.334	.582
.061	.019	1.340	.584
.061	.023	1.337	.585
.066	.028	1.336	.581
.047	.011	1.355	.587
.057	.022	1.319	.595
.056	.019	1.358	.579
.061	.023	1.341	.583
.053	.015	1.363	.579
.064	.030	1.312	.593
.064	.025	1.340	.581
.059	.022	1.361	.576
.062	.025	1.354	.576
.065	.027	1.347	.578
.060	.022	1.342	.584
.061	.024	1.325	.590
.062	.024	1.319	.592
.061	.022	1.328	.589

TABLE 49

BURNING RATE DATA-COMPOSITION 7

Depth of Column		Fuze	Composition
Before Igniter Loading (in.)	After Igniter Loading (in)	Burning Time (sec)	Burning Rate (in./sec)
.048	.011	1.016	.792
.653	.017	1.026	.778
.061	.022	1.078	.732
.055	.017	1.009	.791
.065	.030	1.018	.771
.047	.009	1.042	.738
.059	.022	1.007	.752
.054	.017	1.012	.788
.053	.014	1.055	.757
.053	.005	1.026	.783
.057	.020	1.042	.762
.055	.017	1.029	.775
.063	.024	1.001	.789
.058	.069	.949	.821
.057	.016	1.045	.761
.050	.027	1.034	.780
.068	.025	1.041	.755
.055	.021	1.056	.752
.048	.008	1.032	.780
.058	.064	1.041	.760
.052	.014	1.011	.793
.045	.009	1.038	.776
.050	.014	1.037	.772
.045	.008	1.009	.801

TABLE 50

BURNING RATE DATA—COMPOSITION 8

Depth of Column		Fuze	Composition
Before Igniter	After Igniter	Burning	Burning Rate
Loading (in.)	Loading (in.)	Time (sec)	(in./sec)
.043	.004	1.079	.749
.045	.005	1.114	.723
.044	.019	1.065	.753
.045	.012	1.085	.741
.045	.001	1.109	.728
.040	.006	1.079	.750
.037	.002	1.084	.750
.044	.007	1.099	.733
.046	.004	1.102	.731
.043	.003	1.083	.747
.038	.002	1.114	.728
.042	.003	1.094	.739
.047	.010	1.088	.738
.040	-	1.111	.730
.042	.002	1.109	.730
.037	.002	1.109	.732
.036	.015	1.113	.726
.045	.010	1.085	.741
.044	-	1.104	.732
.045	.002	1.088	.743
.045	.002	1.106	.730
.045	.006	1.060	.761

TABLE 51

BURNING RATE DATA-FOR COMPOSITION 9

Depth of Column		Fuze	Composition
Before Igniter	After Igniter	Burning	Burning Rate
Loading (in.)	Loading (in.)	Time (sec)	(in./sec)
.043	.010	1.188	.666
.042	.007	1.215	.652
.057	.018	1.141	.683
.042	.007	1.166	.680
.051	.017	1.198	.653
.049	.011	1.163	.677
.043	.014	1.182	.668
.044	.007	1.188	.666
.044	.007	1.165	.680
.046	.010	1.136	.695
.042	.009	1.186	.668
.045	.010	1.173	.673
.040	.013	1.190	.666
.049	.014	1.164	.675
.040	.008	1.175	.675
.044	.003	1.219	.653
.043	.010	1.149	.689
.042	.007	1.164	.681
.042	.019	1.153	.684

TABLE 52

BURNING RATE DATA—COMPOSITION 10

Depth of Column		Fuze	Composition
Before Igniter	After Igniter	Burning	Burning Rate
Loading (in.)	Loading (in.)	Time (sec)	(in./sec)
.043	.006	1.330	.594
.039	.016	1.329	.594
.046	.011	1.329	.592
.048	.017	1.318	.594
.044	.019	1.321	.594
.044	.007	1.349	.585
.045	.007	1.371	.575
.048	.010	1.335	.589
.043	.007	1.352	.584
.045	.008	1.340	.588
.048	.005	1.342	.587
.047	.013	1.299	.605
.044	.006	1.336	.591
.043	.004	1.339	.591
.050	.009	1.327	.590
.041	.016	1.312	.601
.044	.006	1.353	.584
.053	.013	1.340	.583
.040	.006	1.333	.594
.045	.013	1.327	.593

TABLE 53

BURNING RATE DATA-COMPOSITION 11

Depth of Column		Fuze Burning Time (sec)	Composition Burning Rate (in./sec)
Before Igniter Loading (in.)	After Igniter Loading (in.)		
.055	.029	1.317	.588
.056	.010	1.370	.569
.055	.024	1.415	.548
.057	.025	1.338	.579
.054	.007	1.340	.584
.062	.011	1.348	.575
.063	.032	1.350	.569
.069	.014	1.296	.594
.052	.020	1.325	.588
.053	.022	1.325	.587
.053	.020	1.344	.579
.058	.004	1.392	.560
.059	.026	1.325	.583
.054	.029	1.344	.577
.062	.029	1.318	.584
.057	.024	1.326	.584
.059	.024	1.319	.586
.065	.032	1.382	.554
.059	.025	1.340	.577
.060	.030	1.345	.568
.058	.026	1.325	.584
.062	.011	1.334	.581
.060	.028	1.351	.567
.060	.026	1.331	.576

TABLE 54

BURNING RATE DATA-COMPOSITION 14

Depth of Column Before Igniter Loading (in.)	Depth of Column After Igniter Loading (in.)	Fuze Burning Time (sec)	Composition Burning Rate (in./sec)
.051	.014	2.860	.270
.042	.006	2.832	.276
.037	.003	2.836	.277
.064	.074	2.344	.322
.075	.038	2.471	.303
.038	.003	2.831	.277
.035	.001	2.817	.280
.055	.024	2.567	.299
.062	.026	2.596	.294
.066	.050	2.912	.259
.058	.022	2.591	.296
.033	.001	2.839	.278
.038	.002	2.801	.280
.072	.037	2.513	-
.050	.016	2.801	.276
.037	.002	2.587	-

TABLES 55

BURNING RATE DATA-COMPOSITION 15

Depth of Column		Fuze	Composition
Before Igniter	After Igniter	Burning	Burning Rate
Loading (in.)	Loading (in.)	Time (sec)	(in./sec)
.055	.020	2.283	.340
.068	.036	2.380	.320
.055	.021	2.354	.329
.055	.023	2.231	.348
.055	.027	2.383	.325
.058	.025	2.290	.337
.057	.029	2.346	.329
.052	.020	2.325	.335
.042	.020	2.220	-

TABLES 56

BURNING RATE DATA-COMPOSITION 16

Depth of Column		Fuze Burning Time (sec)	Composition Burning Rate (in./sec).
Before Igniter Loading (in.)	After Igniter Loading (in.)		
.037	.013	4.154	.189
.039	.012	4.101	.191
.035	-	4.291	.183
-	.024	4.062	.188
.062	.039	4.041	.188
.043	.012	4.167	.187
.046	.015	4.077	.190
.048	.016	4.032	.192
.040	.010	4.137	.189
.064	.010	3.964	.192

TABLES 57

BURNING RATE DATA-COMPOSITION 17

Depth of Column		Fuze	Composition
Before Igniter	After Igniter	Burning	Burning Rate
Loading (in.)	Loading (in.)	Time (sec)	(in./sec)
.067	.029	5.372	.141
.060	.026	5.341	.143
.064	.028	5.341	.142
.064	.025	5.320	.143
.069	.031	5.370	.140
.067	.030	5.413	.140
.062	.028	5.410	.141
.064	.017	5.276	.144
.057	.022	5.517	.139
.067	.029	5.357	.141
.056	.022	5.425	.141
.065	.027	5.273	.144
.063	.026	5.301	.143
.055	.018	5.414	.142
.065	.029	5.262	.144
.065	.029	5.403	.140
.060	.026	5.499	.139
.062	.026	5.406	.141

TABLES 58

BURNING RATE DATA-COMPOSITION 19

Depth of Column		Fuze	Composition
Before Igniter	After Igniter	Burning	Burning Rate
Loading (in.)	Loading (in.)	Time (sec)	(in./sec)
.037	-	.945	.867
.051	.010	.967	.832
.050	.006	.974	.829
.018	.003	.983	.824
.047	.008	.983	.822
.064	.012	.949	.840
.054	.014	.949	.846
.050	.005	.961	.842
.051	.006	.970	.832
.045	.003	.967	.840
.047	.006	.982	.823
.057	.015	.930	.862
.050	.007	.960	.842
.049	.007	.955	.847
.051	.009	.978	.823
.045	.005	.963	.843
.040	.001	.947	.862
.048	.008	.947	.854
.046	.005	.936	.867
.043	.002	.955	.852

TABLES 59

BURNING RATE DATA - COMPOSITION 20

Depth of Column		Fuze Burning Time (sec)	Composition Burning Rate (in./sec)
Before Igniter Loading (in.)	After Igniter Loading (in.)		
.035	.003	2.391	.333
.039	.005	2.325	.341
.049	.016	2.359	.331
.051	.010	2.353	.332
.037	.003	2.371	.335
.044	.010	2.384	.330
.041	-	2.368	.334
.037	.004	2.320	.342
.036	.002	2.330	.341
.044	.001	2.354	.335
.041	-	2.427	.326
.035	.005	2.387	.333
.038	.002	2.387	.332
.041	.001	2.291	.346
.038	.002	2.462	.322
.041	.001	2.355	.336
.035	.003	2.402	.331
.044	.010	2.255	.349
.044	.006	2.369	.332

TABLES 60

BURNING RATE DATA - COMPOSITION 21

Depth of Column		Fuze Burning Time (sec)	Composition Burning Rate (in./sec)
Before Igniter Loading (in.)	After Igniter Loading (in.)		
.045	.035	2.267	.348
.027	.015	2.347	.343
.048	.033	2.318	.339
.034	-	2.326	.343
.030	.019	2.340	.342
.030	.017	2.356	.340
.034	.018	2.389	.334
.030	-	2.274	.352
.033	.022	2.283	.350
.034	.029	2.215	.359
.032	.024	2.304	.346
.041	.029	2.272	.348
.035	.025	2.284	.349
.035	.021	2.268	.352
.034	.025	2.258	.353
.036	.019	2.314	.345
.032	-	2.367	.338
.035	.020	2.284	.350
.029	.017	2.242	.358

TABLES 61

BURNING RATE DATA—COMPOSITION 23

Depth of Column		Fuze	Composition
Before Igniter	After Igniter	Burning	Burning Rate
Loading (in.)	Loading (in.)	Time (sec)	(in./sec)
.052	.015	4.874	.158
.048	.012	4.872	.159
.042	.004	4.954	.158
.043	.009	4.823	.162
.044	.005	4.884	.160
.046	.009	4.894	.159
.048	.010	4.905	.158
.046	.006	4.881	.159
.040	.004	4.874	.161
.046	.001	4.814	.162
.046	.007	-	-
.050	.010	4.790	.162
.044	.005	4.783	.163
.041	.002	5.009	.156
.039	.007	4.787	.164
.041	.004	4.945	.158
.044	.004	4.858	.160
.039	.002	-	-
.039	.002	4.844	.162
.040	.001	4.811	.163

TABLES 62

BURNING RATE DATA-COMPOSITION 24

Depth of Column		Fuze	Composition
Before Igniter	After Igniter	Burning	Burning Rate
Loading (in.)	Loading (in.)	Time (sec)	(in./sec)
.046	.006	2.960	.264
.043	.006	3.021	.260
.057	.017	2.930	.263
.044	.003	2.908	.270
.048	.007	3.008	.259
.047	.006	3.019	.259
.060	.022	2.909	.264
.047	.009	2.939	.266
.053	.012	2.913	.266
.057	.017	2.991	.258
.047	.010	2.939	.266
.043	.006	2.927	.268
.046	.005	2.944	.266
.046	.010	2.953	.265
.040	.025	2.975	.264
.045	.005	2.926	.268
.045	.002	2.942	.267
.047	.005	2.968	.263
.055	.017	2.940	.263
.047	.001	2.956	.265

GLOSSARY

APD

Average Particle Diameter, as determined with the Fisher Sub-Sieve Sizer.

B&C

Barium and Chemicals Corporation.

Baker

J. T. Baker Chemical Company.

HCST

Hermann C. Stark Company, Division of Shieldalloy Corporation.

MP

Mineral Pigments Corporation.

MSA

Mine Safety Appliances Company.

MSA d_m

Mean particle diameter, calculated by integration of the particle size - frequency curves.

MSA 50 Percent Point

Point corresponding to intersection particle size distribution curve (particle size vs. percent greater than size),

drawn from MSA particle size analysis results, and "50 percent greater than size" line.

Trona

American Potash and Chemical Company.

UMC

United Minerals and Chemicals Corporation.